THE PRIMARY PHOTOCHEMICAL PROCESS IN HEXAFLUOROACETONE VAPOUR

by

PETER GEORGE BOWERS
B. A.(Cantab.), 1961

A THESIS SUBMITTED IN PARTIAL FULFILMENT OF
THE REQUIREMENTS FOR THE DEGREE OF

DOCTOR OF PHILOSOPHY

in the Department
of
Chemistry

We accept this thesis as conforming to the
required standard

THE UNIVERSITY OF BRITISH COLUMBIA
July, 1964

In presenting this thesis in partial fulfilment of the requirements for an advanced degree at the University of British Columbia, I agree that the Library shall make it freely available for reference and study. I further agree that permission for extensive copying of this thesis for scholarly purposes may be granted by the Head of my Department or by his representatives. It is understood that copying or publication of this thesis for financial gain shall not be allowed without my written permission.

Department of Chemistry

The University of British Columbia,
Vancouver 8, Canada

Date 8/VII/64

The University of British Columbia

FACULTY OF GRADUATE STUDIES

PROGRAMME OF THE

FINAL ORAL EXAMINATION

FOR THE DEGREE OF

DOCTOR OF PHILOSOPHY

of

PETER GEORGE BOWERS

B.A., University of Cambridge, 1961

MONDAY, JULY 6th, 1964, AT 10:30 A.M.

IN ROOM 261, CHEMISTRY BUILDING

COMMITTEE IN CHARGE

Chairman: I. McT. Cowan

W.R. Cullen	G.B. Porter
F.W. Dalby	Ross Stewart
B.A. Dunell	J. Trotter

External Examiner: B.S. Rabinovitch

University of Washington

THE PRIMARY PHOTOCHEMICAL PROCESS IN HEXAFLUOROACETONE VAPOUR

A B S T R A C T

The photochemical dissociation of hexafluoroacetone vapour (HFA) has been studied at room temperature using five exciting wavelengths between 2500 and 3500 Å, and at -78°, using 3130 Å excitation. The effect of the presence of biacetyl during the photolysis has been investigated.

Complementary experiments on the visible emission from HFA were performed, paying particular attention to the quenching action of oxygen and biacetyl.

Plots of reciprocal quantum yield of carbon monoxide versus HFA pressure have either a positive and constant, or positive and decreasing slope, down to 1 mm pressure: there is virtually no evidence that a weak (multistage) collision mechanism is operative in deactivation of the excited molecules.

A simple extension of classical unimolecular theory is examined, in order to account for observed photodissociation rate constants, $k_2(\lambda, T)$. The model shows that Arrhenius plots of $k_2(T)$ at constant wavelength will not, in general, be linear, but that upper and lower limits for the critical (activation) energy, may still be obtained. For HFA, this energy is placed between 5.7 and 8.6 kcals/mole. Agreement in order-of-magnitude is found between calculated and observed values of $k_2(T)$, only if it is assumed that a fraction (rather more than half) of the normal modes participate in intramolecular energy exchange. This fraction has to be increased with decreasing wavelength to explain the observed $k_2(\lambda)$ values. The inadequacy of a classical treatment of the system is recognized.

The emission spectrum of HFA consists of both fluorescence and phosphorescence. Small concentrations of biacetyl quench phosphorescence and triplet dissociation. The phosphorescence to fluorescence ratio is 2.77 at 25° and 9.95 at -78°, while the total emission yield increases by a factory of 16.7 on decreasing the temperature over this range. From a study of biacetyl emission, direct and sensitized by

HFA, it is shown that nearly 50% of HFA molecules excited with 3130 Å, eventually reach the triplet state at 25°. The phosphorescence yield of HFA at -78° was estimated to be 0.51.

At relatively high pressures, dissociation yields are apparently greater when less energetic excitation is used. Various modifications to the intersystem crossing mechanism are discussed to account for this, but no definite conclusion can be reached.

GRADUATE STUDIES

Field of Study: Chemistry

Topics is Physical Chemistry	J.A.R.Coope A.V. Bree R.F. Snider
Statistical Mechanics	R.F. Snider
Molecular Spectroscopy	K.B. Harvey A.V. Bree L.W. Reeves
Advanced Theoretical Chemistry	R.F. Snider
Chemical Kinetics	E.A. Ogryzlo G.B. Porter D.G.L. James
Quantum Chemistry	R. Hochstrasser

Other Studies:

Computer Programming	Charlotte Froese
Differential Equations	S.A. Jennings
Topics in Organic Chemistry	D.E. McGreer J.P. Kutney R.E.I. Pincock
Topics in Inorganic Chemistry	W.R. Cullen N. Bartlett

PUBLICATION

G. B. Porter and P. G. Bowers

The Primary Photochemical Process in Hexafluoroacetone

6th Photochemistry Conference, Davis, California, June,1964.

ABSTRACT

The photochemical dissociation of hexafluoroacetone vapour (HFA) has been studied at room temperature using five exciting wavelengths between 2500 and 3500 Å, and at -78°, using 3130 Å excitation. The effect of the presence of biacetyl during the photolysis has been investigated.

Complementary experiments on the visible emission from HFA were performed, paying particular attention to the quenching action of oxygen and biacetyl.

Plots of reciprocal quantum yield of carbon monoxide versus HFA pressure have either a positive and constant, or positive and decreasing slope, down to 1 mm pressure: there is virtually no evidence that a weak (multistage) collision mechanism is operative in deactivation of the excited molecules.

A simple extension of classical unimolecular theory is examined, in order to account for observed photodissociation rate constants, $k_2(\lambda, T)$. The model shows that Arrhenius plots of $k_2(T)$ at constant wavelength will not, in general, be linear, but that upper and lower limits for the critical (activation) energy, may still be obtained. For HFA, this energy is placed between 5.7 and

8.6 kcals/mole. Agreement in order-of-magnitude is found between calculated and observed values of $k_2(T)$, only if it is assumed that a fraction (rather more than half) of the normal modes participate in intramolecular energy exchange. This fraction has to be increased with decreasing wavelength to explain the observed $k_2(\lambda)$ values. The inadequacy of a classical treatment of the system is recognized.

The emission spectrum of HFA consists of both fluorescence and phosphorescence. Small concentrations of biacetyl quench phosphorescence and triplet dissociation. The phosphorescence to fluorescence ratio is 2.77 at 25° and 9.95 at -78°, while the total emission yield increases by a factor of 16.7 on decreasing the temperature over this range. From a study of biacetyl emission, direct and sensitized by HFA, it is shown that nearly 50% of HFA molecules excited with 3130 Å, eventually reach the triplet state at 25°. The phosphorescence yield of HFA at -78° was estimated to be 0.51.

At relatively high pressures, dissociation yields are apparently greater when less energetic excitation is used. Various modifications to the intersystem crossing mechanism are discussed to account for this, but no definite conclusion can be reached.

TABLE OF CONTENTS

		Page
I.	INTRODUCTION.	1
	A General Scheme for the Primary Process.	2
	Previous Work on Hexafluoroacetone.	9
	Related Studies:	15
	(i) Stepwise Deactivation: Ketene.	15
	(ii) The Vibrational Temperature Model.	19
	(iii) Excitation by Non-Photochemical Techniques.	23
	(iv) Transfer of Electronic Energy.	26
	The Purpose of this Investigation.	28
II.	EXPERIMENTAL ARRANGEMENT AND PROCEDURE.	30
	Materials.	30
	Optical Arrangement.	31
	Reaction Cells.	32
	Gas Analysis.	33
	Actinometry.	34
	Measurement of Absorption Coefficients.	34
	Reflection Corrections.	35
	Fluorescence Spectroscopy.	37

Page

III. RESULTS. 41

Absorption. 41

Photolysis at 25°. 42

Low Temperature Photolysis. 43

Photolysis of Hexafluoroacetone-Biacetyl Mixtures. 44

Reliability of the Quantum Yields. 44

Emission Spectra: Hexafluoroacetone. 45

Emission Spectra: Hexafluoroacetone-Biacetyl Mixtures. 46

IV. DISCUSSION: COLLISIONAL DEACTIVATION AND DISSOCIATION. 63

General Observations. 63

Collisional Deactivation. 64

Evaluation of Some Rate Constants. 66

A Model for Photodissociation 69

Comparison with Experiment. 86

V. DISCUSSION: INTERSYSTEM CROSSING, ENERGY TRANSFER, AND EMISSION. 95

The Hexafluoroacetone-Biacetyl System. 95

Fluorescence and Phosphorescence. 99

The Intersystem Crossing Reaction. 105

BIBLIOGRAPHY 114

FIGURES

		Page
1.	Energy diagram: electronic excitation of a molecule.	8
2.	Quantum yields of carbon monoxide from HFA (Ayscough and Steacie)	16
3.	Wavelength dependence of the relative fluorescence yield (Giacometti, Okabe and Steacie.	16
4.	Temperature dependence of the relative fluorescence yield (Giacometti, Okabe and Steacie).	16
5.	Calculated quantum yields for a weak collision model (Porter and Connelly).	20
6.	Calculated quantum yields including triplet dissociation (Porter and Connelly).	20
7.	Optical arrangement for photolysis and the low temperature cell.	39
8.	Optical arrangement for recording emission spectra.	39
9.	Spectral characteristics of the radiation used in photolysis.	40
10.	Reflection at quartz windows.	36
11.	A typical absorption curve.	48
12.	Absorption spectrum of HFA.	49
13.	Emission spectrum of HFA-biacetyl under photolysis conditions.	57
14.	Emission spectrum of HFA-biacetyl at higher pressures.	58
15.	Emission spectrum of HFA at 25°: the effect of oxygen.	59

Page

16. Emission spectra of HFA at -78° and 25°. 60

17. Emission spectrum of HFA at -78°: the effect of oxygen. 61

18. Reciprocal quantum yields at lower pressures, 25°. 70

19. Reciprocal quantum yields at 3340 Å, 25°. 71

20. Reciprocal quantum yields at higher pressures, 25°. 72

21. Reciprocal quantym yields at higher pressures: 2652 Å, 25°. 73

22. Reciprocal quantum yields at -78°. 74

23. Quantum yield at 2804 Å. 75

24. Energy diagram for photodissociation. 87

25. Predicted behaviour of $1/\phi$ vs. $[A]$. 82

26. Calculated rate constants, $k_2(T)$. 88

27. Comparison between experimental and calculated rate constants $k_2(T)$. 93

28. The form of $f(E)$ and $k_2(E_1)$. 94

29. Photolysis of HFA-biacetyl mixtures at 25°. 100

30. Variation of triplet dissociation with pressure. 101

31. Phosphorescence and fluorescence at -78°. 106

32. Total emission at -78° and 25°. 107

33. Phosphorescence and fluorescence at 25°C. 108

TABLES

		Page
1.	Absorption coefficients.	49
2.	Photolysis at 3340 Å, 25°.	50
3.	Photolysis at 3130 Å, 25°.	51
4.	Photolysis at 3130 Å, -78°.	52
5.	Photolysis at 3020 Å, 25°.	53
6.	Photolysis at 2804 Å, 25°.	54
7.	Photolysis at 2652 Å, 25°.	55
8.	Photolysis of HFA-biacetyl mixtures at 25°.	56
9.	Comparative emission intensities.	62
10.	Rate constants for photodissociation.	75
11.	Experimental and predicted rate constants, $k_2(\lambda)$.	94
12.	Quantum yields of triplet dissociation.	97

ACKNOWLEDGMENT

I wish to express sincere thanks to Dr. G. B. Porter, whose generous advice, criticism and suggestion guided this research at many stages.

I have had useful conversations with Dr. K. O. Kutschke of the National Research Council, Ottawa, and with Dr. R. F. Snider.

The electronic circuitry attendant to the fluorescence spectrometer was originally constructed by Dr. S. Lower. I am indebted to Dr. E. Ogryzlo for being allowed to use this equipment.

I would also like to thank the National Research Council of Canada, and the University of British Columbia for supporting Fellowships.

INTRODUCTION

From the large amount of work which has been carried out on the photochemical behaviour of ketones in the gas-phase, it is apparent that the absorption of light by such molecules can give rise to a system of considerable kinetic complexity. The Primary Process of the electronically excited molecules embodies, by definition, all those events which result in eventual dissociation or return to the ground state. The latter reactions may include loss of vibrational energy by collision; intersystem crossing between various electronic states; re-emission of radiant energy; radiationless return to the ground state (internal conversion), and energy transfer to other molecules.

The overall picture is further complicated, because the radicals or molecules formed from a primary dissociation may react amongst themselves, or with the parent ketone, to give a diversity of final products. Unless a complete account can be given of these Secondary reactions, the magnitudes and often even the nature, of reactions constituting the primary process, are largely obscured. Thus it is with acetone, where as many as eight products have been recognised, and except under well chosen conditions, estimates of the primary quantum yield of dissociation are subject to large uncertainties.

In only a few cases are the secondary reactions simple enough to make it practicable to study the primary process in detail. Notable amongst these are the perfluoro-aliphatic ketones, ketene, and diazomethane.

A General Scheme for the Primary Process

It is customary to illustrate the course of events in a photo-excited molecule by means of the Jablonski diagram (Fig. 1). Historically, the scheme discussed here has evolved from the early fluorescence experiments of Stern and Volmer (1), modified in the light of more recent spectroscopic knowledge, and as extensive data became available. There have been several recent reviews (2,3,4).

The first absorption band of ketones, which generally has a maximum around 2800 Å, results from excitation of one of the non-bonding electrons of the carbonyl oxygen into an antibonding π orbital. The excited singlet state so produced is referred to, by photochemists, as $^1(n\pi^*)$. Description of the electronic states is often abbreviated to S_o (ground); S_1, S_2, ...(excited singlets); T_1, T_2, ...(excited triplets).

Reaction 1. The act of absorption produces a species $^1A^m$, where part of the excitation energy appears as excess

vibrational energy, of which the index m is a measure. The integrated absorption coefficient is related to the natural (radiative) lifetime, τ_o, of a molecule in S_1. An approximate expression is

$$\tau_o \sim \frac{10^{-4}}{\epsilon_{max.}} .$$

τ_o is generally between 10^{-5}-10^{-7} seconds, but the actual lifetime may be shorter, depending on the rate of subsequent reactions of ^1A.

Reaction 2. The stationary-state concentration of excited species is so small, that they are essentially surrounded by a heat bath of unexcited molecules. The excess vibrational energy is rapidly dissipated by collision: it has generally been assumed that one collision suffices to reduce the excited ($^1A^m$) molecule to low vibrational levels.

$$^1A^m + A \longrightarrow {}^1A^o + A$$

One may then consider all other primary reactions as taking place from either or both of two species, $^1A^m$ or $^1A^o$. Kinetic data, at any rate are often consistent with this oversimplification.

Reaction 3. Both $^1A^m$ and $^1A^o$ could be involved in dissociation from S_1, but in most cases there is evidence that only

$^1A^m$ need be considered. For example, at high concentrations, where collisional deactivation is almost complete, the primary quantum yield for dissociation ϕ may approach zero. Further discussion of the dissociation will be deferred until we consider reaction 9.

Reaction 4. The allowed transition $S_1 \rightarrow S_0$ may or may not be accompanied by emission of radiation. The radiationless process - internal conversion - is visualized as involving crossing to high vibrational levels of S_0, followed by rapid collisional stabilization. This first-order process competes with reaction 3, so that if ϕ is found to approach unity at low concentrations, one need not consider internal conversion from $^1A^m$. The reaction $^1A^o \rightarrow A$ can be considered kinetically with fluorescence: it has to be included to account for the very low fluorescence yields usually found.

The internal conversion process is not at all well understood. If indeed it does involve the intermediate formation of ground state molecules with a great excess of vibrational energy, then there would exist the possibility of rapid decomposition of these with an activation energy quite different from that for reaction 3. The alternatives have to be borne in mind, even though kinetic data may not facilitate a distinction.

Reaction 5 is a fluorescent emission. Resonance fluorescence in ketones has not been observed ($^1A^m \rightarrow A + h\nu$). The evidence is that emission comes from $^1A^o$, and often the absorption and emission bands have a mirror image relationship, with a small region of overlap that allows the 0-0 band to be placed. The fluorescence lifetime is about 10^{-6} seconds, and the yields often relatively insensitive to the presence of oxygen, and to temperature.

Reactions 6, 7 and 8. Besides fluorescence there may be another emission band, characterized by a much longer lifetime, and lying at longer wavelengths. It is now well established that this emission - phosphorescence - arises by a transition from a metastable triplet state, T_1, with a lower energy than S_1. The energy difference originates from difference in electron interaction in the two states. Transitions involving change of multiplicity are strongly forbidden, hence a triplet molecule (^3A) has a much longer lifetime: generally around 10^{-3} seconds, in these systems.

Little is known about the relative positions of potential energy curves representing singlet and triplet states, for even the simplest ketones: the intersystem crossing reaction 6 must be isoenergetic and satisfy the Franck-Condon principle. It would be followed by collisional deactivation:

$$ {}^1A^m \longrightarrow {}^3A^q \xrightarrow{A} {}^3A^o $$
$$ {}^1A^o \longrightarrow {}^3A^n \xrightarrow{A} {}^3A^o $$

An important point is that the rate of singlet-triplet transitions is greatly affected by the presence of paramagnetic molecules such as oxygen. In a photochemical study, this may show itself either as an enhancement of the rate of reaction 6, and therefore a decrease in the fluorescence yields, or enhancement of the radiationless transition 8, and a decrease in both phosphorescence and triplet dissociation. In a number of simple ketones the latter effect (phosphorescence quenching) appears to be more important: thus the short-lived blue emission from biacetyl is apparently unaffected by added oxygen, whereas the long-lived green emission is completely quenched (2). Dissociation in the oxygen-perturbed systems is difficult to study experimentally because of the complexity of photo-oxidation products.

Reaction 9. The triplet molecule, $^3A^o$, may be long-lived enough to be re-energized by collision and dissociate. This is analagous to thermal dissociation, and there are important differences between reactions 3 and 9.

In the first place, if monochromatic radiation is

used for excitation, the $^1A^m$ molecules dissociate from a narrow range of high vibrational levels, and not from an equilibrium disposition. Indeed in the simple model being considered, any move towards thermal equilibration by collision will, ipso facto, preclude dissociation. The range of total vibrational energy of $^1A^m$ will depend upon the spectral purity of the exciting wavelength, and the distribution of thermal energy in the ground state. This last factor gives rise to a temperature dependence for reaction 3, but much smaller than that for the thermal-like reaction 9. On the other hand k_3 will show an increase with increasing excitation energy, whereas k_9 should be wavelength-independent.

Another point is that reaction 9 could be pressure dependent in accordance with the ideas of thermal unimolecular reactions, although no such effect has so far been observed.

There have been few attempts to account quantitatively for the variation of the photodissociation constant (reaction 3) with wavelength and temperature, mainly because unambiguous data over a wide range have not been available.

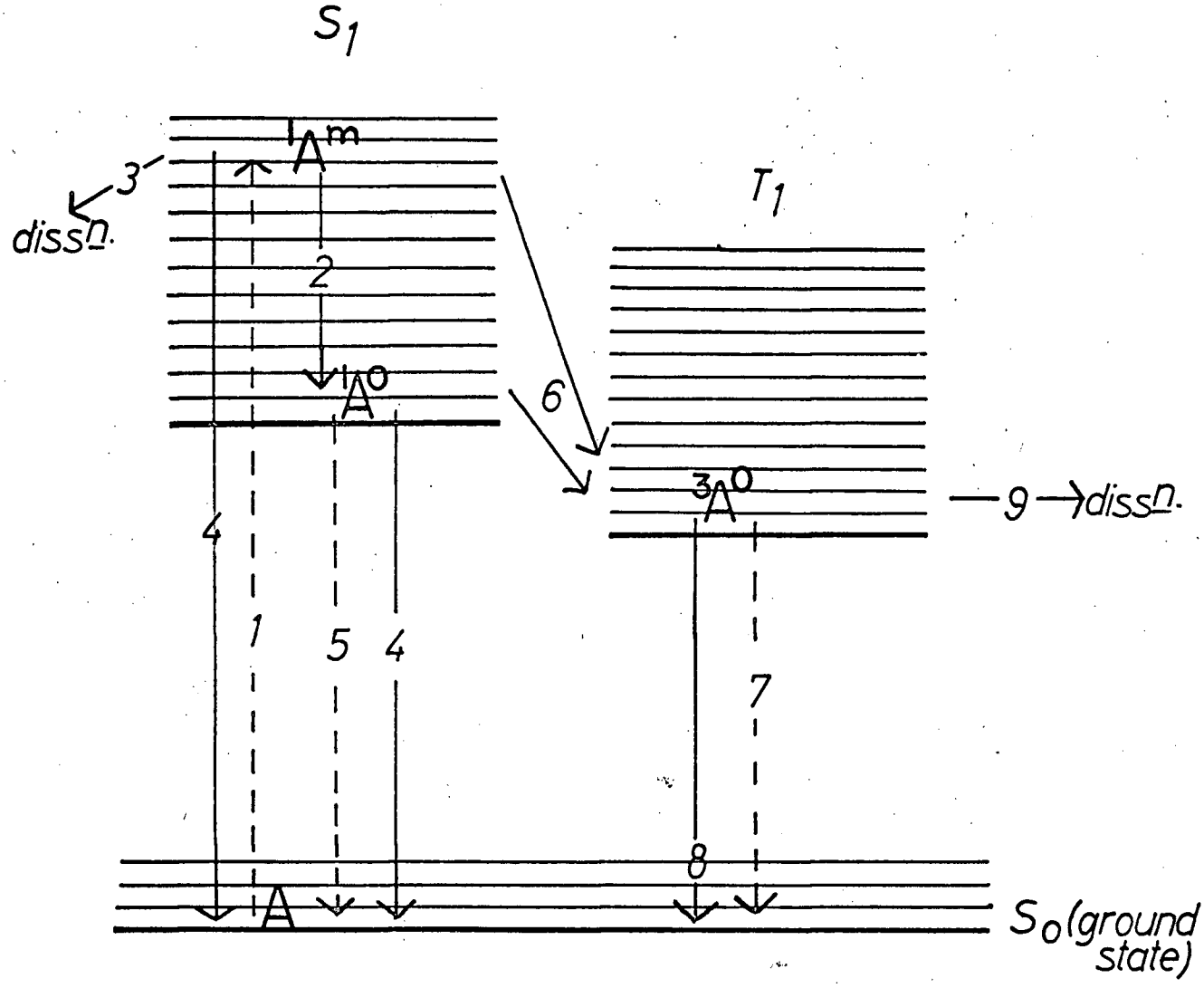

Fig. 1. Energy diagram: electronic excitation of a molecule and the subsequent events. Radiative processes are indicated by a broken line.

Previous Work on Hexafluoroacetone.

The photochemical behaviour of hexafluoroacetone (HFA) was first investigated by Steacie and his co-workers (5,6,7). They carried out extensive photolysis using 3130 Å monochromatic radiation, and a few experiments with 2640 Å. The fluorescence behaviour was studied at a number of wavelengths.

Carbon monoxide, and perfluoroethane, C_2F_6, were the only products formed up to 250°C, in equal proportions to within the experimental error. The quantum yield of carbon monoxide Φ_{CO} was independent of light intensity, and at 27° decreased from near unity at the lowest ketone concentrations (7 mm), to around .07 at 100 mm. Above 200°, Φ_{CO} was unity, almost independent of pressure. At a given temperature, Φ_{CO} was greater at the shorter wavelength, whatever the ketone concentration. The general form of the results is shown in Fig. 2.

The fluorescence band, with a maximum around 4200 Å was found to be unaffected in spectral distribution by pressure, temperature, exciting wavelength, or the presence of oxygen. Relative fluorescence yields (Q) increased with increasing wavelength, tending at higher concentrations to converge to the same value for all wavelengths (Fig. 3). The decrease of Q with increase in temperature was most marked at high concentrations (Fig. 4).

It was fairly clear that Φ_{Co} was equal to the primary dissociation yield of HFA (Ø). No hexafluorobiacetyl was formed, and the overall simplicity of products ruled out attack on HFA by any intermediate radical. This is in sharp contrast to acetone, and one of the few cases where direct equation of a measured product yield to the primary yield can be made with reasonable certainty under all conditions.

The mechanism proposed included many of the reactions outlined in the previous section*

$$A + h\nu \longrightarrow {}^1A^m \qquad I_a$$

$${}^1A^m \longrightarrow \text{Dissociation} \qquad (2)$$

$$A + {}^1A^m \longrightarrow {}^1A^o + A \qquad (3)$$

$${}^1A^o \longrightarrow {}^3A^o \qquad (4)$$

$${}^1A^o \longrightarrow A + h\nu \qquad (5)$$

$${}^1A^o \longrightarrow A \qquad (6)$$

$${}^3A^o \longrightarrow \text{Dissociation} \qquad (8)$$

$${}^3A^o \longrightarrow A \qquad (9)$$

It was necessary to include the two modes of dissociation, since plots of $1/\phi$ vs. [A] did not show the linearity which would be consistent with $k_4=0$. That is,

* The reactions here are re-numbered for convenience. This new numbering is adhered to throughout the remainder of the thesis.

including only reactions 2, 3, 5 and 6, and making the usual stationary state assumptions:

$$1/\phi = 1 + \frac{k_3[A]}{k_2} \qquad (1.1)$$

The primary yield at high concentrations would then tend to zero, with all $^1A^m$ species being collisionally deactivated before having time to dissociate.

With the full mechanism, however,

$$\left(1/\phi\right)^{-1} = \frac{k_2}{k_2+k_3[A]} + \frac{k_3k_4k_8[A]}{(k_4+k_5+k_6)(k_8+k_9)(k_2+k_3[A])} \qquad (1.2)$$

The limiting high concentration yield is now non-zero, since the stabilized $^1A^o$ molecules are able to cross and dissociate from the triplet state. The first term in equation 1.2 represents dissociation from the singlet state; the second, triplet dissociation.

A note on nomenclature is perhaps required. It will be frequently necessary to refer to the primary quantum yield for a particular reaction. Thus ϕ_2 is the yield for singlet dissociation, ϕ_4 is the yield of formation of triplet molecules, and so on. In this nomenclature, even though reaction 8, say, were perfectly efficient in the sense that all triplet molecules decomposed, ϕ_8 need not necessarily be unity.

Superscripted ϕ° and ϕ^{∞} indicate limiting values at extreme concentrations, of ϕ (unscripted), the total primary dissociation yield. Q is a relative fluorescence yield, proportional to the absolute yield ϕ_5.

Rearranging equation 1.2, and putting

$$\phi^{\infty} = \frac{k_4 k_8}{(k_4+k_5+k_6)(k_8+k_9)} \qquad (1.3)$$

$$\text{gives} \quad 1/\phi = \frac{k_2/k_3 + [A]}{k_2/k_3 + \phi^{\infty}[A]} \qquad (1.4)$$

The experimental data fitted equations of the form of expression 1.4, with $1/\phi$ being linear at low pressures and curving off at large [A] to an upper limit. Values for ϕ^{∞} and k_3/k_2 were obtained using the alternative form (equation 1.5), from linear plots of $\phi/(1-\phi)$ vs. $1/[A]$:

$$\frac{\phi}{1-\phi} = \frac{\phi^{\infty}}{1-\phi^{\infty}} + \frac{k_2}{k_3[A](1-\phi^{\infty})} \qquad (1.5)$$

ϕ^{∞} decreased from unity at 219° to about .04 at 25°, with 3130 Å excitation. At the shorter wavelength, with data much less extensive, no unequivocal parameters could be given.

Because the low concentration limit, ϕ°, was close to unity under most conditions, it was not necessary to

include internal conversion from $^1A^m$.

While the direct dissociation of $^1A^m$ showed only a small temperature dependence, the second mode was greatly enhanced by temperature. From the photolysis data alone it was possible that the species $^1A^o$ were themselves dissociating. If this were the case, then at high concentrations, fluorescence and dissociation from $^1A^o$ would be competing reactions, and the change in apparent activation energies of ϕ^∞ and Q^∞ should be complementary. This was not the case: the negative temperature coefficient of Q^∞ was about 1 kcal/mole, constant between 25° and 200°, while that of ϕ^∞ changed from 11 kcal/mole at 25°, to 1.5 kcal/mole at 200°. Thus it was postulated that this second mode of dissociation occurred from another electronic state, which by analogy with acetone would probably be the low-lying triplet state, even though no oxygen-quenched emission was found.

By assuming a collision diameter of 6.0 Å for the HFA molecule, and that reaction 3 took place at every encounter, values for k_2 were obtained at various temperatures. The Arrhenius plot of these was linear, corresponding to an activation energy of 5.7 kcal/mole. However the significance of this assignment was regarded as doubtful,

for dissociation from the non-equilibrium ensemble.

What radicals are formed as a result of the primary dissociation remained a matter of some doubt. Gordon (8) has reported a thorough search for more products, in which he found that a perfluoroether is formed at elevated temperatures:-

$$CF_3\cdot + CF_3COCF_3 \rightarrow \begin{matrix} CF_3 \\ CF_3 \end{matrix}\!\!>\!\dot{C}OCF_3 \xrightarrow{CF_3\cdot} (CF_3)_3C\text{-}O\text{-}CF_3$$

Fortunately this secondary reaction does not affect the carbon monoxide yield as a measure of the primary dissociation yield.

Tucker and Whittle (9) have shown that the presence of bromine during photolysis gives CF_3COBr, and almost no CO. This could mean that $CF_3CO\cdot$ is an intermediate, but can equally well be interpreted in terms of attack on excited HFA by Br_2. Such behaviour is shown in the photooxidation (10), where Φ_{CO_2} is much greater than Φ_{CO} under the same conditions in the absence of oxygen.

If $CF_3CO\cdot$ radicals do play a part, then one might expect $CF_3COCOCF_3$ (HFBA) to be formed. A search for this product in particular has not been made, since it has only

recently been prepared (11). A noteworthy point is that HFBA itself apparently photolyses in the gas phase, to give only C_2F_6 and CO in the ratio 1:2, but no HFA (12).

Related Studies

(i) Stepwise Deactivation: Ketene.

Ketene is another of the ketones whose overall photochemistry is simple enough for the primary process to be investigated in some detail. Briefly, it has been established that the quantum yield of carbon monoxide is equal to twice the primary dissociation yield. The reaction scheme is somewhat simpler than for HFA, with no evidence for the participation of a triplet state. Plots of $^1/\phi$ vs. concentration are linear up to the highest pressures studied. Reaction 5 (page 5) may not occur, as no fluorescence has been observed.

Connelly and Porter (13) considered the effect on ϕ if more than one collision were required for complete deactivation. They assumed that a constant amount of vibrational energy was removed per collision from $^1M^n$, the excited ketene molecule initially produced, and that each partially deactivated species ($^1M^j$) could dissociate, until a certain vibrational level (m) was reached, when the

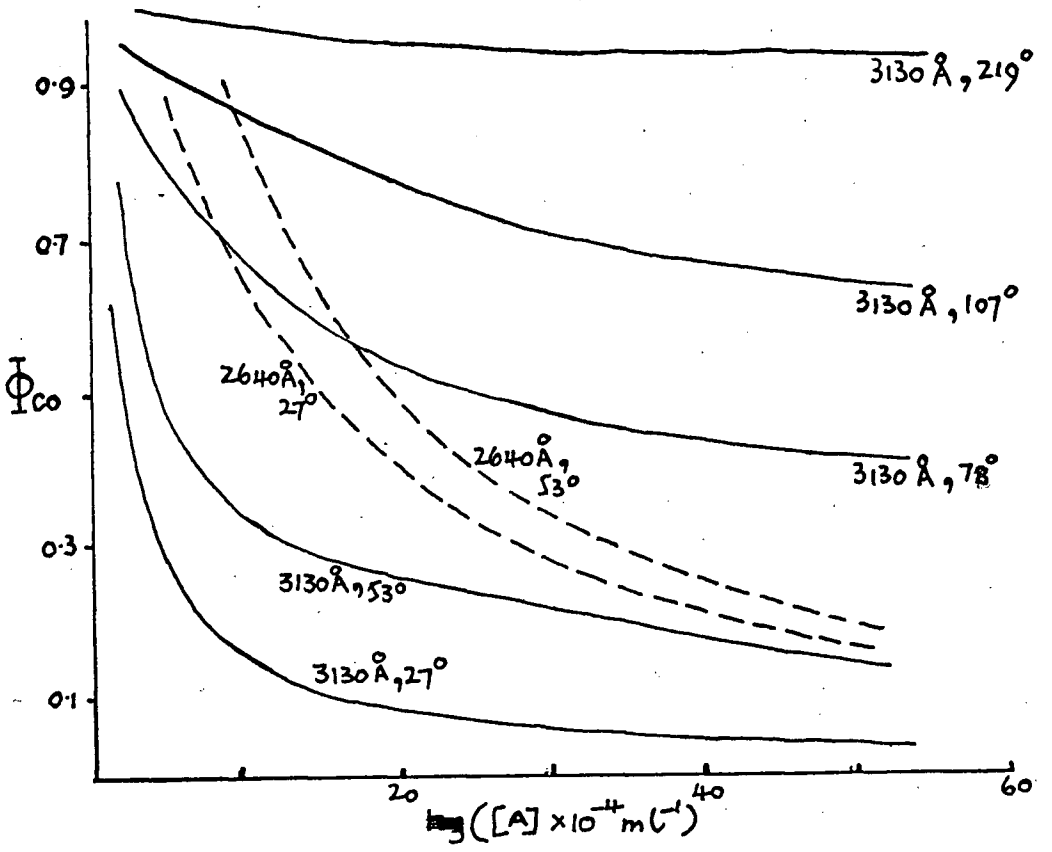

Fig. 2. Quantum yields of carbon monoxide in the photolysis of HFA (Ayscough and Steacie).

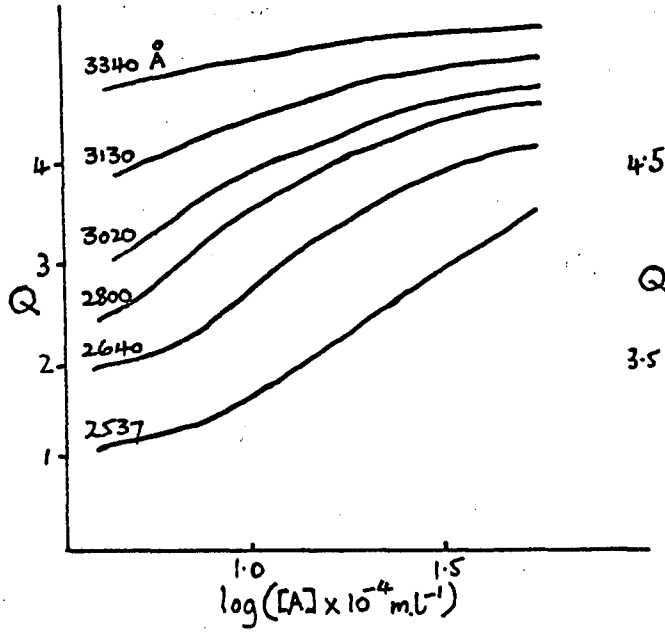

Fig. 3. Relative fluorescence yields at various wavelengths, at room temperature. (Giacometti, Okabe and Steacie).

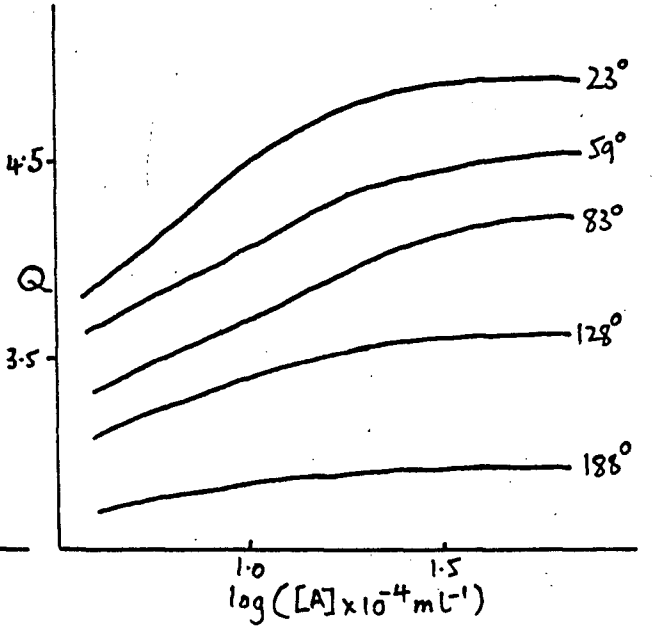

Fig. 4. Temperature variation of the relative fluorescence yield with 3130 Å excitation. (Giacometti, Okabe and Steacie).

molecule could no longer dissociate:

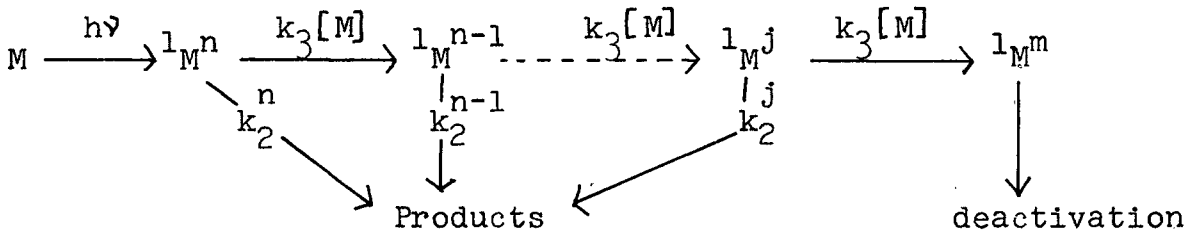

Indices m, n and j are measures of vibrational energy in units of the energy lost per collision.

Application of steady-state assumptions for all intermediate species gave the equation:

$$\phi = 1 - \prod_{i=m+1}^{n} \left[\frac{1}{1 + \frac{a_i}{[M]}} \right] \qquad (1.6)$$

Where $a_i = k_2^i / k_3$. Expression 1.6 compares with the single-stage deactivation relationship, equation 1.1, above.

To construct theoretical curves in accordance with equation 1.6 required further assumptions that the form of k_2^i was given by a Rice-Kassel-Ramsberger (14,15,16) type of expression:

$$k_2^i = \nu \left(1 - \frac{\epsilon_m}{\epsilon_i} \right)^{S-1} \qquad (1.7)$$

ϵ_m and ϵ_i are vibrational energies associated with states m and i (i.e. ϵ_m is the activation energy). ν is a frequency factor, and S is the number of non-degenerate vibrational modes of the molecule. Definitions of ν and S, and the values to be assigned, vary from author to author, but the form of equation 1.7 is common.

Plotting $1/\phi$ vs. [M] then gave curves which were concave upwards at low pressures, and became linear at higher pressures (Fig. 5). Values for ν, k_3 and S were reasonably assumed.

If triplet participation were included, then the modified expression was

$$\phi = 1 - (1 - \phi^{\infty}) \prod_{m+1}^{n} \left[\frac{1}{1 + \frac{a_i}{[M]}} \right] \qquad (1.8)$$

with $1/\phi$ vs. [M] now sigmoid in shape (Fig. 6).

Precise measurements were subsequently made on the primary dissociation yield of ketene in lower pressure regions (17). These did not, however, reveal any curvature in $1/\phi$ vs. [M]. From this it was tentatively concluded that not more than about three collisions were required to deactivate the molecule.

The work of Wilson, Noble and Lee (18) dealt essentially with this same idealized model, and considered whether fluorescence measurements would be helpful in investigating the collision process. Similar conclusions were reached, namely that precise data at low pressures would be required to distinguish between a strong and a weak process.

(ii) The Vibrational Temperature Concept.

A somewhat different approach to the problem of collisional deactivation has been taken by Boudart and his collaborators (19,20). Observations on the increase of relative fluorescence yields of β-naphthylamine in the presence of foreign gases, led to values for the average amount of energy transferred from the fluorescent molecule by collision. For example, using exciting wavelength of 2652 Å, the excess vibrational energy, ΔE, of β-naphthylamine was about 10,000 cm^{-1}: of this, it was calculated that 70 cm^{-1} were lost per collision with H_2, 550 cm^{-1} with CO_2, and 1240 cm^{-1} with C_5H_{12}.

Derivation of these values pivoted around the hypothesis that ΔE could be related to a vibrational temperature:

$$T_{vib} = T + \frac{\Delta E}{C_{vib}} \qquad (1.9)$$

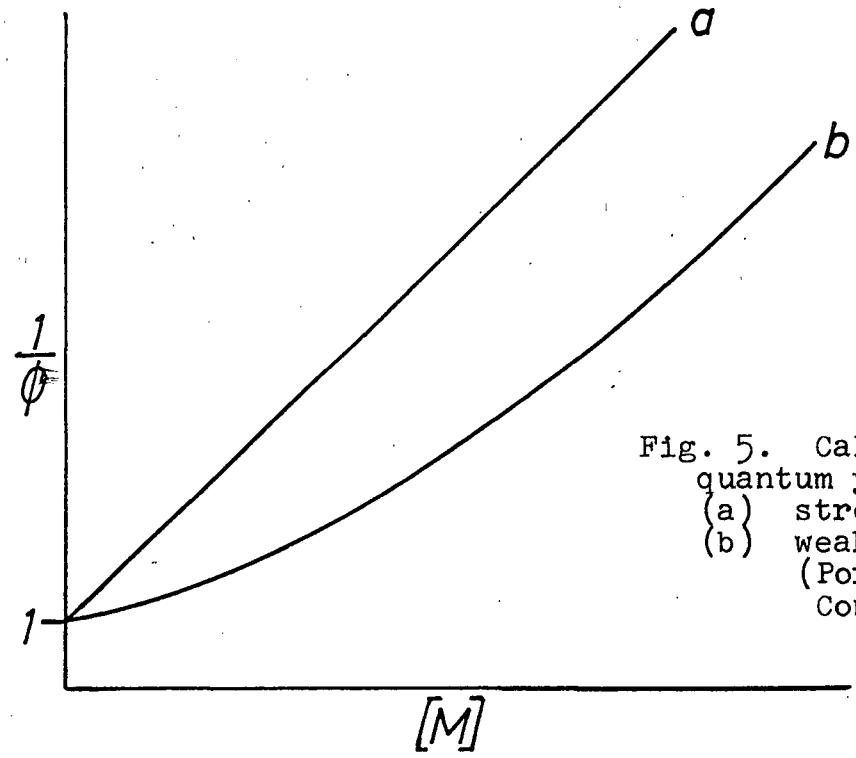

Fig. 5. Calculated quantum yields using (a) strong collisions, (b) weak collisions. (Porter and Connelly).

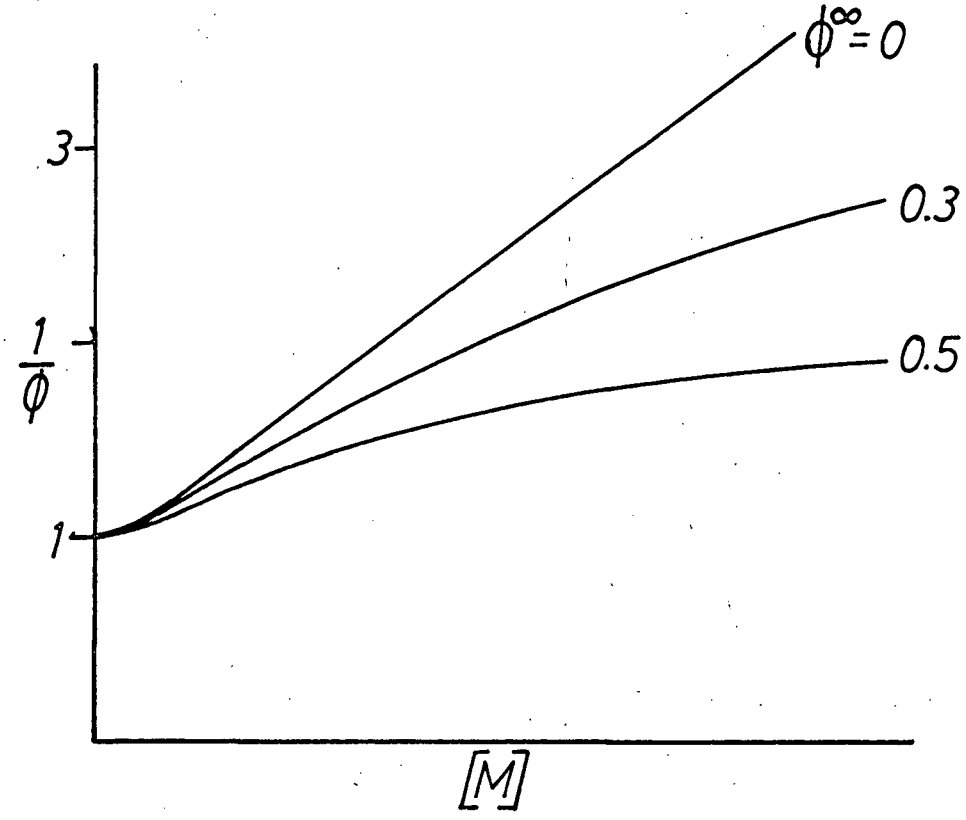

Fig. 6. Calculated quantum yields including triplet dissociation, for a weak collision model (Porter and Connelly).

with $$\Delta E = h(\nu_a - \nu_o). \qquad (1.10)$$

T is the ambient temperature, C_{vib} the vibrational heat capacity, ν_a the exciting frequency, and ν_o the height of the lowest vibrational levels of the electronically excited molecule above the ground state.

The deactivation mechanism resembled the ketene case considered above, with an excited $^1M^j$ molecule being cascaded down the vibrational scale by collisions with a foreign molecule X. The competing unimolecular processes at each stage were fluorescence and internal conversion:

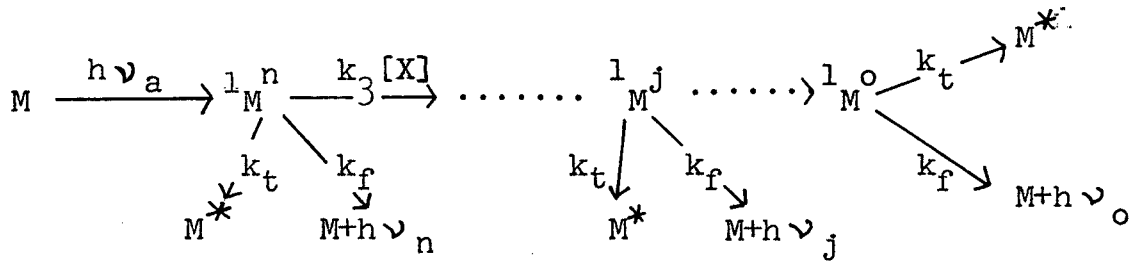

Associated with each intermediate $^1M^j$ was a vibrational temperature T^j_{vib} and a lifetime τ^j. These two parameters were related by a smooth curve obtained from quenching data at a number of wavelengths. Loss of vibrational energy would increase the lifetime of an excited molecule and account for the enhancement of relative fluorescence yield, Q, with increasing amounts of inert gas. The scheme gave an explicit but complicated relationship:

$$Q = f(\tau^j, k_3, [X]) \qquad (1.11)$$

which reduced to

$$\frac{dQ}{d[X]} = k_3(\tau^{n-1} - \tau^n) \qquad (1.12)$$

T^n_{vib} and hence τ^n were evaluated using equations 1.9 and 1.10, so that observations of the initial slope of Q vs$[X]$ plots allowed an estimate to be made of E, the energy lost per collision:

$$E = C_{vib}\,(T^n_{vib} - T^{n-1}_{vib}).$$

The use of the vibrational temperature concept in this way has provoked some comment (20). By definition, a temperature is assigned to a group of molecules in a canonical ensemble (i.e. thermally equilibrated). Such a distribution is itself the result of continual collisional encounters, so there is some doubt about the validity of applying equation 1.9 to molecules which have still to undergo <u>inter</u>molecular energy relaxation by collision.

Rapid <u>intra</u>molecular energy redistribution (which may make it allowable to define some sort of internal "temperature" of the vibrators within a molecule), is quite a distinct problem, and closely allied to the rate of spontaneous dissociation.

(iii) Excitation by Non-Photochemical Techniques.

It has been possible to study the kinetics of complex molecules with a large excess of vibrational energy using methods of excitation other than irradiation in the near ultraviolet region. Mass spectrometry has been used to investigate the unimolecular dissociation of molecule-ions produced either by photo-ionization (21) or electron impact (22). Much attention has been given, for example, to the photoionization of alkanes.

$$C_2H_6 \xrightarrow[1000\ \text{Å}]{h\nu} C_2H_6^+ \longrightarrow \text{fragmentation}$$

Unlike the photochemical case, concentrations are small enough ($\sim 10^{-2}$ mm) for the competing collisional process to play no important part.

Such studies were largely stimulated by the quasi-equilibrium theory (23), broadly analogous to the transition-state theory in conventional kinetics. The vibrational energy (E to $E+\Delta E$) of the molecule-ion is postulated to be rapidly randomized amongst the various degrees of freedom, by numerous radiationless transitions between a large number of potential surfaces (electronic states). If the ion consists of N loosely coupled harmonic oscillators, frequency

ν_i, and the activated complex N-1 oscillators, ν_j ; then specific rate constant for dissociation is

$$k(E) = \left(\frac{E - \epsilon_o}{E}\right)^{N-1} \prod_{i=1}^{N} \nu_i \Bigg/ \prod_{j=1}^{N-1} \nu_j \qquad (1.13)$$

Here ϵ_o is the potential energy of the activated complex - the activation energy. The quasi-equilibrium theory also led to a more detailed expression taking into account internal rotations.

Equation 1.13 is formally analogous to the RKR (page 17) and Slater (24) expressions, but whereas these started with the premise that dissociation was from a thermally-equilibrated population, the quasi-equilibrium theory assumes an initial microcanonical ensemble. It is noteworthy that such similar forms for $k(E)$ have resulted from considering completely different models.

The original form of the quasi-equilibrium theory largely failed to account for the observed rate constants, especially at low excitation energies, unless an arbitrary fraction of the total number of oscillators be employed. This has been taken to mean that complete randomization of

of the excess energy does not occur. (Apparent non-participation of every normal mode is of course a familiar problem in many thermal dissociations).

A more recent treatment (25) has shown that some of the difficulties are resolved if the unimolecular formulation of Marcus is used (26,27).

Rabinovitch and his collaborators have done extensive investigations on both decomposition and collisional stabilization of radicals and molecules, produced by chemical reaction with a large excess of vibrational energy (28,29,49). Thus the sec. butyl radical formed by addition of a hydrogen atom to cis-butene has 45 kcal/mole of excess energy. Subsequent competition between dissociation (D) and stabilization (S) of the hot radicals was studied by measuring the relative amounts of products formed by the two reactions. The theoretical expression for the observed dissociation constant, k_a was

$$k_a = \omega \cdot \frac{D}{S} = \frac{\omega \int \frac{k(E)}{k(E)+\omega} \cdot f(E)dE}{\int \frac{\omega}{k(E)+\omega} \cdot f(E)dE} \quad , \qquad (1.14)$$

where ω is the second-order constant for stabilization. $f(E)$ is the calculated energy distribution function for the

excited radicals. The model predicted that an increase in k_a at low pressures would be evident if energy was lost by a weak, rather than a strong, collision process. No such increase was observed down to .005 mm pressure, and it was concluded that deactivation occurred in large steps of at least 11 kcal/mole per collision. Rate constants, and their energy dependence, were calculated according to the Marcus theory, using a quantum statistical formulation for f(E). Such calculations have generally given a very fair measure of agreement with observed values in such systems.

The hypotheses and results of work done in these related fields bear closely on the problems involved in understanding photochemical dissociation.

(iv) Transfer of Electronic Energy.

The transfer of electronic energy from one excited ketone (or aromatic hydrocarbon) to a second is now a well-established phenomenon. One example taken at random, is the sensitization of biacetyl (short-lived) fluorescence by benzene, in oxygenated cyclohexane solution (30).

$$C_6H_6 \xrightarrow{3130\ \text{Å}} {}^1(C_6H_6) \xrightarrow{Ac_2} {}^1(Ac_2) + C_6H_6$$

$$\downarrow \qquad\qquad \downarrow$$

$$C_6H_6 + h\nu \qquad\qquad Ac_2 + h\nu$$

The benzene fluorescence is sharply quenched in the presence of even a small amount of biacetyl. Oxygen is necessary in this case to quench any triplet species: the long lived phosphorescence from triplet biacetyl would completely mask the fluorescence.

Inter-triplet energy transfer is also common and has been reported for many donor-acceptor pairs over a wide variety of conditions. The energetic requirement is that the acceptor triplet state be lower than that of the donor. Biacetyl is frequently used as an acceptor, chiefly because of the high yield of emission from its triplet state, observable even in solution, and also because biacetyl itself does not absorb appreciably at the most convenient mercury line (3130 Å). Flash photolysis techniques have enabled energy transfer to be studied by measuring the triplet absorption spectrum of both donor and acceptor, even in the absence of emission.

The value of this phenomenon to studies of the primary process in gases is considerable, for in principle it allows one to investigate either triplet or singlet reactions selectively. Hitherto there have been few attempts to measure primary dissociation yields under such conditions, but there are a number of instances where change in emission yields of

a donor ketone have been observed in the presence of biacetyl. An important point in a given case is whether singlet-singlet or triplet-triplet transfer is the major reaction. This can be decided, for example, by measuring relative yields of emission from a constant concentration of donor, with increasing concentrations of biacetyl. In the case of triplet-triplet interaction only, the donor yield decreases up to a certain concentration of biacetyl and then remains constant when only singlet-emission remains. This is the case for acetone-biacetyl (32,33), and 3-pentanone-biacetyl (34). Where no inter-triplet exchange is observed (e.g. in 2-pentanone-biacetyl (35)), it is doubtful whether the triplet state plays any appreciable part in the primary process of the donor molecules.

The Purpose of this Investigation

Although the ketene experiments described above had not revealed evidence for a multistage deactivation process, the situation with HFA was more promising, because the data of Ayscough and Steacie showed that $1/\Phi$ vs[A] plots extrapolated back to well below unity at zero pressure, at both wavelengths studied. It was therefore decided to make more precise measurements of the primary quantum yield at lower pressures, and hence detect any curvature in these plots,

from which details of the collisional process could be elucidated. This would require drastic assumptions about the competing rate of decomposition, on the basis of existing unimolecular theories.

On the other hand, if it were found that complete deactivation apparently occurred at every collision, then by using a number of different exciting wavelengths, an attempt could be made to correlate the observed rate constants, $k_2(\lambda, T)$, and assign an activation energy. Furthermore the simplicity of the products might allow complementary studies to be made of both dissociation and sensitized emission, from HFA-biacetyl mixtures under suitable conditions.

It was felt that evidence for triplet state participation in the photolysis of HFA would be more convincing if phosphorescence were to be observed. This might be recognized by working at low temperatures (e.g. -78°), where thermal dissociation of the triplet state should be completely suppressed.

EXPERIMENTAL ARRANGEMENT AND PROCEDURE

Materials.

Starting materials and products were manipulated in a conventional all-glass vacuum system, evacuated by a standard oil pump and a single-stage mercury diffusion pump. Stopcocks were greased with Apiezon L.

Hexafluoroacetone hydrate, supplied by Merck (Canada), was dehydrated in vacuo, by passing it through phosphorus pentoxide: unchanged hydrate was condensed out by two dry-ice traps, and the ketone collected in a liquid nitrogen trap. The hydrate was re-circulated a number of times. The IR spectrum of a sample of the ketone thus prepared showed no band in the $-OH$ region. It was stored in a blackened 5-litre bulb, and samples used were outgassed by two trap-to-trap distillations and then pumping on the ketone at -196° for one hour. With larger samples (i.e. for a run at higher pressure), reproducible results could only be obtained by outgassing for about one hour in a LeRoy-Ward still (36) at -125°: the ketone being subsequently collected at -110°. Later in the work, HFA gas supplied in a cylinder by Allied Chemicals became available: this was subjected to a similar LeRoy-Ward fractionation before irradiation, and gave essentially the same results.

Eastman-Kodak biacetyl was fractionally distilled on the vacuum line and a middle fraction taken for use.

Oxygen was prepared by heating AR potassium permanganate and used without further purification.

Initial pressures of reactants were measured with a mercury manometer. For pressures of HFA below 1 cm Hg a pump-oil manometer proved reliable, and did not appear to absorb the gas.

Optical Arrangement.

For photolyses at wavelengths shorter than 2850 Å a mercury-argon compact arc was employed (Hanovia D517-A). At longer wavelengths the B.T.H. Type ME-D medium pressure mercury lamp was satisfactory. The output from both of these lamps underwent rapid fluctuations of up to 5%, about a mean value, but was approximately constant over the period of a run: since simultaneous actinometry was always performed, this was a matter of convenience rather than necessity.

The particular source in use was focussed by a quartz lens on to the entrance slit (1 mm) of a diffraction grating monochromator (previously constructed in this laboratory). The divergent light emergent from the exit slit (1 mm) was focussed to a parallel beam 1 cm in diameter, which

passed through a Corning 9863 glass filter, along the axis of the reaction cell, and on to the actinometer, without touching any of the side walls (Fig. 7). In this way no light was lost by edge effects. Since the quantum yield measured was intensity independent, steady-state assumptions were not violated by light not filling the cell(37).

The spectral characteristics of the "monochromatic" radiation used in photolysis were ascertained using a second (Bausch and Lomb) grating monochromator, placed at the exit slit of the first. Emergent light from this analyser fell on to an RCA 935 photocell in conjunction with a 2000 μV recorder. The line shapes are summarized in Fig. 9. The half-widths could only be bettered at the expense of considerable intensity, and this last factor determined the practicability of quantitative photolysis under most conditions.

Reaction Cells.

Cylindrical reaction vessels were of pyrex, with quartz windows whose transmission properties at various wavelengths had been measured before attachment to the cell with 'Araldite' resin cement. Four cells, each fitted with a side-arm for condensation, were constructed, with dimensions 4 and 122 cms length (2 cms diameter); 14 and 46 cms length

(4 cms diameter). The 4 cm cell was T-shaped with a third quartz window through which emission could be recorded.

For runs at room temperature, these cells were simply blackened on the outside and used without further thermostatting. The earlier work (5) on HFA had shown that the quantum yield was not very sensitive to the $\pm 1.5^{\circ}$ temperature variations which occurred in the room. For work at -78°, after several unsuccessful attempts to use a flow system for cooling, the reaction cell (Fig. 7), with evacuated guard tubes on either end, was enclosed in an aluminium casing insulated by a 1 cm layer of paraffin wax and 2 cms of "Polyfoam" foam plastic. The casing could be filled with pulverized dry-ice, which was frequently stirred and topped up during the course of a run to ensure continued thermal contact with the cell walls. The resin cement with which the cell windows were affixed remained efficient at this temperature.

Gas Analysis.

The contents of the reaction cell at the end of a run were allowed to flow through two successive traps at -196° (liquid N_2). These condensed out C_2F_6 and unchanged HFA, and carbon monoxide was measured as the only non-condensable

product, on a calibrated McLeod-Toepler gauge. One re-evaporation of the condensed products was necessary to release occluded CO. In one run the non-condensable product was dosed into the silica-gel column of a Perkin-Elmer 104 gas chromatograph. The CO peak was identified as constituting more than 99% of the product.

Actinometry.

The potassium ferrioxalate actinometer of Hatchard and Parker (38) was used for all quantitative runs. The quartz actinometer cell, diameter 4 cm, depth 1 cm, was placed immediately behind the reaction vessel. Optical densities of exposed and developed solutions were determined on a previously calibrated Unicam 500 spectrophotometer, at 510 mμ. The usual blank correction was made with unexposed solution, and significant mis-matching of spectrophotometer cells was also taken into account.

Measurement of Absorption Coefficients.

Before commencing photolysis at a particular wavelength, the absorption of the ketone at that wavelength was measured, over the range of pressures to be studied, using the photocell and recorder. HFA could be almost instantaneously frozen down in the side-arm of the cell, so that successive recorder readings I_t(cell full), I_t(cell empty) were

made rapidly enough to minimise errors due to fluctuation of lamp intensity. A mean of several such determinations was taken at each pressure.

Where the absorption of the gas in the cell to be used for photolysis was greater than about 7%, this could be accurately determined by the method described. For smaller absorptions - generally at gas pressures below 10 mm - a longer cell was used, and a Lambert's-Law extrapolation invoked for subsequent quantum yield determinations. The validity of this is discussed below (page 41).

Reflection Corrections.

If all reflection and absorption by reaction vessel and actinometer cell windows is neglected, there is introduced an error of about 20% in an experimental quantum yield. Corrections must be made with great care to eliminate this effect (39).

For a quartz window, the fraction α of a beam, reflected at each interface, can be calculated from the refractive index for any wavelength. The theoretical transmission may then be compared with the experimentally determined transmission to see if β , the fraction of a beam absorbed by a window is appreciably non-zero.

For the full correction, we have to find the total light absorbed (I_a), knowing both the total light transmitted into the actinometer solution (Fig. 10), and γ, the fraction absorbed by HFA during a single passage of the beam.

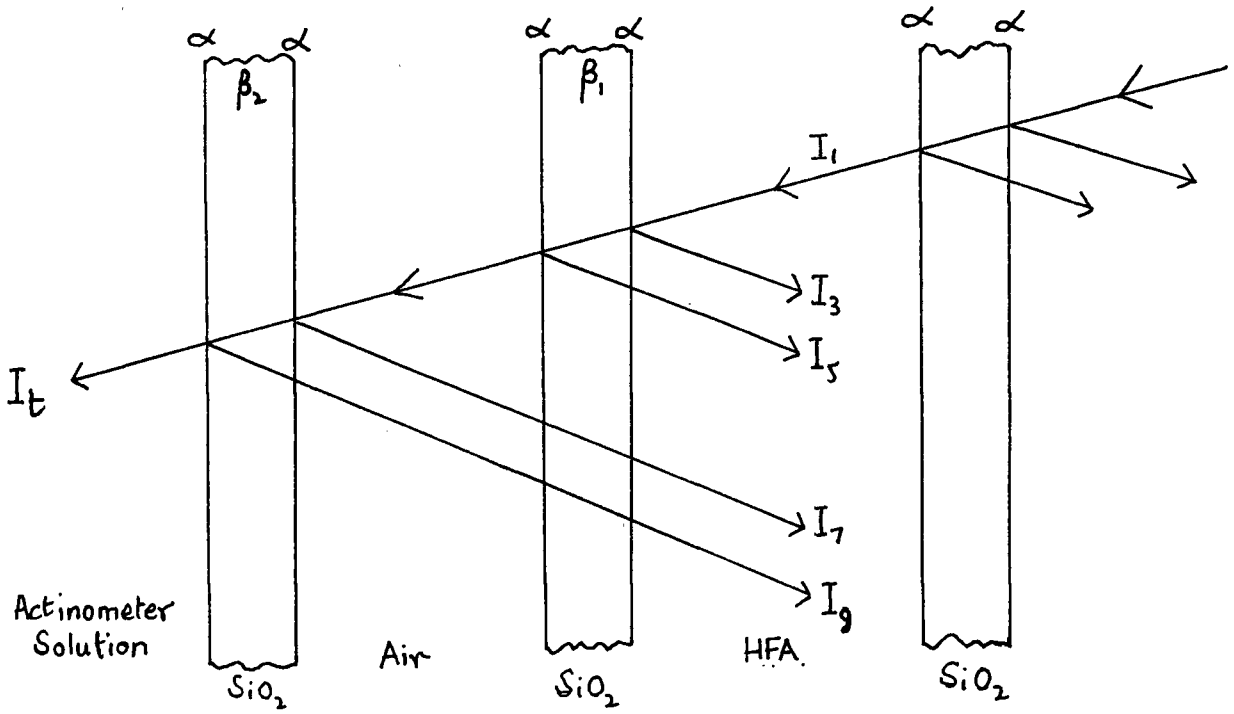

Fig. 10. Reflection at quartz windows.

Thus, using the value of α appropriate to 3130 Å, the correct relationship is

$$I_a = I_1+I_3+I_5+I_7+I_9 = \frac{1.17\,\gamma\,I_t}{1-\gamma}\left[1 + 0.14(1-\gamma)\right] \qquad (2.1)$$

It was found, that β_1 and β_2 only had appreciable values ($\sim$1.5%) at the shortest wavelength, 2652 Å. This was allowed for by a further small correction in equation 2.1.

Fluorescence Spectroscopy.

Fig. 8 shows the arrangement used for observing emission spectra. With the lamp-monochromator combination used in photolysis, it was difficult to obtain a suitably steady exciting intensity: this was overcome by using the more compact Bausch and Lomb grating monochromator with an Osram HB200 medium pressure source, which could be moved much closer to the cell.

Approximately parallel incident radiation passed through the cell, whose T-arm faced the entrance slit of a Hilger f/4.4 D285 spectrometer, with glass optics. Fluorescent light emergent from the spectrometer fell on to an RCA 7265 photomultiplier tube. Emission spectra could be recorded from 7000 - 3800 Å by means of an automatic scan

which took about six minutes. (Hence the need for a steady exciting intensity over this time). The spectrometer slit widths were kept constant at 750 μ for all spectra.

When it was desired to make quantitative comparisons of total emission (e.g. before and after adding oxygen), the cell was not moved in between scans. Corrections were applied for variation in spectral response of both photocell and photomultiplier. Allowance was also made for variation in the dispersion of the D285 spectrometer over the wavelengths recorded. The manufacturers specifications were used in considering these corrections.

A photographic method, using Kodak 103F plates and a small Hilger f/8 D182 spectrometer gave essentially the same spectra.

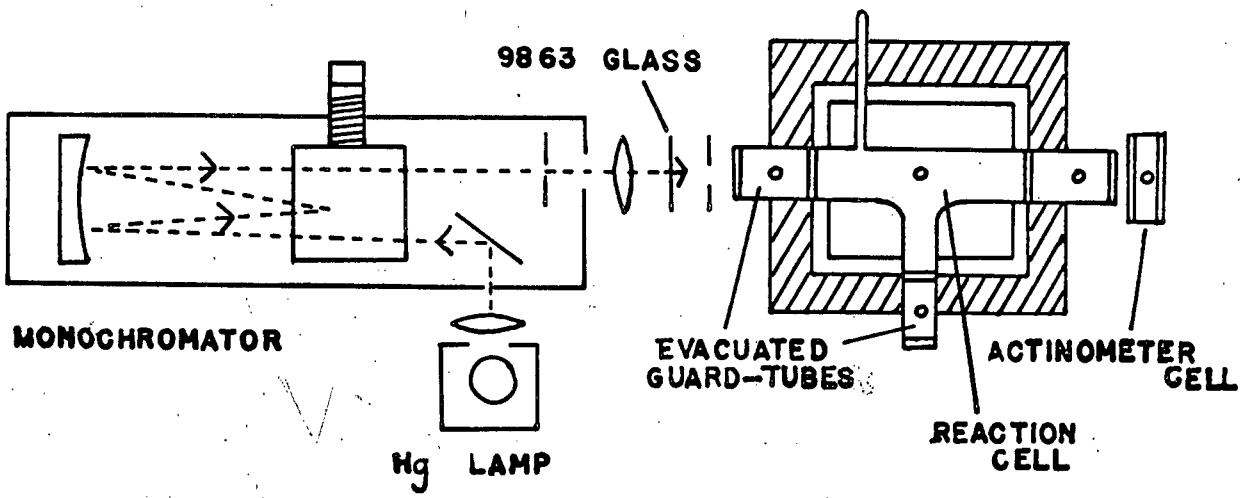

Fig. 7. Optical arrangement for photolysis, and the low temperature cell.

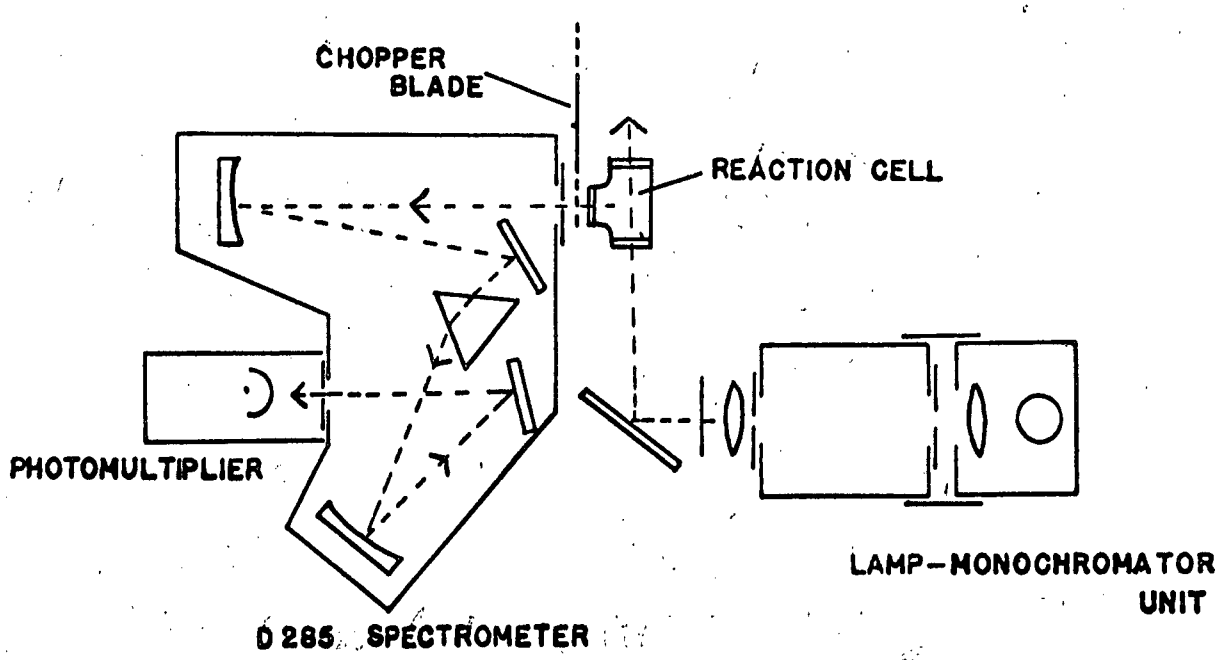

Fig. 8. Optical arrangement for recording emission spectra.

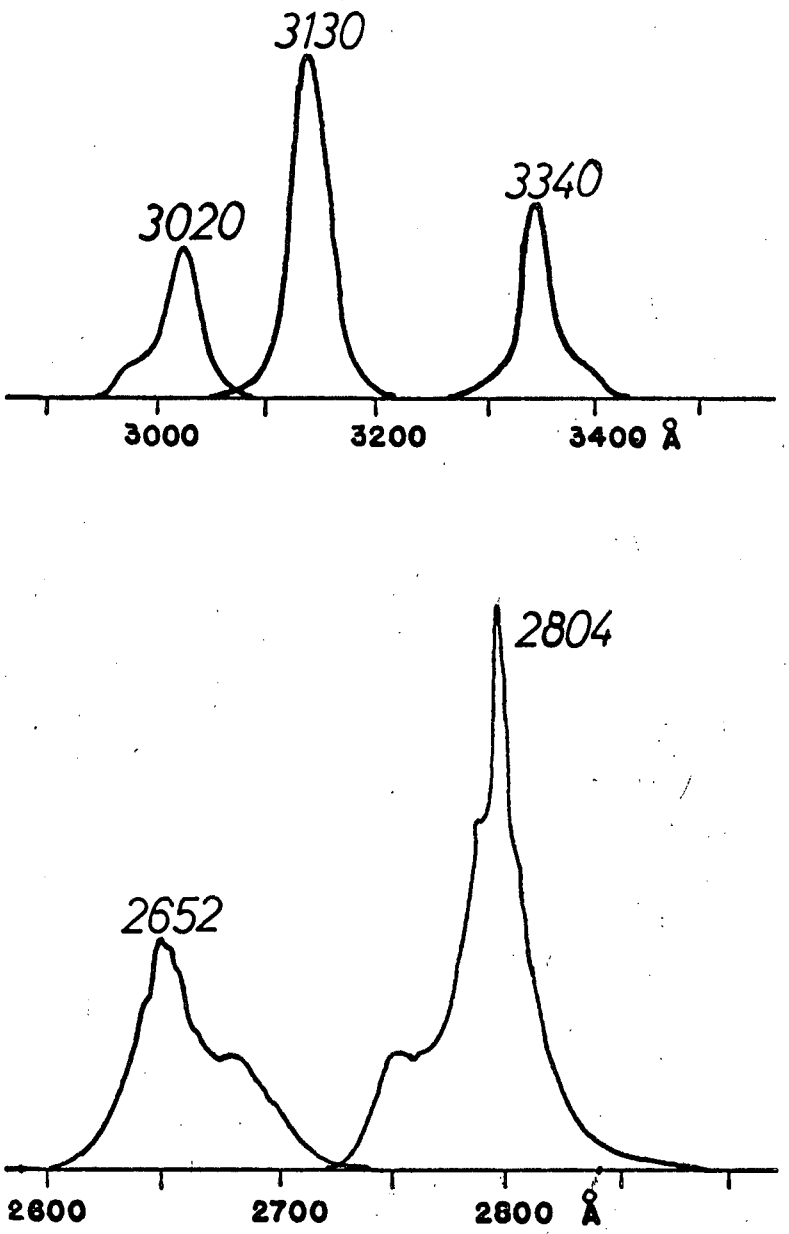

Fig. 9. Spectral characteristics of the wavelengths used for photolysis. Relative intensities have no significance.

RESULTS

Absorption.

Table 1 lists the mean molar absorption coefficients, found by measuring the percent transmission over a range of pressures, by the method described above. In general, unless the absorption coefficient ε is truly constant over the spectral width of the exciting radiation, neither Beer's nor Lambert's Laws can be expected to hold exactly (37). A structured absorption spectrum in the region of excitation could lead to quite marked deviations.

Fig. 12 shows the first absorption band of HFA. The apparent lack of structure could indicate either a true continuum, or a superposition of many vibration-rotation lines. The former is perhaps unlikely, since it carries the implication of direct transition to a repulsive upper state, in which case the quantum yield would most likely be independent of exciting wavelength.

However, for pressures below 10 mm no deviations from Beer's Law were observed at any wavelength. We may thus reasonably assume that Lambert's Law will also hold for this pressure range. On this basis, the fractional absorptions, γ, under photolysis conditions at low pressures were calculated, from values at similar pressures, but measured

in a longer cell.

In an intermediate pressure range, where measurements could be made at several path lengths, Lambert's Law was indeed found to hold. In fact, at 3340, 3130 and 2652 Å, Beer's Law was also obeyed up to the highest pressures studied. Small high-pressure deviations at 3020 and 2804 Å did not introduce any error, since the absorption was measured directly, rather than by extrapolation.

These points are illustrated by a typical case, (Fig. 11) where the absorption of 1 cm length of gas has been calculated from values obtained using cells of various length.

Photolysis at 25°.

The exposure time for a run at room temperature varied from 15 minutes to 27 hours, and was generally around 2 hours. At low absorptions, this time was determined by the minimum amount of CO which could be measured on the McLeod gauge ($\sim 0.8 \times 10^{-7}$ moles). At high absorptions, the smallest amount of transmitted radiation which could be recorded with a developed actinometer solution determined the exposure time. In all runs, less than 2% of the HFA was decomposed.

The parameters measured in each run could be easily combined to give Φ_{CO}:

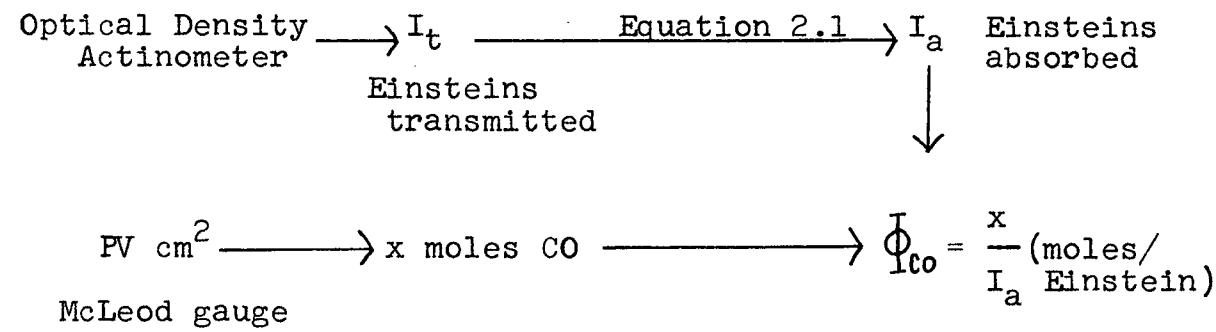

The results are presented in Tables 2, 3, 5, 6, and 7.

Low Temperature Photolysis.

A measured pressure of HFA was dosed into the low temperature cell before it was cooled. After adding the dry-ice, the gas was allowed to cool 20-30 minutes before exposure. About 4 hours irradiation then gave a minimum amount of CO. The analysis involved transferring the cell contents at -78° to liquid nitrogen traps through connecting tubing at room temperature.

It was noted that a thermocouple, suspended at the axis of the cooled cell registered only -60° eventually, even when the cell was filled with air. This may have been due to heat conduction along the thermocouple wires, but uncertainty in the exact temperature during the runs must be borne in mind as a possible source of error.

Table 4 shows the CO yields at this temperature: the range of concentration is limited by the S.V.P. of HFA at -78° (about 30 mm).

Photolysis of HFA-biacetyl mixtures.

Measured samples of HFA and biacetyl were outgassed and dosed into the reaction cell separately. Biacetyl pressures were arbitrary between 0.2 - 0.4 mm, and 15 minutes allowed for mixing before exposure. The presence of a trace of biacetyl did not affect the absorption of HFA, while the absorption of biacetyl itself was negligible for HFA pressures above 3 mm (3130 Å) and 10 mm (3030 Å).

Table 8 lists the quantum yields.

Reliability of the Photolysis Data.

Experimental quantum yields are notoriously prone to large random and systematic errors.

Chief sources of random error were in measuring optical density, and in reading manometers and the McLeod gauge. In the method used here, temperature fluctuations would also constitute a random error, but absorption measurements, taken from a smoothed curve, would not.

These random errors are fairly reflected in the scatter of points on $1/\phi$ vs. [A] plots (e.g. Fig. 18), and at low pressures amount to about $\pm 2\%$. At higher pressures the scatter is larger, $\sim \pm 10\%$. This is partially due to the fact that ϕ is more sensitive to temperature fluctuations in this region.

The fact (page 63) that $1/\phi$ vs. [A] plots extrapolate back to give $\phi^{o} = 1.00 \pm .03$, at the three shortest wavelengths, is some indication that no large systematic errors have appeared. This is readily apparent from the discussion on page 67. The point is that a value of ϕ^{o}, constant at several short wavelengths, of significantly different from unity, would definitely suggest systematic error. That this is not the case is consistent with accurate values for (a) reflection corrections, (b) the literature value for the quantum yield of potassium ferrioxalate, (c) absorption coefficients under the experimental conditions, (d) calibration factors for the spectrophotometer and various pressure gauges.

Emission Spectra: Hexafluoroacetone.

Typical emission traces as recorded are reproduced in Figs. 15, 16 and 17.

The band at 25° extends from below 3800 Å (lower limit, glass prism spectrometer), to at least 7000 Å (upper limit, photomultiplier sensitivity), with a broad maximum between 4500 and 4900 Å. Addition of a few mm of oxygen decreases the intensity considerably, and shifts the maximum to shorter wavelengths. No further changes occur on introducing more oxygen: it is probably that much less oxygen than was actually used completes the quenching. Several spectra were taken with ketone pressures between 30 and 150 mm: their form was essentially the same over this range.

The effect of oxygen is even more marked at -78° (Fig. 17).

Runs 1, 2 and 3 of Table 9 show relative magnitudes of the integrated intensities, found by measuring the area Δ, under the appropriate curves after correcting for instrumental sensitivity (c.f. Fig. 33 page 108).

Emission Spectra: HFA-Biacetyl Mixtures.

It was found that irradiation of HFA at 25° with 3130 Å, in the presence of small concentrations of biacetyl sensitized the strong, characteristic green emission from biacetyl. Fig. 13 shows the spectrum, taken under conditions

where dissociation measurements were also made. Because of the low concentrations used, the emission intensity was comparitively weak, and could only just be recorded above background radiation.

In Fig. 14, where much larger concentrations were used, the short wavelength end of the band could be examined more closely. It is seen that the biacetyl emission is followed by a much weaker tail extending to 3800 Å.

In run 4, Table 9, the concentrations of each component were such that the mixture absorbed radiation to the same extent at 3130 Å (due to HFA) as at 4358 Å (due to biacetyl). Hence the direct and sensitized biacetyl emission intensities (4800-7000Å) could be compared.

A comparison was also made (run 5) of the total HFA emission, with that of biacetyl emission sensitized by the same sample.

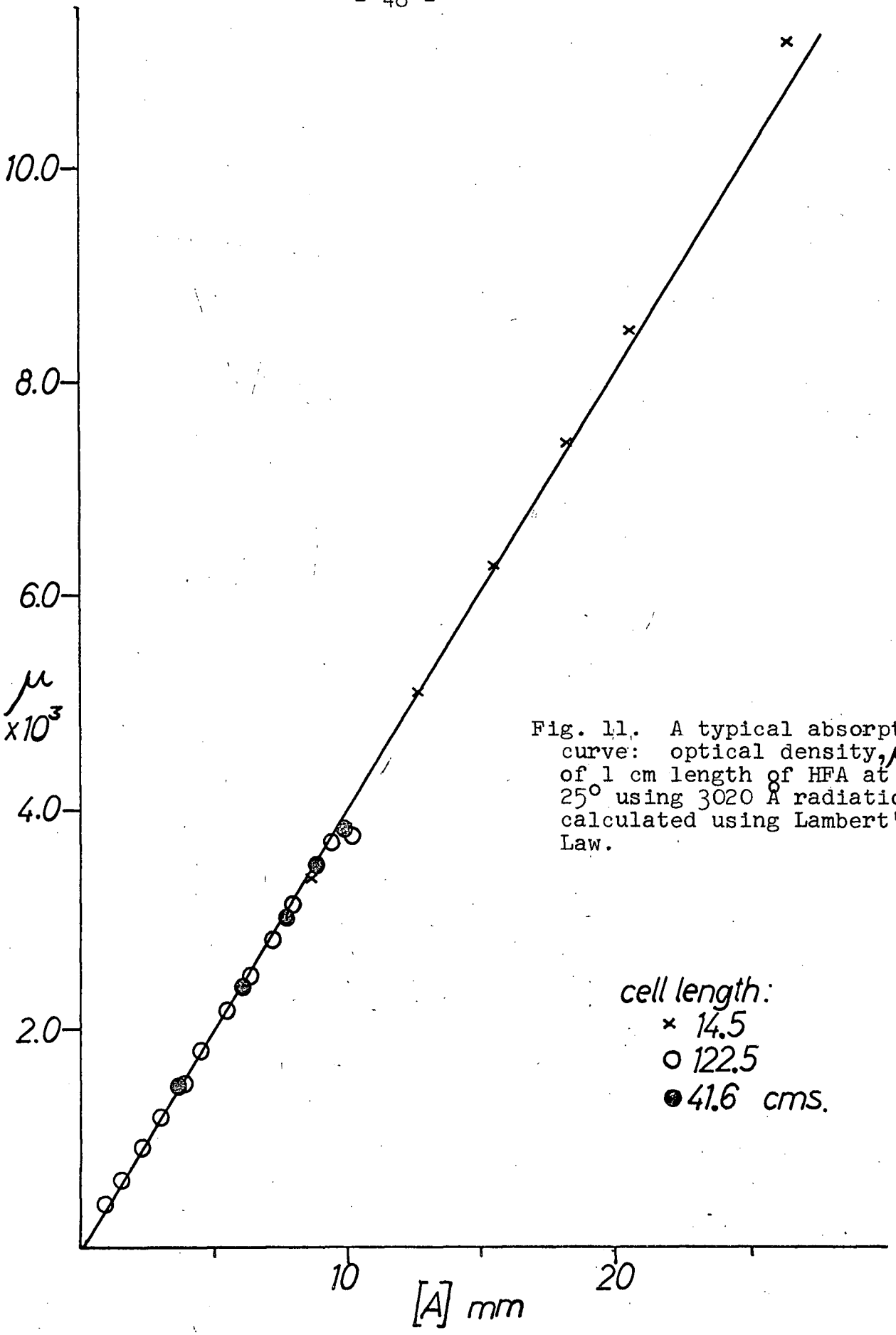

Fig. 11. A typical absorption curve: optical density, μ, of 1 cm length of HFA at 25° using 3020 Å radiation; calculated using Lambert's Law.

Table 1. Mean molar absorption coefficients at the wavelengths used in photolysis, at 25°.

λ(Å)	ε(litre mole^{-1}cm^{-1})
3340	2.27
3130 (25°)	6.93
3130 (-78°)	6.28
3020	7.54
2804	5.42
2652	3.10

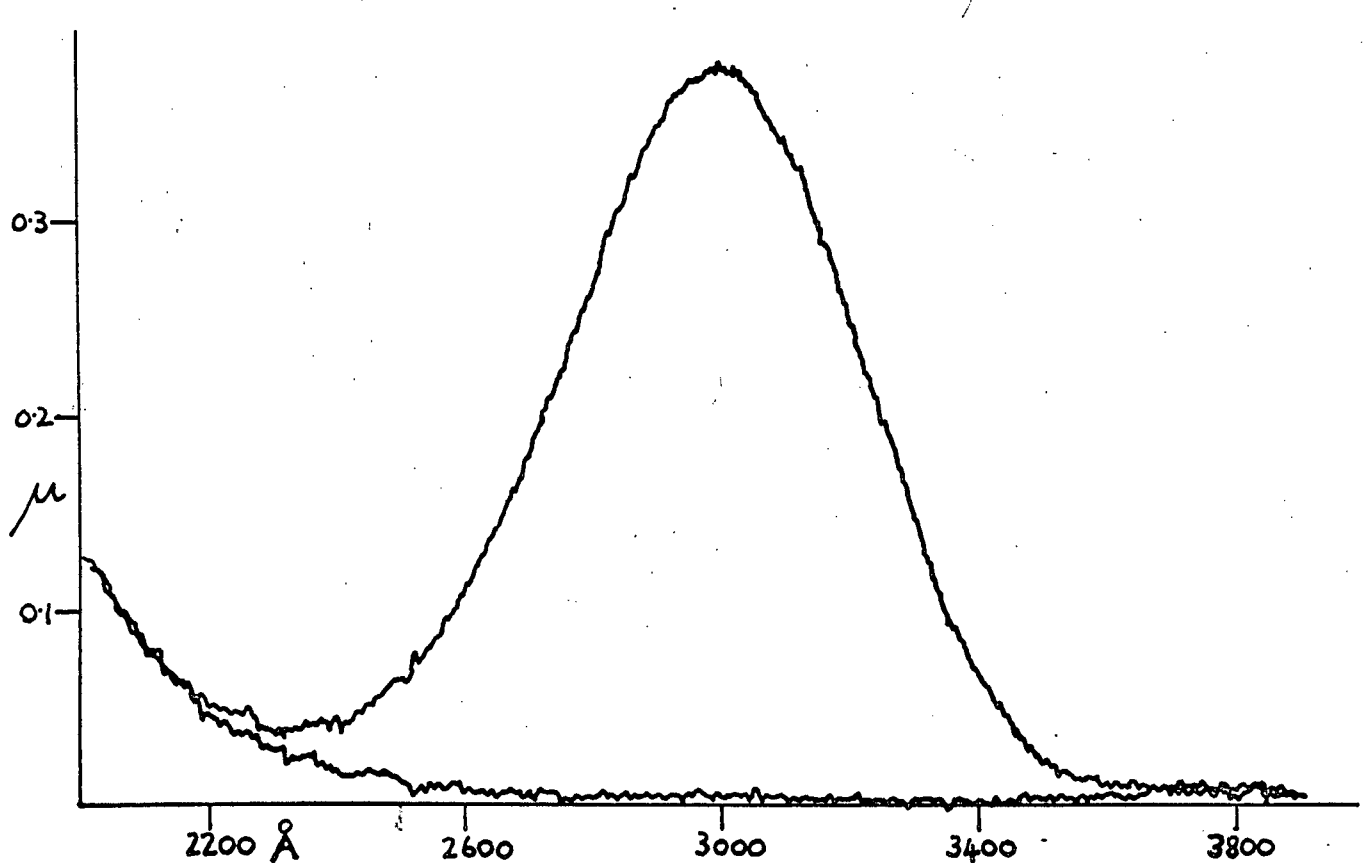

Fig. 12. Absorption band of HFA measured on CARY 14 UV spectrograph. The baseline was taken with the ketone frozen down in the cell. [A] ≃ 100 mm; 25°; 10 cm path.

TABLE 2

Photolysis of HFA at 3340 Å

Cell Length 41.6 cms; Temperature 25°C

Run No.	HFA Concentration (mm Hg.)	Φ_{CO}
144	15.7	.210
145	22.5	.202
146	3.8	.213
147	8.2	.200
148	3.6	.227
149	3.0	.223
150	12.6	.196
151	1.85	.245
152	5.4	.238
153	5.6	.220
154	1.25	.293

TABLE 3

Photolysis of HFA at 3130 Å

Cell Length 14.47 cm (pressures below 80 mm)
4.1 cm (higher pressures)

Temperature 25°C

Run No.	HFA Concentration (mm)	Φ_{CO}	Run No.	HFA Concentration (mm)	Φ_{CO}
43	4.7	.562	228	22.3	.304
44	10.3	.444	224	32.7	.319
45	8.5	.453	221	44.0	.280
47	1.5	.704	225	54.9	.265
48	3.1	.610	222	68.7	.264
49	0.73	.769	257	127.7	.189
50	5.95	.550	259	152.5	.217
51	8.6	.470	261	170.0	.216
52	6.1	.513	262	129.5	.151
53	1.7	.719	263	119.0	.192
54	15.0	.403	264	126.0	.200
56	14.5	.407	265	98.5	.195
57	2.05	.641	265A	112.5	.189
58	11.2	.413			

TABLE 4

Photolysis of HFA at 3130 Å

Cell Length 16 cms; Temperature -78°C

Run No.	HFA Concentration (mm Hg at 25°C)	Φ_{CO}
232	14.8	.0403
235	13.2	.0410
236	10.0	.0614
237	20.0	.0273
238	5.15	.1136
239	18.0	.0296

TABLE 5

Photolysis of HFA at 3020 Å

Cell Length 14.47 cm; Temperature 25°C

Run No.	HFA Concentration mm Hg	Φ_{CO}
127	.65	.862
128	2.85	.746
129	1.10	.885
130	1.70	.833
131	2.35	.807
132	3.4	.719
133	4.75	.671
134	6.35	.571
135	7.8	.571
136	9.85	.541
137	12.85	.470
138	5.75	.610
140	14.6	.457

TABLE 6

Photolysis of HFA at 2804 Å

Cell Length: 41.6 cms (pressures below 20 mm)

14.47 cms (higher pressures)

Temperature: 25°C

Run No.	HFA Concentration (mm Hg)	Φ_{CO}	Run	HFA Concentration (mm Hg)	Φ_{CO}
160	2.70	.917	171	12.6	.662
161	1.05	.990	172	10.3	.735
162	1.55	1.00	173	10.1	.709
163	7.45	.741	174	15.6	.578
165	3.60	.877	175	13.6	.641
166	2.10	.943	175A	18.7	.529
167	.72	.971	198	51.5	.345
168	4.90	.840	200	40.6	.410
169	5.90	.813	201	29.5	.451
170	8.90	.714	202	69.7	.314

TABLE 7

Photolysis of HFA at 2652 Å

Cell Length: 41.6 cm (pressures below 25 mm)
14.47 cm (higher pressures)

Temperature 25°C

Run No.	HFA Concentration (mm Hg)	Φ_{CO}	Run No.	HFA Concentration (mm Hg)	Φ_{CO}
176	3.60	.826	194	46.4	.337
177	8.70	.719	195	62.7	.275
178	12.9	.625	196	87.6	.205
179	1.63	.909	197	121.4	.160
181	5.85	.807	270	126.7	.189
182	15.8	.614	272	14.6	.685
183	2.60	.877	272A	69.0	.305
184	9.95	.719	273	150.5	.153
185	1.57	.926	274	145.0	.180
186	4.3	.855	275	133.0	.193
187	22.9	.490	276	163.0	.173
189	11.1	.714	277	195.4	.147
190	6.85	.775			
191	18.5	.541			
192	12.6	.671			
193	20.0	.556			

TABLE 8

Photolysis of HFA/Biacetyl Mixtures

Cell Length 14.47 cms; Temperature 25°C

Concentration Biacetyl: ~0.3 mm Hg

(a) 3130 Å			(b) 3020 Å		
Run No.	HFA Concentration (mm Hg)	Φ_{CO}	Run No.	HFA Concentration (mm. Hg)	Φ_{CO}
59	11.3	.208	155	9.15	.373
60	8.00	.265	156	11.7	.316
61	5.50	.332	157	17.2	.230
63	4.80	.389	158	14.0	.283
68	3.75	.457	159	15.7	.244
70	11.0	.217			
71	6.7	.315			

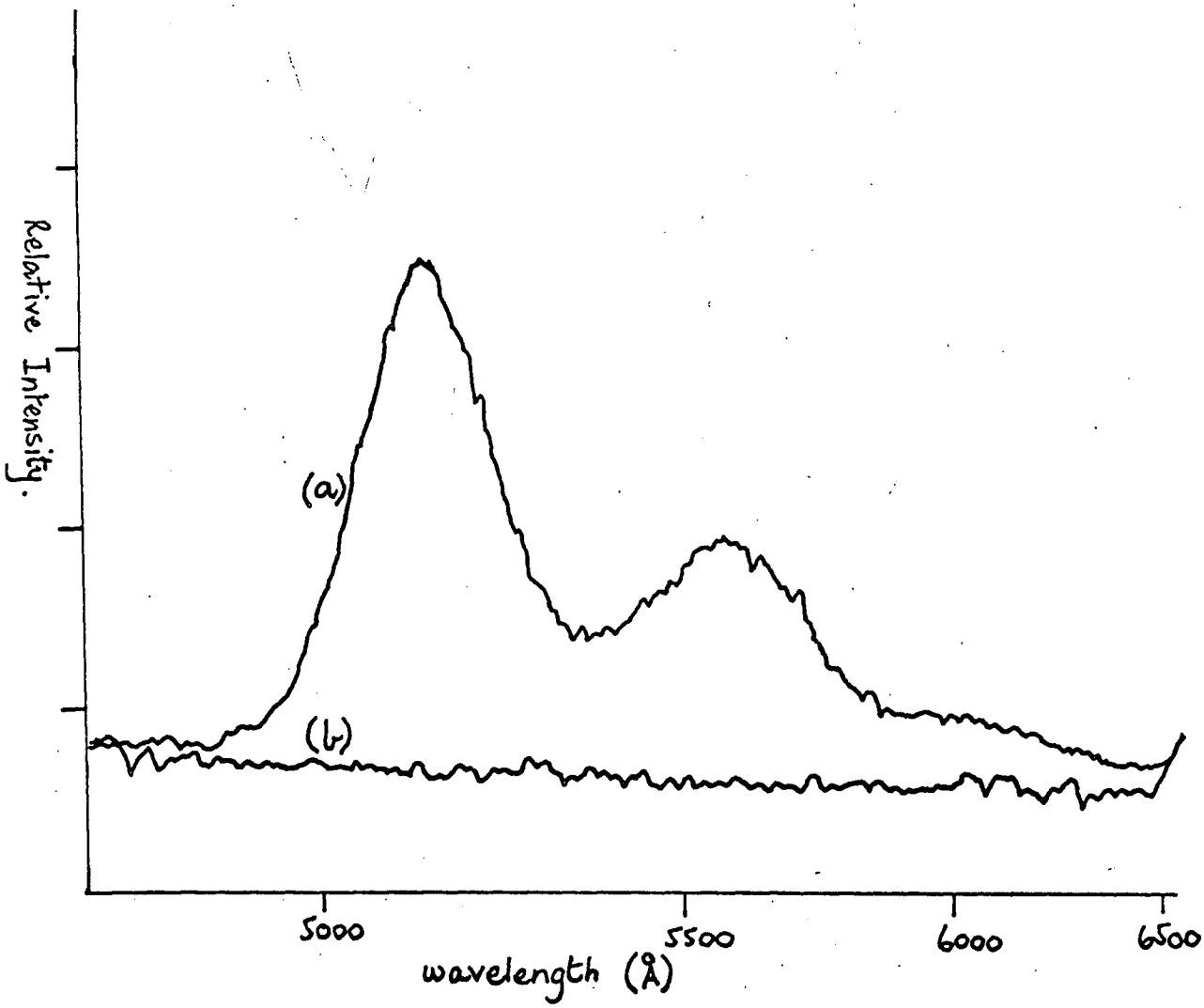

Fig. 13. (a) Emission from 3.0 mm HFA + 0.3 mm biacetyl. λ=3130 Å; T=25°.

(b) Gases frozen down; background radiation

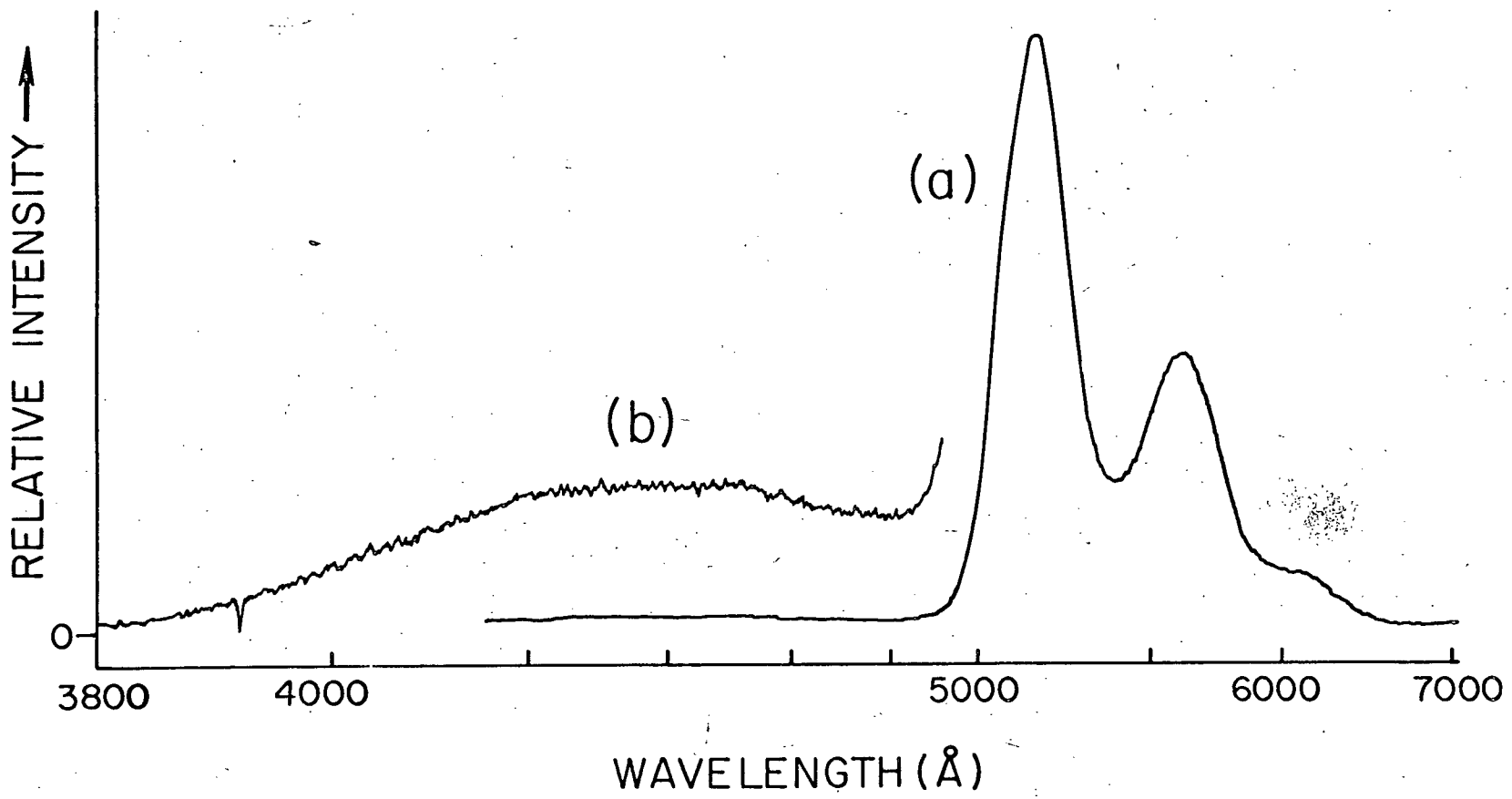

Fig. 14. Emission from 70 mm HFA + 1.3 mm biacetyl. Relative intensity of (b) has been increased by a factor of 9 compared with that of (a). λ= 3130 Å; T = 25°.

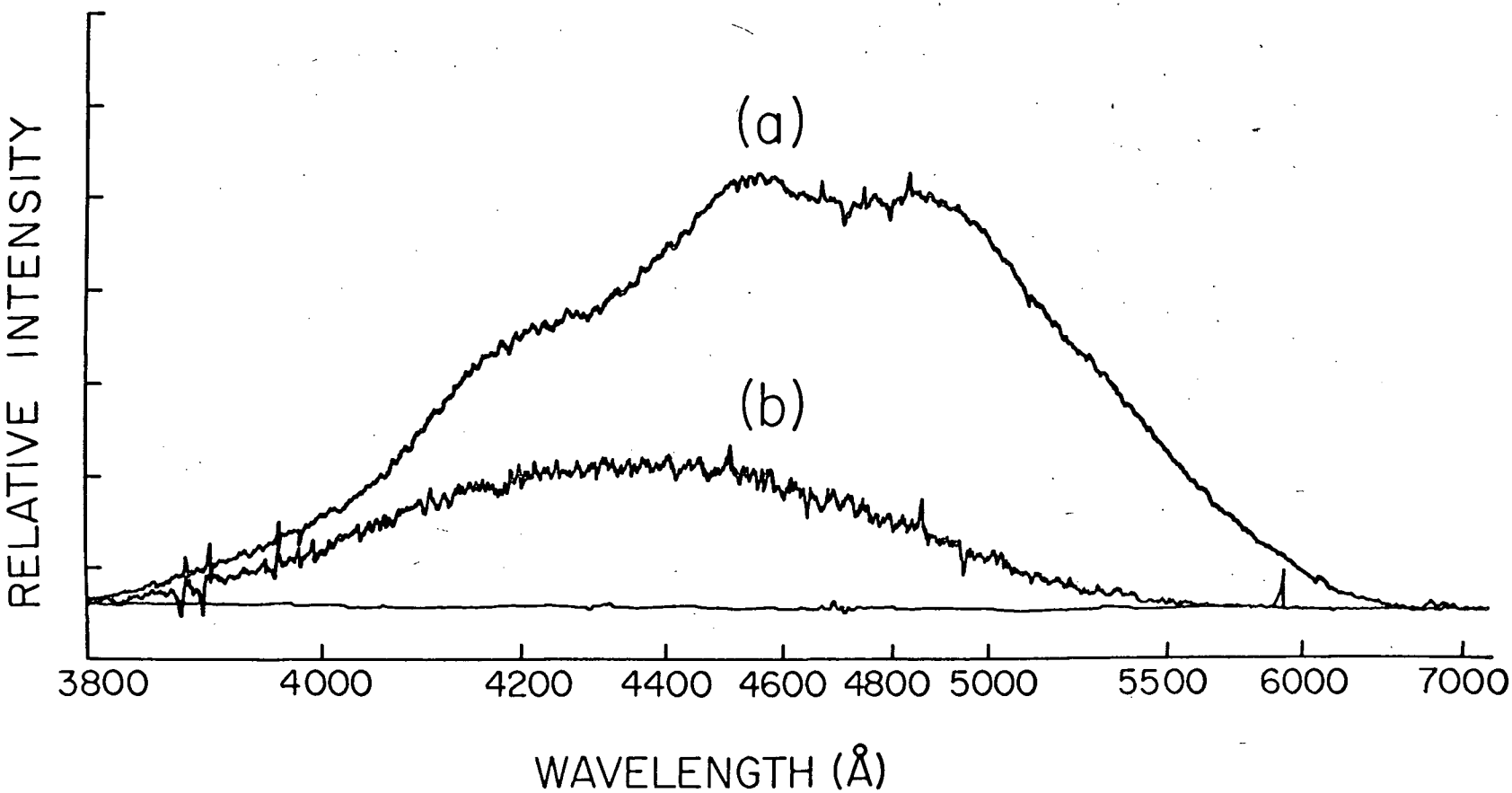

Fig. 15. Emission spectrum of HFA at 25° using 3130 Å excitation.
(a) 110 mm HFA alone.
(b) After adding 1.9 mm O_2.

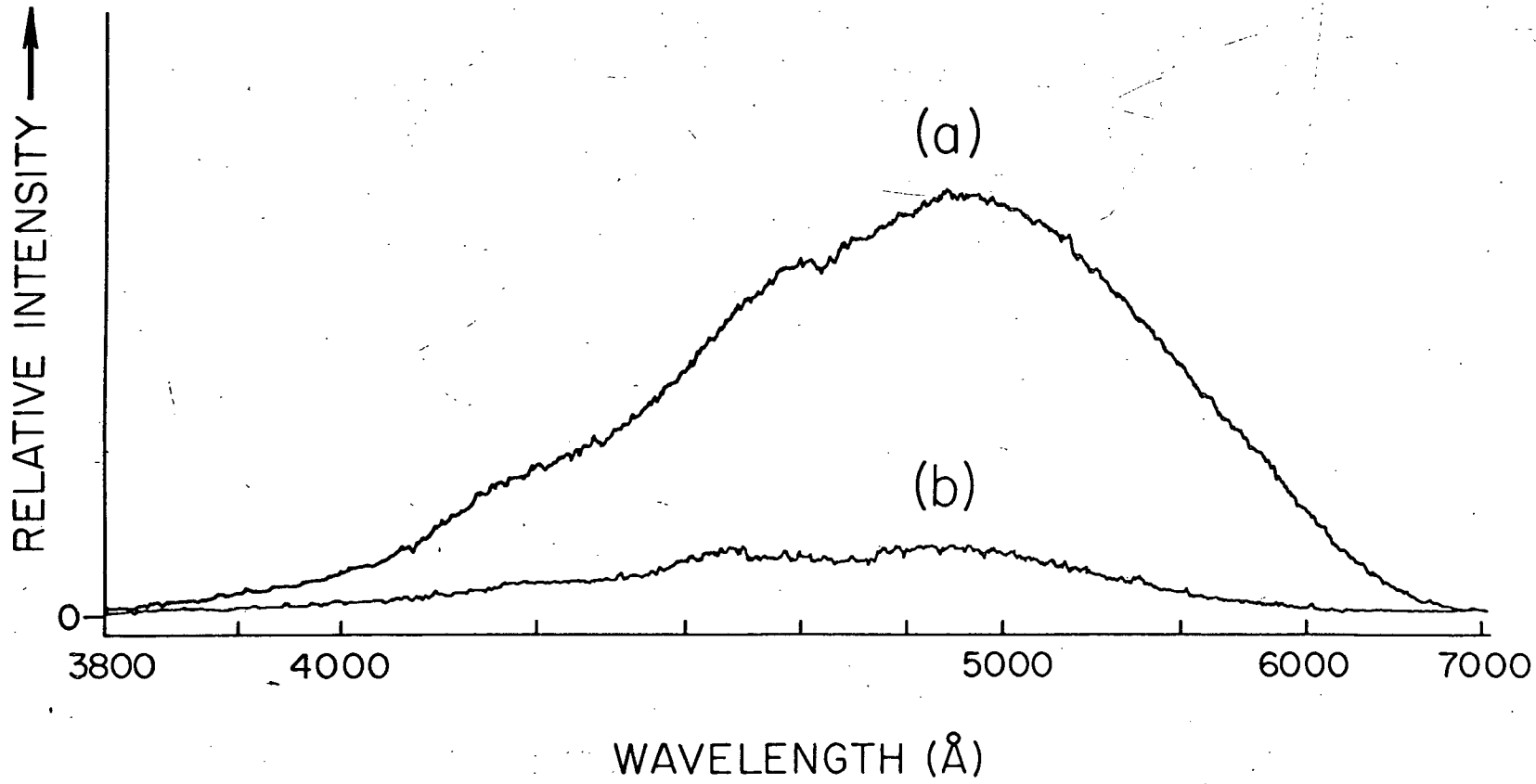

Fig. 16. Emission spectrum of HFA vapour (30 mm) at (a) -78° (b) 25°, excited by 3130 Å. The relative intensity of (a) has been reduced by a factor of $^1/_2$ compared with that of (b).

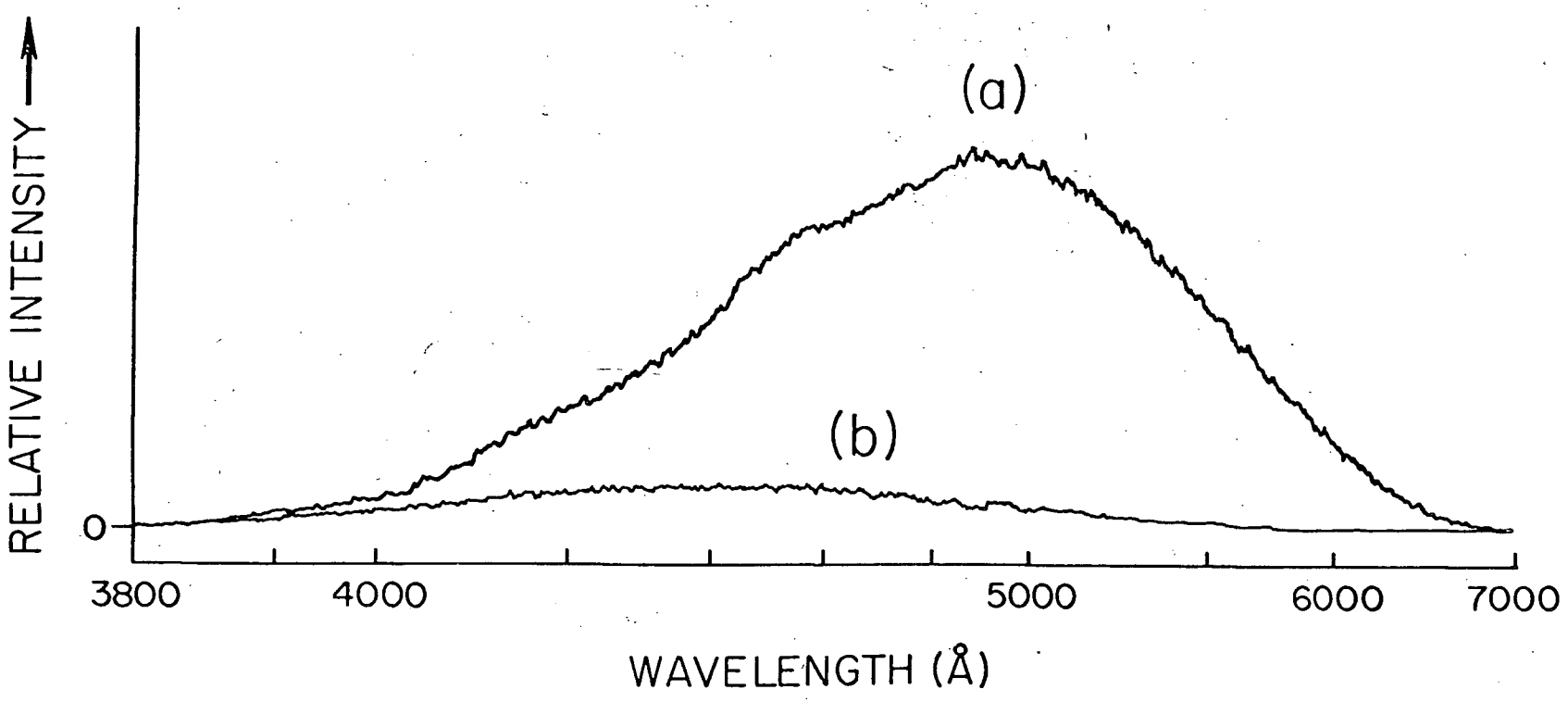

Fig. 17. Emission spectrum of HFA vapour at -78° using 3130 Å excitation.
(a) 30 mm HFA alone
(b) after adding 0.87 mm O_2

Run	System	T°C	$\Delta(A)/\Delta(B)$
1 A	HFA (110 mm)	25	3.77
B	" + O_2 (1.9 mm)		
2 A	HFA (30 mm)	-78	10.95
B	" + O_2 (0.9 mm)		
3 A	HFA (30 mm)	-78	15.38
B	"	25	
4 A	HFA (33 mm); biacetyl (14.7 mm)	25	0.24
B	"		
5 A	HFA (33 mm)	25	0.50
B	" + biacetyl (2 mm)		

Table 9. Comparative emission intensities from HFA vapor, and the effect of biacetyl and oxygen. 3130 Å radiation was used for excitation, except in run 4B (4358 Å)

COLLISIONAL DEACTIVATION AND DISSOCIATION

General Observations.

We use the mechanism of Ayscough and Steacie (equation 1.4) as a basis for discussion, and plot at each wavelength, reciprocal quantum yield of CO as a function of HFA concentration [A]. It will be taken as an established fact that $\Phi_{CO} = \phi$, the primary dissociation yield. The plots are shown in Figs. 18 to 22.

Immediate observations can be summarized:

(i) ϕ° is very close to unity at all wavelengths, with the possible exception of 3340 Å, where no reliable extrapolation can be made. Even at -78°, ϕ° cannot differ greatly from one.

(ii) At 3340 Å, $1/\phi$ rises to an upper limit of around 5.0, above 10 mm pressure. At 3 successively shorter wavelengths, $1/\phi$ apparently increases linearly at the start, but falls off at higher pressures. At 3130 Å, 25°, the high pressure limit is also about 5, approached at pressures above 100 mm. Curvature of the plots for 2804 and 3020 Å is readily apparent, although the high pressure limit was not reached at these wavelengths.

(iii) At 2652 Å, $^1/_\phi$ vs. [A] is linear up to 150 mm pressure, where $^1/_\phi \sim 7$. The data here fall into two sets, both with ϕ^o close to unity, but with slopes differing by about 25%. For the first set (runs 176-197) a partially deteriorated Hanovia D517-A source was employed, and Merck HFA, prepared from hydrate. In the second set, a previously unused D517-A source, and Allied HFA were used. It is possible that the wavelength distribution of the source changes as a lamp ages, or that the monochromator characteristics changes between the two sets of runs. Both batches of HFA gave identical absorption and emission spectra.

(iv) All $^1/_\phi$ vs. [A] plots have either a constant or positive decreasing slope. There is no evidence whatever that the slopes tend to zero at lower pressures, even though extensive data were obtained down to 1 mm.

Collisional Deactivation.

It is clear that under no conditions is there any "reverse" curvature in $^1/_\phi$ vs. [A] , of the kind predicted by Porter and Connelly for a stepwise deactivation mechanism. Any such effect must occur at even lower pressures (below 1 mm), and would be completely masked by experimental scatter, with the order of precision currently attainable in this type of investigation.

In principle, it would be possible to compute theoretical curves, similar to those in Fig. 6, to fit the data, and quote at least an upper limit for the number of collisions required to deactivate the vibrationally excited molecule. In such a calculation however, a number of speculative assumptions would have to be made about the rate of the complementary process - dissociation, such as would make the estimate of doubtful significance.

The results are consistent with a single-step deactivation mechanism (but in no way prove the point). This need not necessarily mean that the vibrationally equilibrated species ($^1A^o$) is formed directly from $^1A^m$ with unit collision efficiency, but simply that the first collision reduces the probability of dissociation to a negligible value.

In this respect, the exponential model for multistage deactivation (40), where a constant fraction α of the excess energy is removed per collision is more plausible than the stepladder model, where the energy decrement at each encounter is constant. A "strong" collision, such as is indicated by the data here, would perhaps mean that α is near its maximum allowed value ($\leq 1/2$), corresponding

to complete vibrational equilibration between the two colliding molecules.

The discussion to follow will be based on the assumption that a $^1A^m$ molecule formed by absorption cannot dissociate from the singlet state once it has encountered a heat-bath molecule A.

Evaluation of Some Rate Constants.

We may re-write equation 1.4 as

$$1/\phi = \frac{a(b+[A])}{c+[A]} \qquad (4.1)$$

where the constants a, b, and c are ratios to be found from the curves, and $ab/c = 1/\phi^o = 1$

$$a = 1/\phi^\infty = \left(\frac{k_8+k_9}{k_8}\right)\left(\frac{k_4+k_5+k_6}{k_4}\right) \qquad (4.2)$$

$$b = k_2/k_3 \text{ mm}$$

$$c = \frac{k_2}{k_3\phi^\infty} \text{ mm}$$

We could for generality include a direct internal conversion,

$$^1A^m \longrightarrow A, \qquad (1)$$

then $b = \frac{k_1+k_2}{k_3}$ and $1/\phi^o > 1$. However, the observed fact that ϕ^o is unity means that $k_1(\lambda) \ll k_2(\lambda)$, for all λ. Much less likely, it could imply that $k_1(\lambda)/k_2(\lambda)$ is constant for all λ, and compensated exactly by a systematic error. We shall discount this possibility. The point is not trivial, because there is another implication in $\phi^o = 1$, which will become apparent later.

3130 Å. The experimental curve may be fitted quite well to a whole family of curves of the form of equation 4.1. However, the data on biacetyl-HFA mixtures (page 95) indicate the value b=3.0 mm. This, together with the high pressure limit ϕ^∞ =0.2 gives

$$1/\phi = \frac{5.0(3.0 + [A])}{15.0 + [A]} \quad . \qquad (4.3)$$

The broken line in Fig. 20 is drawn according to equation 4.3, and in the intermediate pressure range is seen to predict yields definitely smaller than those actually observed. A possible reason for this is considered later (page 110): in this chapter we are mainly interested in extracting values for the constant b.

Taking the gas-kinetic cross section of HFA as [redacted] 6.0 Å we can calculate $k_3 = 1.88 \times 10^{11}$ litre mole^{-1} sec^{-1}, and hence get $k_2 = 3.0 \times 10^7$ sec^{-1} under these conditions. At -78°, as we might expect, thermal triplet dissociation is completely retarded, leaving $1/\phi$ linear in [A] according to equation 1.1. Using k_3(at -78) = 1.51×10^{11} litre mole^{-1} sec^{-1} we obtain $k_2 = 4.7 \times 10^6$sec^{-1}.

3020 Å. Here again we resort to the biacetyl experiments, which give b=5.28 mm and hence $k_2 = 5.3 \times 10^7$ sec^{-1}.

Taking the value of ϕ at the highest pressure studied (15 mm), the calculated value of a is 4.0, and computed yields at lower pressures agree well with those measured (Fig. 18).

2804 Å. No complementary biacetyl data are available, so we use an alternative form, equation 1.5, and estimate ϕ from the intercept of a $\phi/(1 - \phi)$ vs. $1/[A]$ plot.

This plot has been avoided in other cases, because it magnifies the experimental scatter rather badly: where ϕ approaches unity, $\phi/(1 - \phi)$ is subject to increasingly large errors, and this occurs for the large $1/[A]$ values which have major prominence on the graph. Nor can a mean square analysis be justifiably used, for the errors are not proportionate.

In Fig. 23, only the 6 highest pressures have been considered. The intercept gives $a = 7 \pm 2$.

Then, taking one experimental value ($^1/\phi = 2.50$ at 40 mm) we get $b = 17.1$, $c = 119.7$ and so calculate the remaining yields, using equation 4.1, which fit the experimental values quite well (Fig. 20). The value of k_2 is 1.7×10^8 sec^{-1}.

2652 Å. The apparently linear plot of $^1/\phi$ vs. [A] indicates that very little triplet dissociation occurs. The mean value of k_2 (using equation 1.1) is $2.7 \pm 0.3 \times 10^8$ sec^{-1}. ϕ^∞ is either zero or very small.

The k_2 values are summarized in Table 10, together with those of Ayscough and Steacie. In this respect, agreement between the two sets of data is good.

The Model for Photodissociation.

We will consider a simple system, in which a molecule dissociates only from high vibrational levels of the excited singlet state (c.f. ketene). Where triplet dissociation also occurs, this presents no additional problem if the two contributions to ϕ can be reasonably distinguished, as for the HFA data presented here.

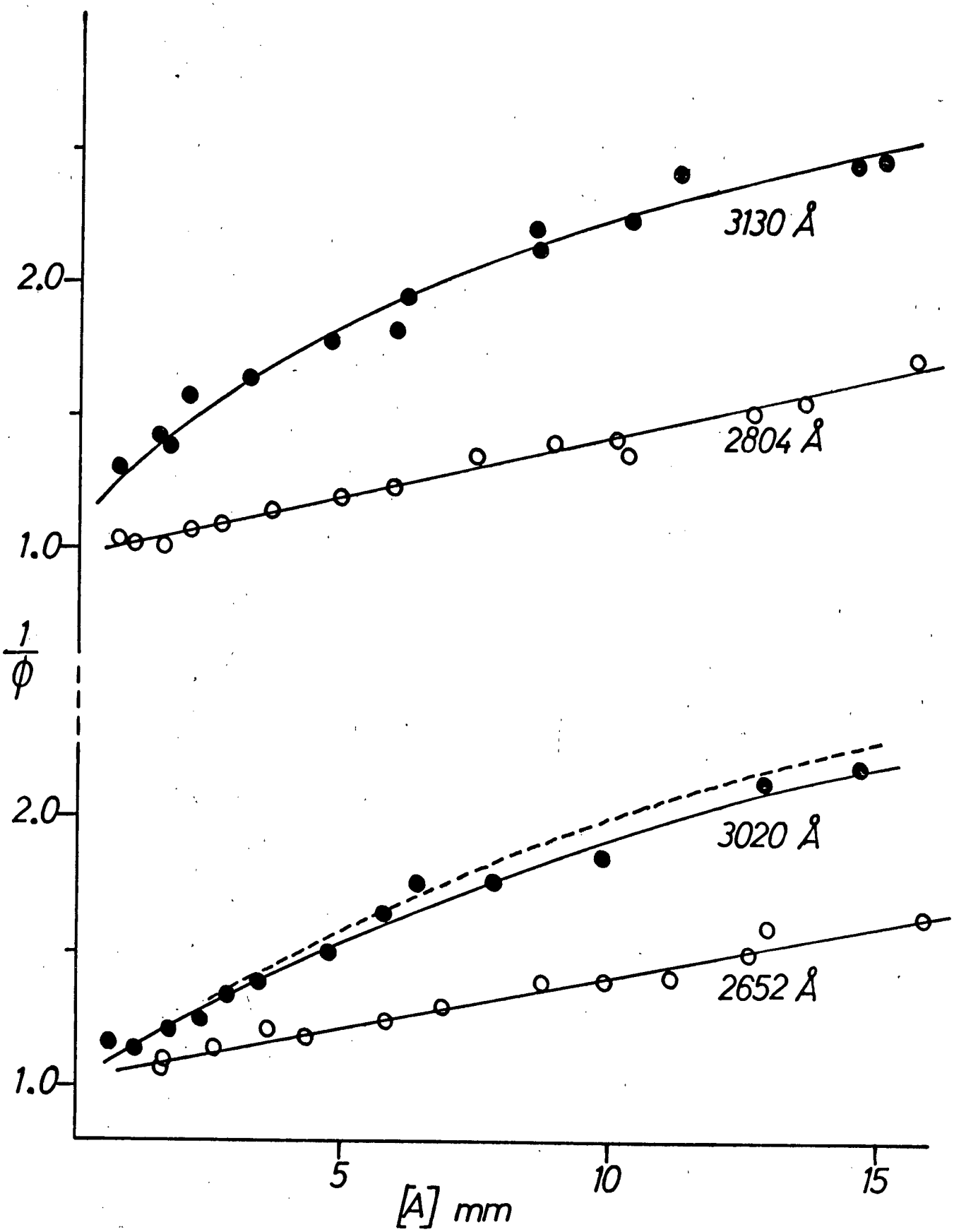

Fig. 18. Reciprocal quantum yields at the lower pressures at 25°.

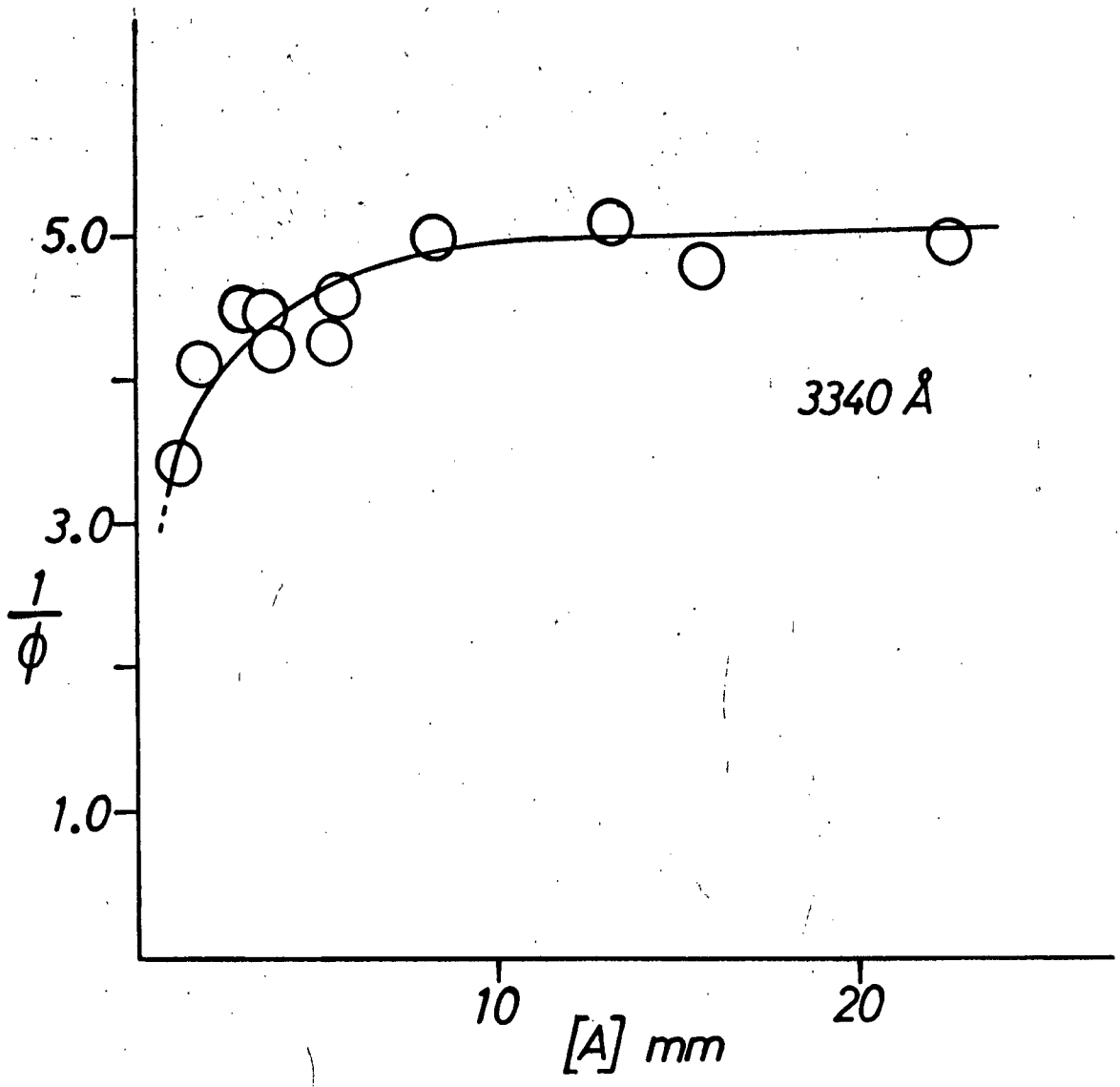

Fig. 19. Reciprocal quantym yields at 3340 Å, 25°.

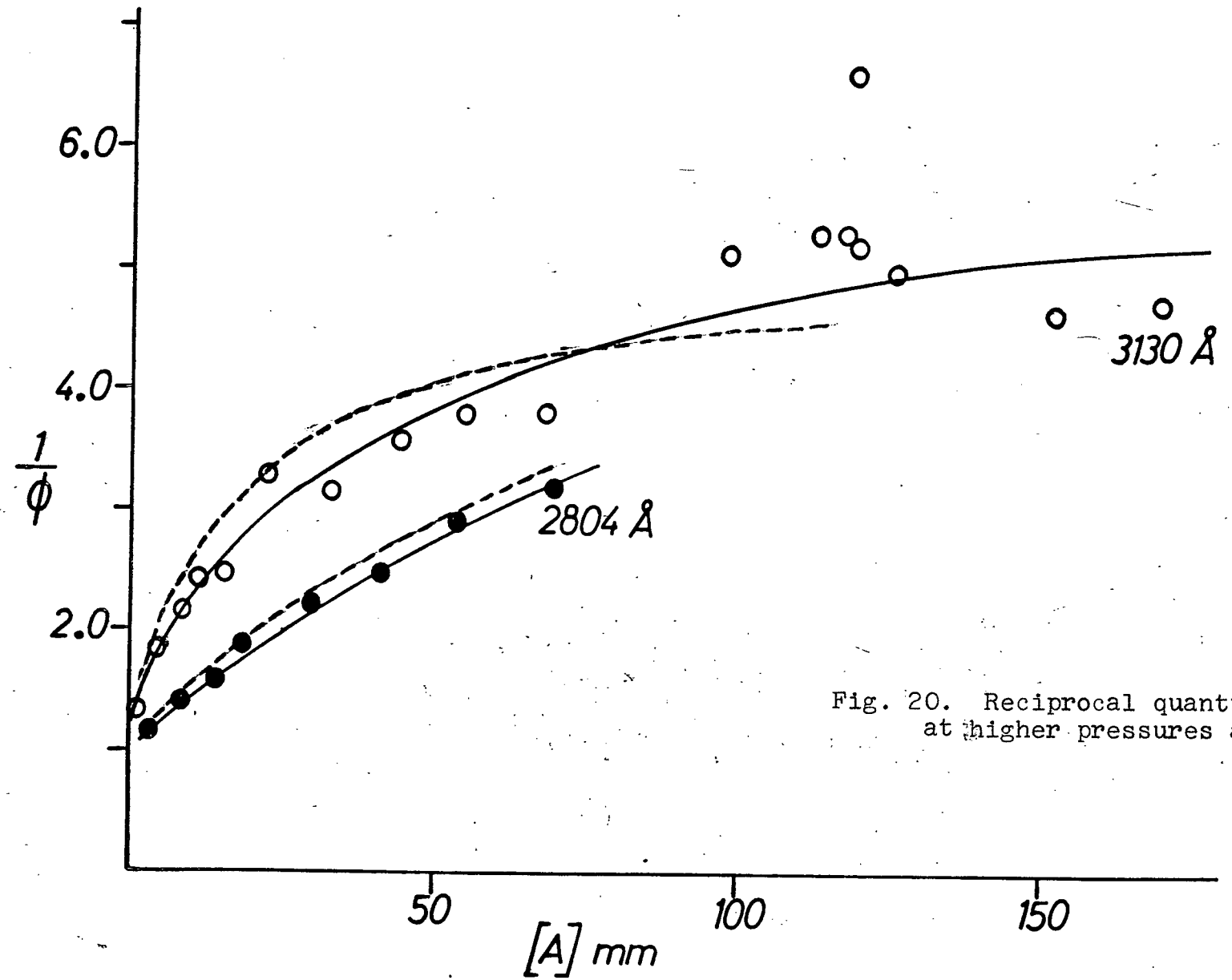

Fig. 20. Reciprocal quantum yields at higher pressures at 25°.

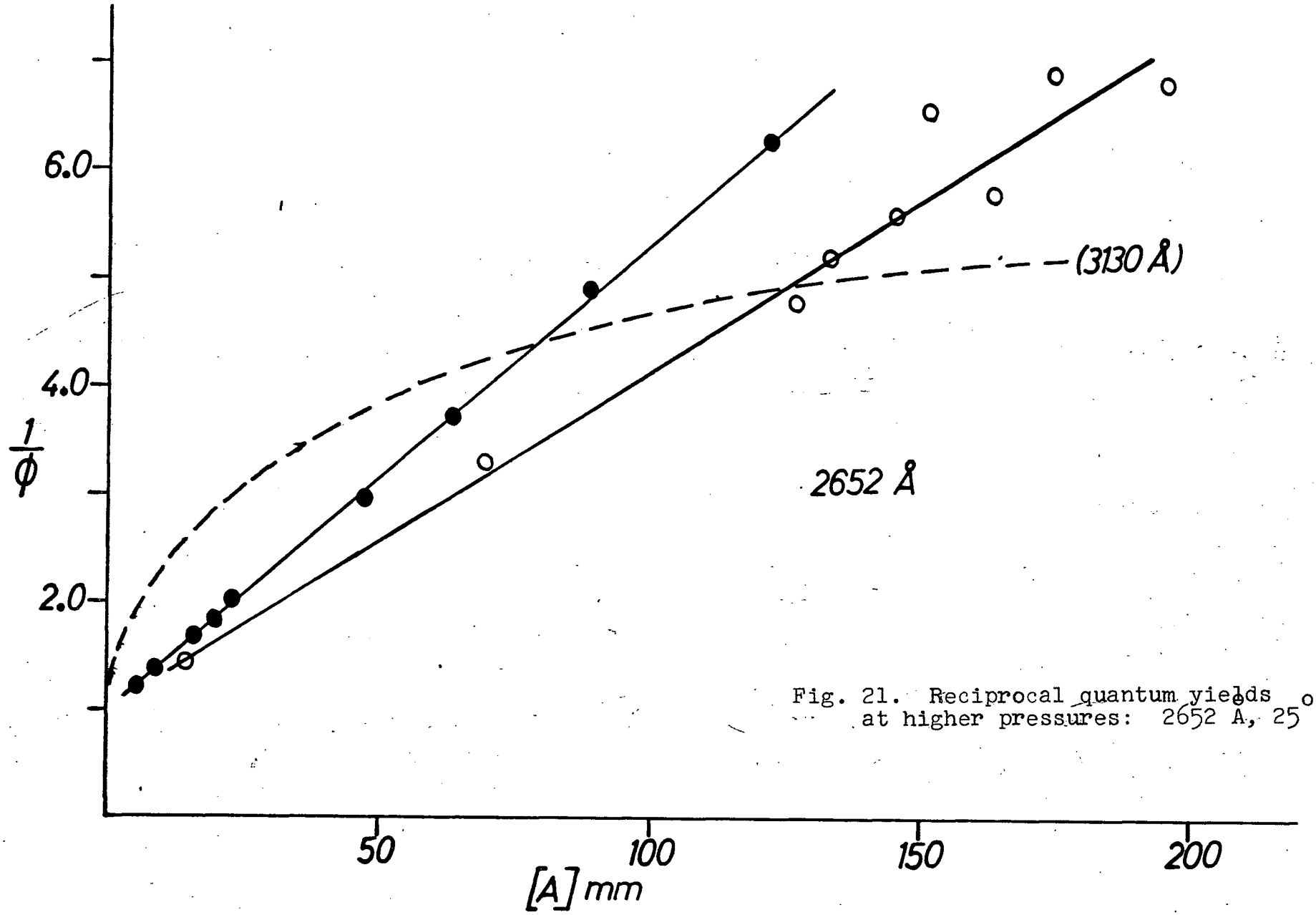

Fig. 21. Reciprocal quantum yields ● ○ at higher pressures: 2652 A, 25 °.

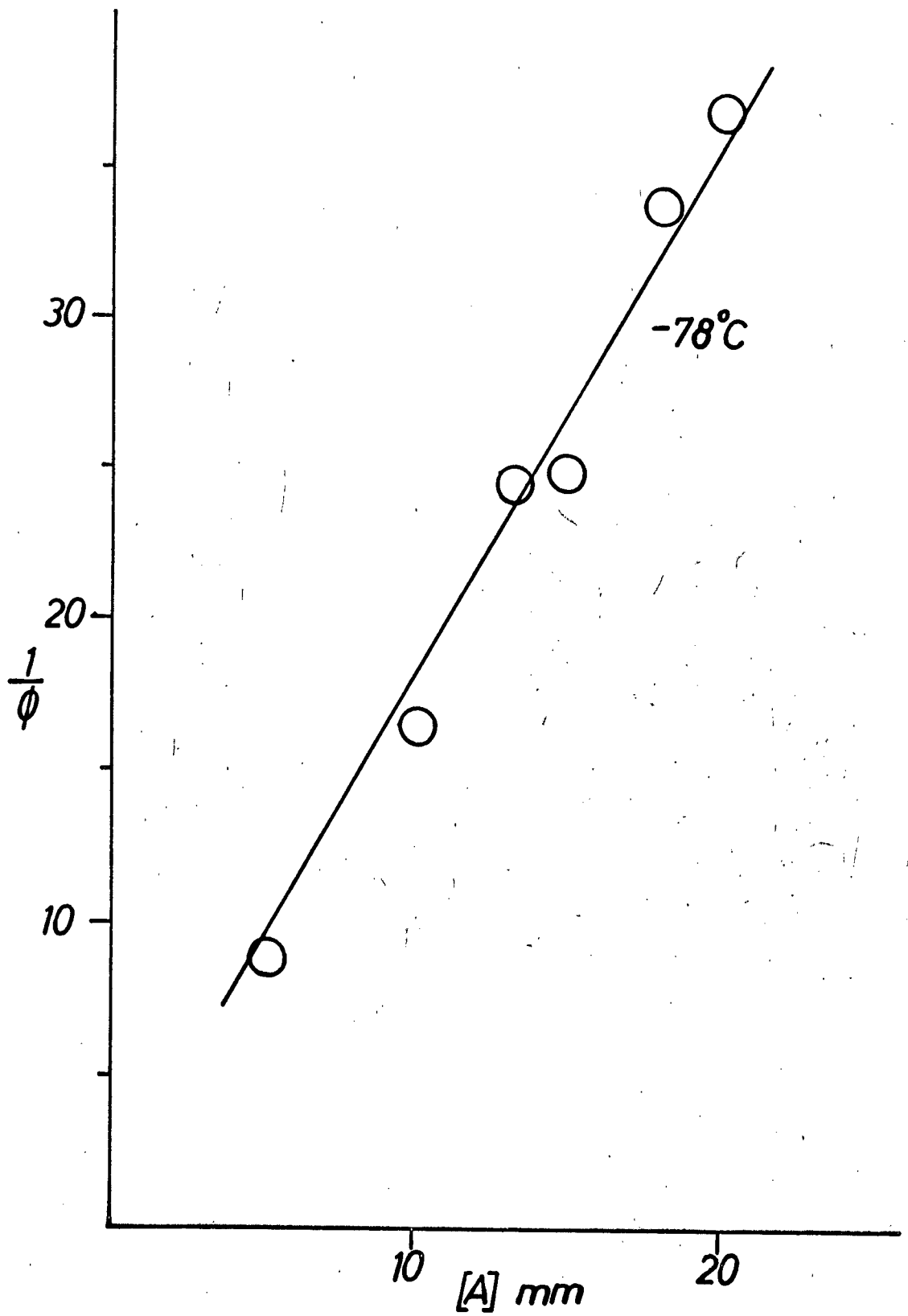

Fig. 22. Reciprocal quantum yields at -78°, using 3130 Å.

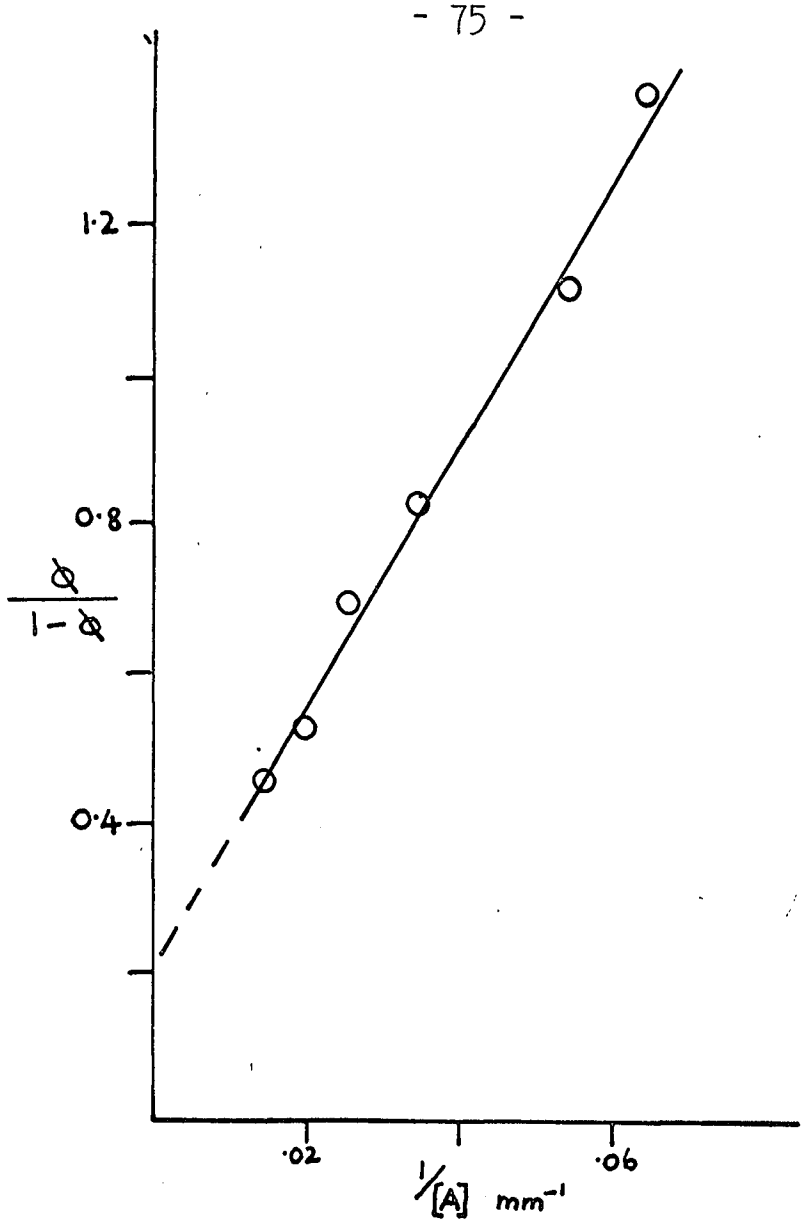

Fig. 23. The quantum yield at 2804 Å, 25°. Only higher pressures are shown.

Table 10. Rate constants for photodissociation. AS refers to reference 5.

T(°C)	$k_2(T)$ sec^{-1} at 3130 Å	λ(Å)	$k_2(\lambda)$ sec^{-1} at 25°
107	2.35×10^8 (AS)	3340	-
78	1.25×10^8 (AS)	3130	3.0×10^7
53	6.25×10^7 (AS)	3020	5.3×10^7
27	3.01×10^7 (AS)	2804	1.7×10^8
25	3.0×10^7	2652	2.7×10^8
-78	4.7×10^6	2640	$\sim 3 \times 10^8$ (AS)

Then, as shown above, we measure a unimolecular rate constant k_2 from

$$^1/\phi = 1 + \frac{k_3}{k_2}[A] \qquad (1.1)$$

This equation is only strictly valid if:

(a) the incident light is truly monochromatic

(b) the ground state molecules A all have the same vibrational energy

An energy diagram for this fictitious case is shown in the sketch:

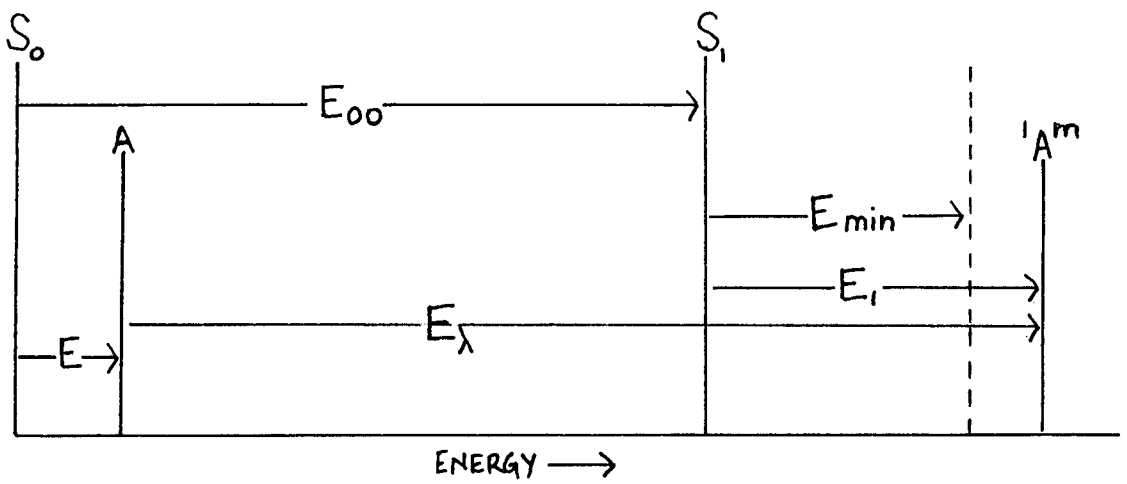

E represents the initial total vibrational energy of A above the fixed zero point energy. Absorption of a

photon with energy $E_\lambda = \frac{hc}{\lambda}$ leaves the molecule with excess vibrational energy E_1 above the zero-point energy of S_1. If E_{oo} is the difference between two zero-point energies, then

$$E_1 = E_\lambda - E_{oo} + E$$

and from the RKR expression,

$$k_2(E_1) = \nu\left(1 - \frac{E_{min}}{E_\lambda - E_{oo} + E}\right)^{S-1} \qquad (4.5)$$

On the Kassel picture, E_{min} is the minimum energy, which when shuttled into the breaking bond, causes immediate dissociation.

The tacit assumption here is that the optical excess energy is distributed randomly amongst S oscillators.

Of course, such a system would only be approached in practice at low temperatures, where $E \rightarrow 0$. In that case, one might hope to correlate k_2 (observed), with values predicted from the simple expression above.

To take into account a distribution of thermal vibrational energy for A, not only is it necessary to express equation 4.5 as a sum over all E_1, but also to review the strict validity of equation 1.1.

Consider a ground state molecule, A^j, with total vibrational energy j, which is raised by absorption to $^1A^q$. If we assume the transition probability to be independent of j, then the steady-state equation is

$$\frac{d[^1A^q]}{dt} = 0 = \frac{I_a[A^j]}{[A]} - k_2(q)[^1A^q] - k_3[^1A^q][A]$$

where I_a = the total rate of absorption

and $[A] = \sum_j [A^j]$, the photolyte concentration,

hence $$\left[\frac{d(\text{Product})}{dt}\right]_{^1A^q} = \frac{k_2(q)I_a[A^j]}{[A](k_2(q) + k_3[A])}$$

and the observed overall yield

$$\phi = \Phi_{\text{Product}} = \frac{\sum_{\text{all } q}\left[\frac{d(\text{Product})}{dt}\right]_{^1A^q}}{I_a}$$

$$= \sum_{\text{all } q}\left[k_2(q)\frac{[A^j]}{[A]} \Big/ (k_2(q) + k_3[A])\right] \qquad (4.6)$$

For a complex polyatomic molecule, the spacing of vibrational levels may be regarded as nearly continuous, with

$\frac{[A_j]}{[A]}$ = f(E) dE, the fraction of ground

state molecules with energy E to E + δE. (Discrete j $\leftrightarrow$ continuous E; discrete q $\leftrightarrow$ continuous E_1).

Equation 4.6 then becomes on inversion

$$\frac{1}{\phi} = \left[\int_{E_{min}}^{\infty} \frac{k_2(E_1)f(E)}{k_2(E_1) + k_3[A]} \, dE_1 \right]^{-1} \qquad (4.7)$$

This relationship is clearly the photochemical equivalent of equation 1.14 for chemical activation. In the latter case, the experimental observable is the stabilization to dissociation ratio, S/D, while here it is the activation to dissociation ratio, $1/\phi$.

The lower limit of integration may be either the critical energy E_{min}, or $E_x (= E_\lambda - E_{oo})$. The energy diagram in Fig. 24 illustrates this point. The case of E_x as the lower limit arises if $E_{min} < E_x$, for then, even for a molecule with very little thermal vibrational energy, the excess optical energy will still raise it to above E_{min}.

This is an important point. The experimental fact for HFA is that $\phi^{\circ} \rightarrow 1$ at wavelength 3130 Å or shorter; that is, essentially every excited molecule decomposes, so that the condition $E_x(3130\ \text{Å}) > E_{min}$ sets an upper limit to the critical energy.

$$\phi^{\circ} = \int_{E_x}^{\infty} f(E)\, dE_1 = 1$$

Conversely, in systems where $\phi^{\circ} < 1$ is found, this need not mean, as has been frequently assumed, that there is another first-order process competing with dissociation. It could be that $E_{min} > E_x$.

The total vibrational energy of a molecule in S_1 remains constant until a collision occurs, after which the molecule cannot dissociate. At low pressures, where the collision interval is very long, intramolecular energy redistribution must occur within this time, (or within the radiative lifetime, which ever is shorter), to get at least E_{min} concentrated in the breaking bond. Otherwise again we would observe $\phi^{\circ} < 1$.

The Slater postulate (24) of no energy exchange between normal modes does not seem to apply here. Perhaps

this is not surprising, since anharmonic coupling of the normal mode frequencies in an upper electronic state may be considerable.

Equation 4.7 gives

$$\frac{d\,1/\phi}{d[A]} = \frac{k_3 \int_{E_x}^{\infty} \frac{k_2(E_1) f(E)}{\left(k_2(E_1) + k_3[A]\right)^2} dE_1}{\left[\int_{E_x}^{\infty} \frac{k_2(E_1) f(E)}{k_2(E_1) + k_3[A]} dE_1 \right]^2}$$

and

$$\left(\frac{d\,1/\phi}{d[A]}\right)_{[A]\to 0} - \left(\frac{d\,1/\phi}{d[A]}\right)_{[A]\to\infty} = k_3 \left(\left\langle \frac{1}{k_2} \right\rangle - \frac{1}{\langle k_2 \rangle} \right) \qquad (4.9)$$

where the mean values are

$$\langle k_2 \rangle = \int_{E_x}^{\infty} k_2(E_1) f(E)\, dE_1$$

$$\left\langle 1/k_2 \right\rangle = \int_{E_x}^{\infty} \frac{f(E)}{k_2(E_1)} dE_1 \qquad (4.10)$$

In general, whatever explicit form for $k_2(E_1)$ is employed, it increases rapidly with E_1. Hence $\langle k_2 \rangle > \langle 1/k_2 \rangle^{-1}$, because in the former, molecules with higher than average energies are most important, while in the latter, low energy molecules are heavily weighted

in the averaging. At extremely high concentrations, only those molecules with the highest energy have time to dissociate before collision, so the relevant average rate constant is $\langle k_2 \rangle$.

We can see that strictly speaking $1/\phi$ vs. $[A]$ would not be linear, but show a decrease in slope according to equation 4.9. These points are illustrated in Fig. 25. Significant deviations from linearity in this plot might only become evident when $k_3[A]$ is comparable to $k_2(E_1)$ for those energies at which the integrand in equation 4.7 has an appreciable value. It is shown later that the effect is unlikely to reveal itself at practicable working pressures, even without the complication of triplet dissociation.

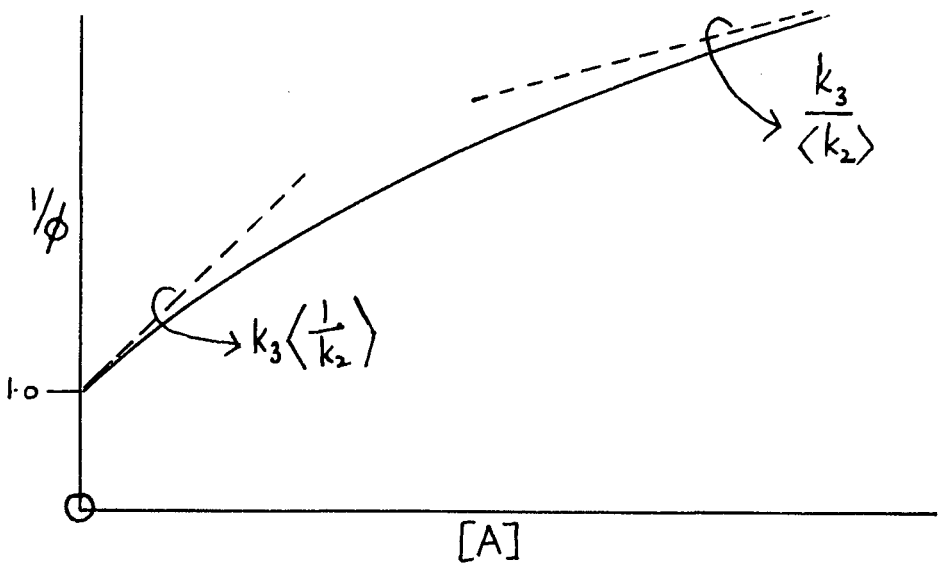

Fig. 25. Predicted behaviour of $1/\phi$ vs. $[A]$.

For this reason we may put approximately:

$$\frac{1}{\phi} = 1 + k_3[A]\left\langle \frac{1}{k_2} \right\rangle \qquad (4.11)$$

which is just the first two terms in the McLaurin expansion of equation 4.7.

To calculate the values of $\left\langle \frac{1}{k_2} \right\rangle^{-1}$ according to equation 4.10, for comparison with experimental values, we have to choose expressions for $k_2(E_1)$ and $f(E)$. This is the type of calculation which has been done in detail by Rabinovitch (49) and other protagonists of the Marcus formulation (c.f. page 25). It requires a knowledge of the normal mode frequencies of the molecule, in both ground and excited states, (for photodissociation). Unfortunately not even the normal mode frequencies for the ground state have been measured for HFA.

As an alternative we may resort to classical forms for $k_2(E_1)$ and $f(E)$, recognising that this is liable to be a severe limitation in making a quantitative comparison.

The probability distribution function for the total vibrational energy of a collection of coupled harmonic oscillators is

$$f(E)\,dE = \left(\frac{E}{kT}\right)^{S_2-1} \cdot \frac{\exp.(-E/kT)}{kT(S_2-1)!}\,dE \qquad (4.12)$$

We shall treat S_2, the number of oscillators contributing to the ground state energy as an unknown parameter, constant with T.

For $k_2(E_1)$ the RKR equation will be used, with $S_1 \leqslant 24$ as the unknown number of oscillators exchanging energy with the breaking bond.

The expression for $\left\langle {}^{1}/_{k_2} \right\rangle$ is then

$$\left\langle \frac{1}{k_2} \right\rangle = \int_{E_x}^{\infty} \left(1 - \frac{E_{min}}{E_1}\right)^{1-S_1} \cdot \left(\frac{E_1 - E_x}{kT}\right)^{S_2-1} \cdot \frac{e^{-\left(\frac{(E_1-E_x)}{kT}\right)}}{\nu\,(S_2-1)!kT} dE_1 \qquad (4.13)$$

The integral cannot be evaluated explicitly. At high enough temperatures the thermal energy $(E_1 - E_x)$ will greatly exceed the optical energy E_x. In this limit we would expect $k_2(T)$ to be of the classical form for a thermal reaction, viz: $\nu \exp(\frac{-E_{min}}{kT})$. The low temperature limit, when the molecules have no thermal energy in excess of the fixed zero point energy, is given by equation 4.5, essentially the simple RKR expression.

These facts are illustrated in Fig. 26, together with a curve (a), computed* by graphic integration of equation 4.13, using the parameters indicated. Over the practicable range of temperature AB, where photolyses can generally be performed, the curvature in the Arrhenius line is very slight. Experimental points in this range would be most unlikely to reveal it. However, if interpreted in the way customary for a thermal decomposition, such data would yield an activation energy of 800 cm^{-1} and a frequency factor of 1.5×10^{13} sec^{-1}. These are clearly only lower limits for the true values chosen (2000 cm^{-1}, 10^{14} sec^{-1}).

The effect of varying each of the parameters in turn is also indicated in Fig. 26. Increasing S_1 or decreasing S_2 decreases the rate constants, but in this calculation, and in other using widely different parameters, the slope and curvature of the line in the region AB is almost constant for quite large changes in S_2.

Change in ν, of course, merely displaces the curve vertically.

* A simple Fortran II programme was written for the IBM 1620 machine at the University of British Columbia. With the machine time available, it was most economical to compute only values for the integrand in equation 4.13. These could be rapidly plotted and integrated by planimeter to give $\langle 1/k_2 \rangle$.

The difference between $\langle k_2 \rangle$ and $\langle 1/k_2 \rangle^{-1}$ may not, in general, be negligible. For the sample calculation (a) in Fig. 26, at 300°K, $\langle 1/k_2 \rangle^{-1} = 3.66 \times 10^{11}$ sec^{-1}, while $\langle k_2 \rangle = 7.11 \times 10^{11}$ sec^{-1}.

Comparison with Experiment.

If $k_2(T)$ from Table 10 is plotted in Arrhenius form, the value at -78° lies well above the linear extrapolation of the 4 crowded points between 25° and 108°. Qualitatively this bears out the prediction that this kind of plot is not linear over a wide enough temperature range.

E_{oo} has been placed at 3500 Å (28570 cm^{-1}) from the small overlap between absorption and fluorescence (6). The excess vibrational energy associated with 3130 Å cm^{-1} is thus 3380 cm^{-1}. As shown above, this is an upper limit for E_{min}. In fact, because of the spectral width of the 3130 Å radiation, used (Fig. 9), a better value is 3000 cm^{-1}: that is, even those molecules which absorb a photon of 3170 Å light eventually decompose in the absence of competing collisions. The lower limit for E_{min}, from the greatest slope in the experimental curve, is 2000 cm^{-1}.

The critical energy for the photodissociation may therefore be placed with some confidence between 5.7 and 8.6 kcal/mole.

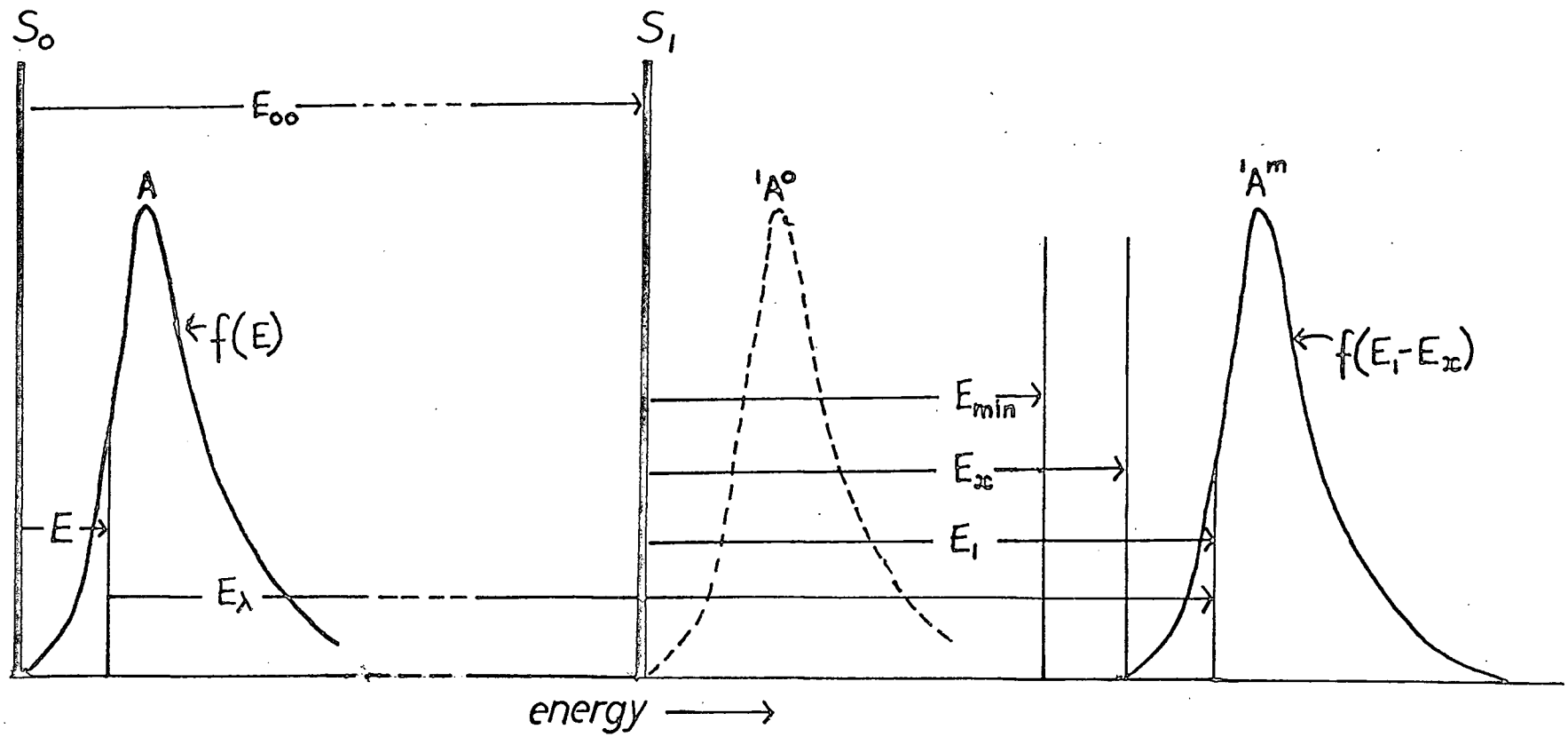

Fig. 24. Energy diagram for photodissociation.

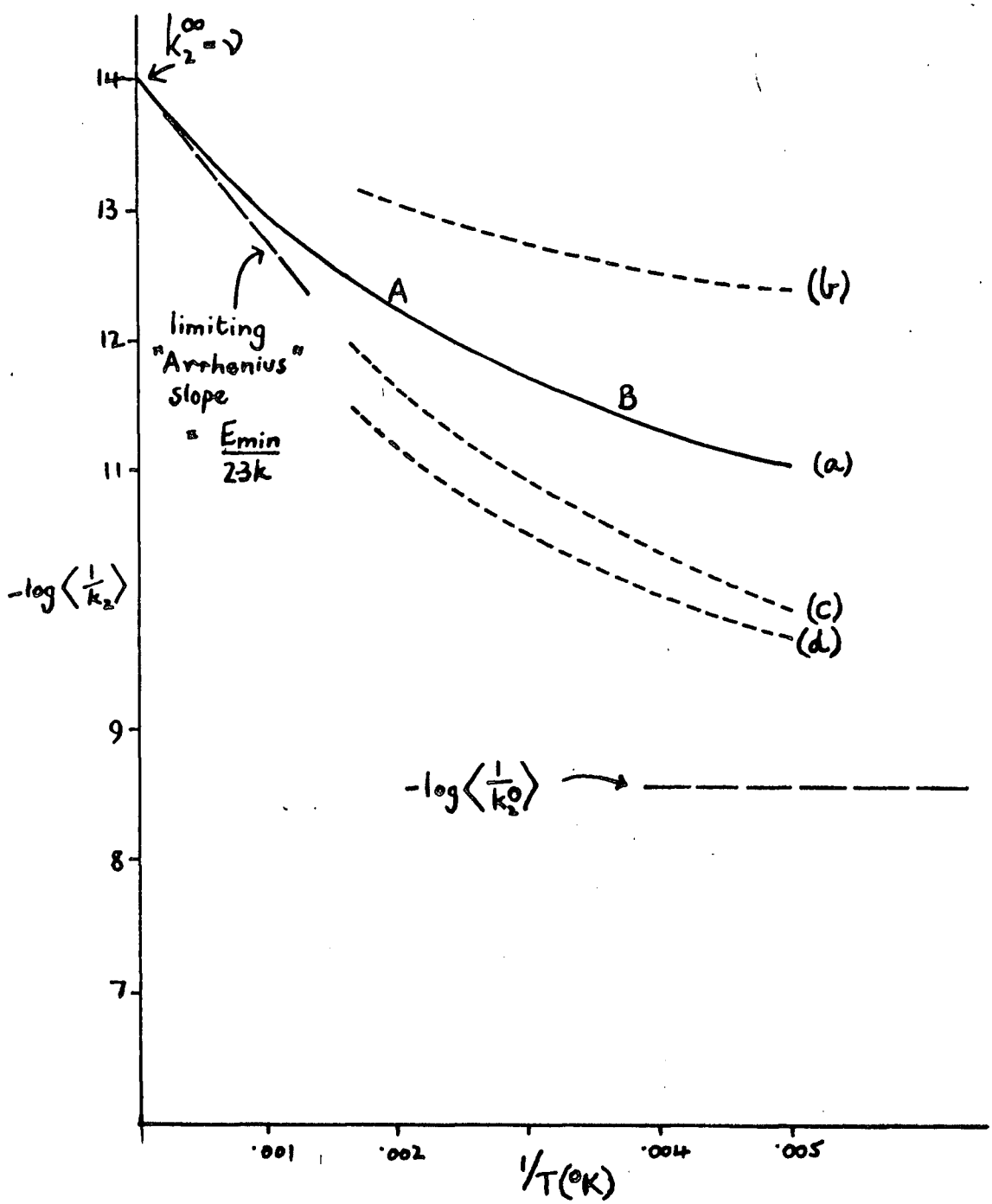

Fig. 26. Calculated rate constants $k_2(T)$. In (a) the parameters used were $E_x=3380\ cm^{-1}$, $E_{min}=2000\ cm^{-1}$, $S_1=S_2=15$, $\nu=10^{14}\ sec^{-1}$. The effect of varying each parameter in turn is shown by (b) $S_1=9$; (c) $E_{min}=2500\ cm^{-1}$, (d) $S_2=9$.

Taking $\nu = 10^{14}$ sec^{-1}, and E_{min} = 2500, 2750 and 3000 cm^{-1} in turn, curves were computed to give the best fit to the experimental data (A,B,C in Fig. 27). Whatever parameters are chosen, the predicted curvature in the Arrhenius line is always much less than that indicated by the experimental points. Nevertheless, one can obtain order-of-magnitude agreement between calculated and observed values for $k_2(T)$ at 3130 Å.

The three sets of parameters A, B, C were used for complementary calculation of $k_2(\lambda)$ at 25°C, for the wavelengths 3020, 2804 and 2652 Å. An approximate correction was made for the spectral width of each of these wavelengths. Thus, reference to Fig. 9 shows that irradiation with 2652 Å is more nearly equivalent to using 2650 and 2700 Å with relative intensities 13 and 8, respectively. It turned out that ignoring this factor would have introduced an error of only about 10%. The use of fairly broad exciting lines may not be a serious restriction in this kind of work.

In all cases, the calculated values of $k_2(\lambda)$ were much higher than those found experimentally. For instance, using approximation B gave k_2(2652 Å) = 7.3 x 10^{11} sec^{-1}, which compares with the experimental value of 2.7 x 10^{8} sec^{-1}.

Some improvement is evident if ν is chosen to be much less*, with S_2 correspondingly larger. With $\nu = 3.2 \times 10^{11}$ sec^{-1} and $E_{min} = 3000$ cm^{-1} (approximation E), the discrepancy between $k_2(\lambda)$, calculated and observed is not much more than an order of magnitude (Table 11).

The origin of the disagreement is not difficult to see. At 108°, with 3130 Å, using the approximation E, the average total vibrational energy of the excited molecule is 7800 cm^{-1}, whereas at 25°, with 2652 Å, this same quantity is 12,700 cm^{-1}. Furthermore $k_2(E_1)$ is still increasing quite rapidly over this range. These points are illustrated in Fig. 28. However the observed rate constants under the two sets of conditions are almost the same (2.3×10^8; 2.7×10^8 sec^{-1}). Digressing for the moment, Fig. 28 also reflects on the likelihood of recognising curvature in $1/\phi$ vs [A] due to the thermal spread of vibrational energy. At 2652 Å, over the region where $f(E)$ is appreciable, $k_2(E_1)$ is about 10^{10} sec^{-1}. The magnitude of k_3 [A] has to be approaching this value, before the predicted change

* $\nu = 10^{14}$ sec^{-1} (~ 3000 cm^{-1}) is perhaps unrealistically high for a molecule containing no hydrogen: Slater (24) has shown that ν must lie within the range of the normal mode frequencies. However, it cannot be less than about 3×10^{11} sec^{-1}, judging from extrapolation of the linear experimental points.

in behaviour becomes important. This would require $[A] \sim 10^3$ mm pressure. At longer wavelengths, although this critical pressure is somewhat lower, the effect would be completely hidden by the preponderance of triplet dissociation.

Returning to the discrepancy in the calculated values for $k_2(\lambda)$, one reason for this could be that the effective number of oscillators S_1 increases with increasing vibrational energy. This possibility has been noted before (41,42). It is justified classically on the basis of increased anharmonicity in the higher vibrational levels, which allows energy to flow between more of the normal modes than at lower energies. Hence, in Kassel language, it takes relatively longer for sufficient energy to get into the breaking bond.

The change in mean thermal energy over the temperature range studied is comparitively small compared with the difference in the optical vibrational energies of the extreme wavelengths. This is why the data for $k_2(T)$ can be reasonably fitted using one value of S_1.

In approximation F(Table 11), the value of S_1 was increased from 15 at 3130 Å, to its maximum value of 24,

at 2652 Å, and proportionately at the intermediate wavelengths. Calculated values for $k_2(\lambda)$ then show much better agreement with the experimental data.

Such arbitrary adjustment of the unknown parameters in no way saves the day for the simple extension of classical unimolecular theory considered here. A more satisfactory correlation between $k_2(\lambda)$ and $k_2(T)$ must await a knowledge of the normal mode frequencies for HFA, and an indication as to how these may change in the excited state.

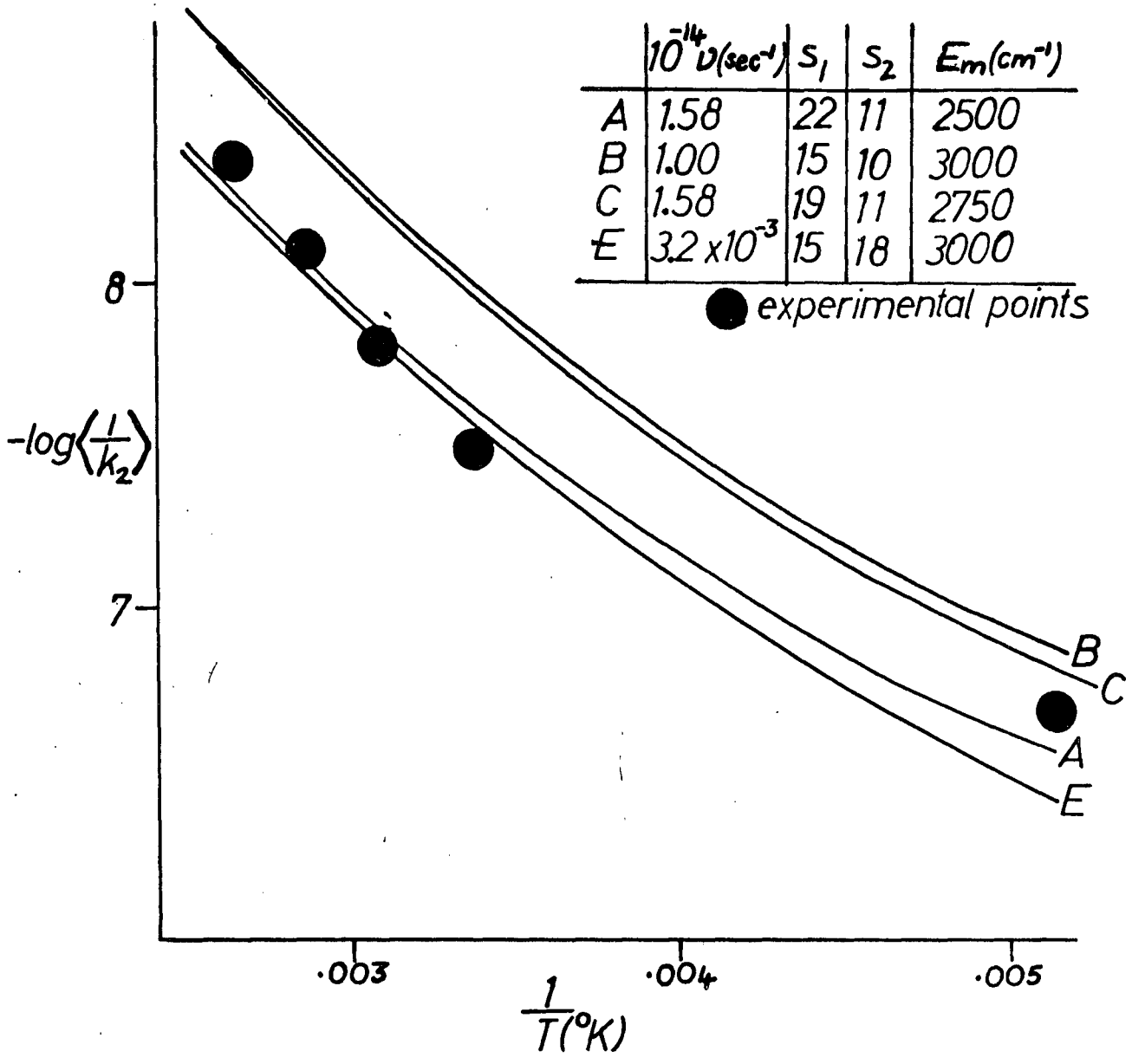

Fig. 27. Calculated $k_2(T)$ at 3130 Å, compared with experimental values. Curves B and C have been displaced 0.2 units upwards to avoid confusion.

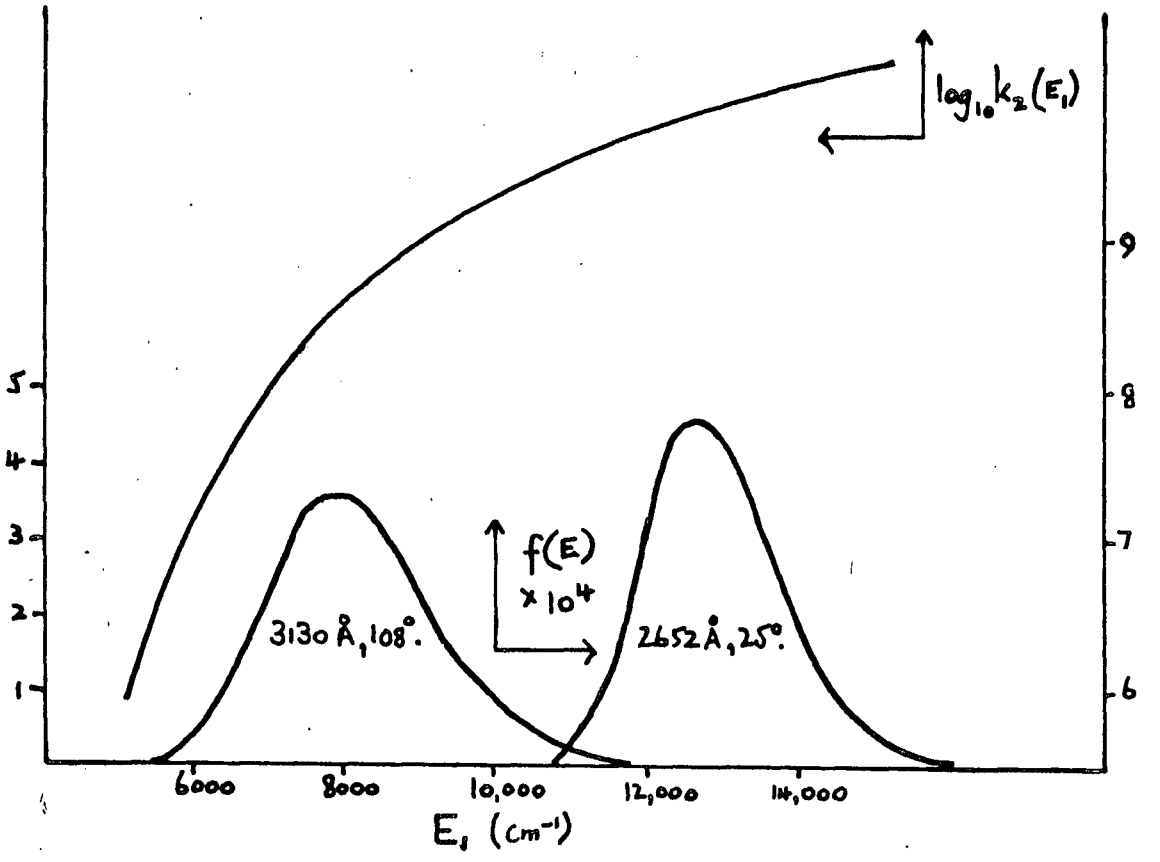

Fig. 28. Distribution of total vibrational energy, and the form of $k_2(E_1)$. The parameters of approximation E were used in calculating the curves.

Table 11. Comparison of experimental and calculated $k_2(\lambda)$ at 25°. Approximations E and F differ only in the values assigned to S_1.

λ(Å)	Observed $k_2(\lambda)$ sec^{-1}	"E" S_1	"E" $\langle k_2^{-1}\rangle^{-1}$ sec^{-1}	"F" S_1	"F" $\langle k_2^{-1}\rangle^{-1}$ sec^{-1}
3130	3.0×10^7	15	2.76×10^7	15	3.76×10^7
3020	5.3×10^7	15	4.8×10^8	17	1.36×10^8
2804	1.7×10^8	15	4.2×10^9	21	4.5×10^8
2652	2.7×10^8	15	8.6×10^9	24	5.4×10^8

INTERSYSTEM CROSSING, ENERGY TRANSFER AND EMISSION

The Hexafluoracetone-biacetyl System.

In the presence of small concentrations of biacetyl, quantum yields of carbon monoxide from HFA irradiated at 3130 Å are greatly decreased. Thus with 11 mm of HFA, the yield changes from 0.41 to 0.21 (c.f. Tables 3 and 8).

This can be explained if we include the energy transfer reaction,

$$^3A^\circ + B \longrightarrow {}^3B + A \qquad (10)$$

where B represents biacetyl. At room temperature, triplet biacetyl is thought to decompose by the bimolecular reaction (45):

$$^3B + {}^3B \longrightarrow B + \text{product} \qquad (10\,a)$$

Even when biacetyl alone is excited directly at 4358 Å, where photo-oxidation studies show that the triplet state is formed with almost unit efficiency (43,44), the dissociation yield by reaction 10a is only .01 (45). In this system we may therefore neglect this reaction, so that essentially all CO would come from reaction 2, singlet dissociation of HFA, assuming all triplet HFA is quenched by reaction 10.

This is borne out by a linear plot (Fig. 29) of $^1/\phi$ vs. [A] (i.e. according to equation 1.1). The slope of these plots give values for k_2/k_3. The figures are 3.0 mm (3130 Å), 5.28 mm (3030 Å).

The triplet biacetyl formed by reaction 10 phosphoresces back to the ground state:

$$^3B \longrightarrow B + h\nu \qquad (11)$$

The emission spectrum in Fig. 13 is due to this reaction: weak emission below 4500 Å in Fig. 14 corresponds closely to the fluorescence of singlet HFA (discussed below). Neither phosphorescence nor fluorescence from biacetyl extend to wavelengths shorter than 4400 Å (46).

We must also consider the possibility of singlet-singlet energy transfer:

$$^1A^o + B \longrightarrow {}^1B + A \qquad (12)$$

The fact that the fluorescence band of HFA still remains in the presence of biacetyl indicates that reaction 12 must be far less efficient as an energy transfer path, than reaction 10. The linearity of the plot in Fig. 29 is further evidence for this point: dissociation from singlet biacetyl formed by reaction 12 might be considerable,

and it is unlikely that such a simple relationship between ϕ and [A] would be observed. We therefore assume that reaction 12 does not occur to an appreciable extent under the conditions used in these experiments. This is similar to the case of acetone (32).

The magnitude of ϕ_8, triplet dissociation yields, can be evaluated by difference, and are listed in Table 12. The experimental values for ϕ_2 from Fig. 29 were subtracted from values of $\phi_2+\phi_8$, obtained from the best curve through the experimental points in Fig. 18.

Table 12. Quantum yields for triplet dissociation of HFA at 25°.

3130 Å		3020 Å	
[A] mm	ϕ_8	[A] mm	ϕ_8
11.3	.219	9.15	.165
8.00	.209	11.7	.177
5.50	.194	17.2	.209
4.80	.161	14.0	.182
3.75	.128	15.7	.208
11.0	.216		
6.70	.185		

According to equation 1.2, ϕ_8 should be given by

$$\frac{1}{\phi_8} = \frac{1}{\phi^\infty} + \frac{k_2}{k_3 \phi^\infty [A]} \qquad (5.1)$$

The data are plotted according to expression 5.1 in Fig. 30. The process of taking differences magnifies the experimental scatter considerably, but within this limitation, reasonable straight lines can be drawn through the data at 3020 Å and 3130 Å, which have the same intercept. The extrapolated value of ϕ^∞ so obtained is about 0.3: significantly larger than that observed at 3130 Å at this temperature (0.2). Additional reactions to explain this point are discussed later. Obviously much more extensive data would be required before the variation of ϕ_8 with pressure could itself give any useful information.

The sensitized and direct phosphorescence intensities measured in run 4, Table 9, allow ϕ_4 to be estimated. Since biacetyl emission excited by 4358 Å at 25°C is 98% phosphorescence (46), we obtain

$$\frac{\phi_{11} \text{ (sensitized by HFA at 3130 Å)}}{\phi_{11} \text{ (direct, at 4358 Å)}} = 0.45,$$

where the tabulated value of 0.24 has been adjusted for the relative intensities of the 4358 Å and 3130 Å exciting lines.

It is not unreasonable to suppose that the proportion of triplet biacetyl molecules which emit is the same, whether the excitation is direct or indirect. This, together with the fact above, that triplet biacetyl is formed with almost unit quantum yield at 4358 Å, gives

$$\phi_{10} \simeq \phi_4 = 0.45$$

That is, about 50% of the HFA molecules which absorb eventually reach the triplet state. ϕ_8 would be about 0.22 under these same conditions (33 mm at 25°C, with 3130 Å).

Fluorescence and Phosphorescence.

On the basis of the marked effect of oxygen on the emission spectrum of HFA, it is clear that phosphorescent reaction must be included in the primary process:

$$^3A^\circ \longrightarrow A + h\nu \qquad (7)$$

This is, of course, kinetically similar to the radiationless reaction 9, and its inclusion does not invalidate any of the previous discussion. The behaviour of HFA then falls into line with that of acetone and trifluoroacetone, where except at elevated temperatures, phosphorescence predominates (32,47).

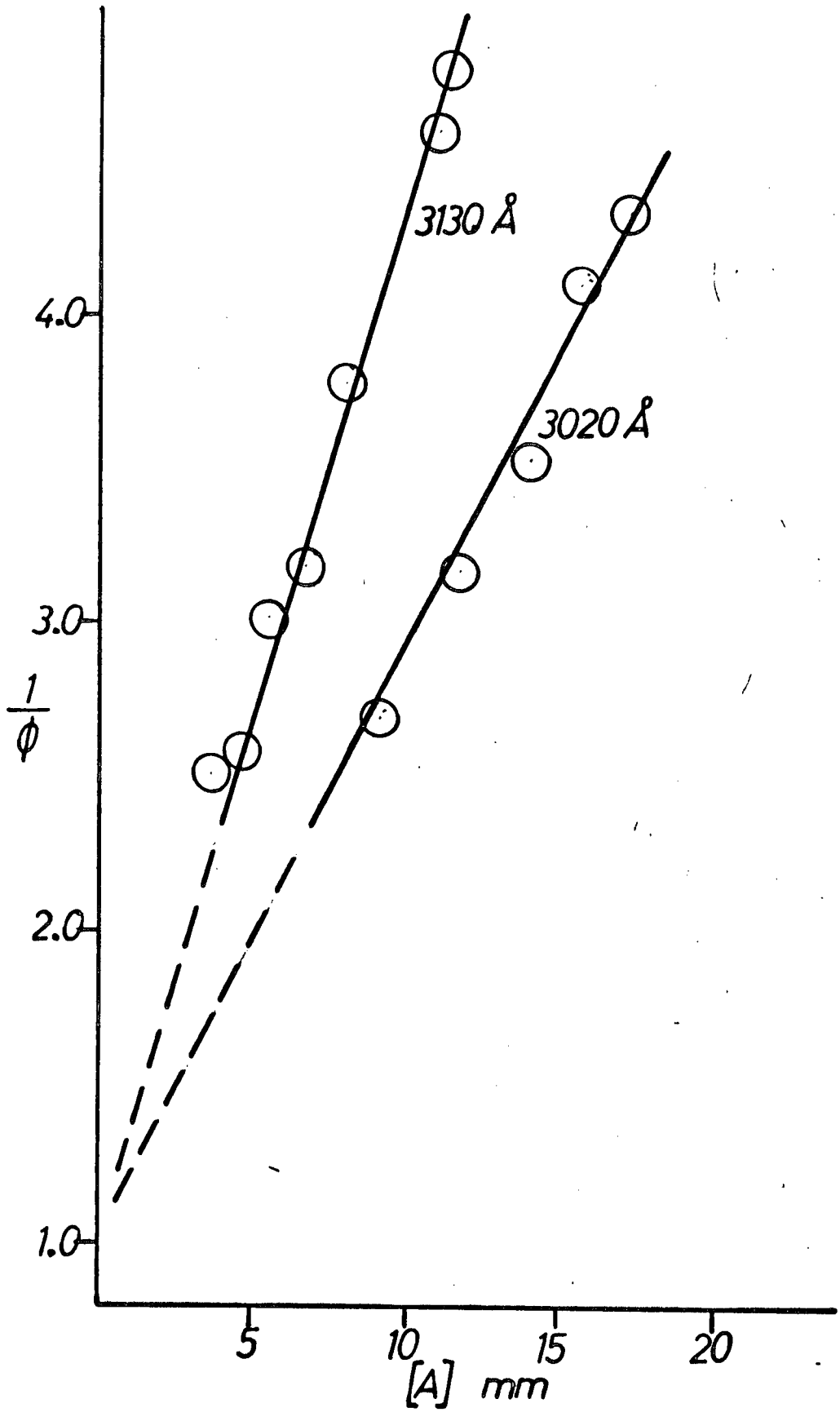

Fig. 29. Photolysis of HFA - biacetyl mixtures at 25°C. The biacetyl pressure was constant at about 0.3 mm.

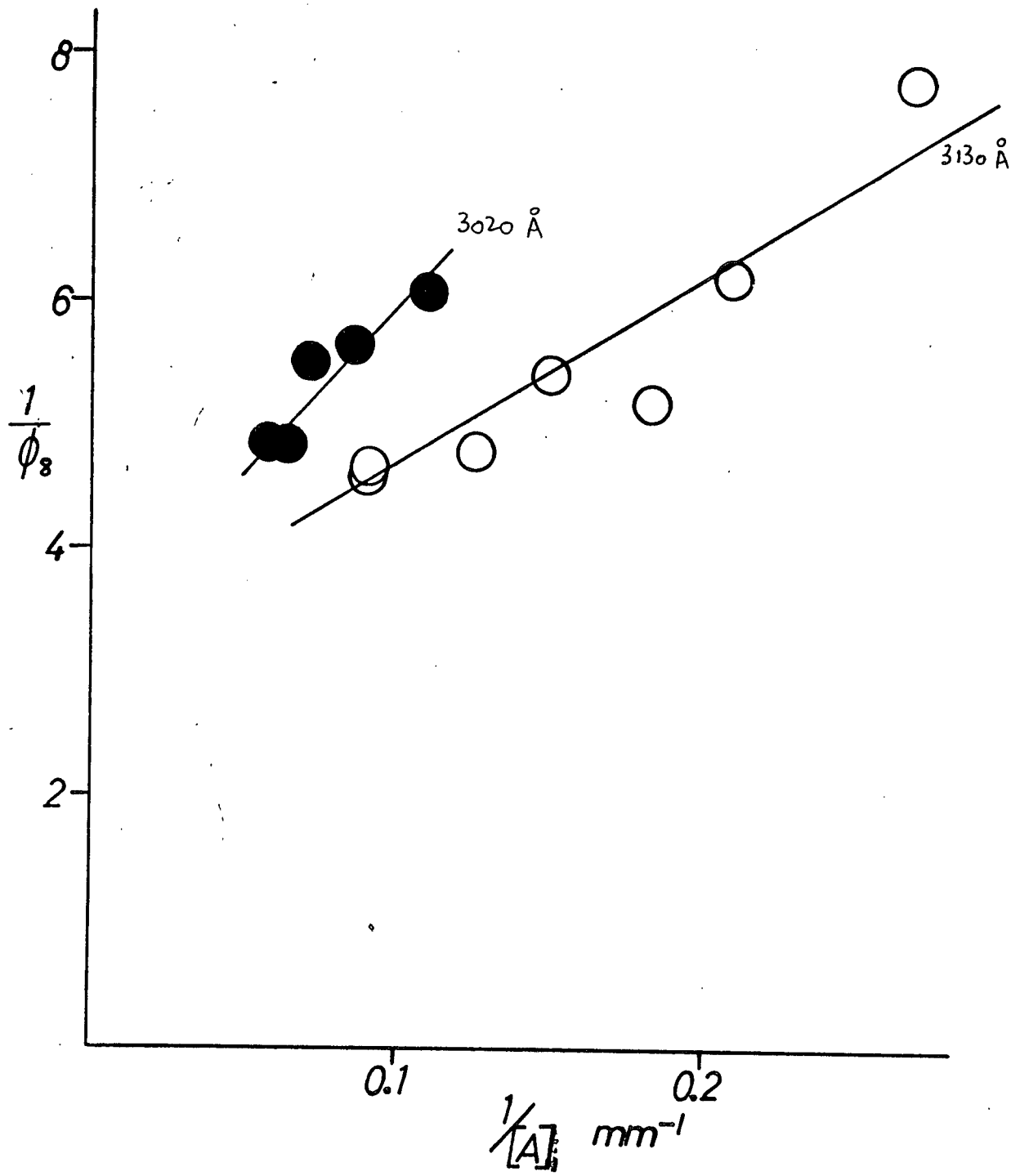

Fig. 30. Variation of triplet dissociation with pressure at 25°.

The spectra recorded in these experiments differ somewhat from the spectrum obtained in the previous study of HFA (page 9). The fluorescence band, seen directly in our experiments only when oxygen is present, corresponds closely to the total emission band reported by Okabe and Steacie. A corresponding discrepancy is evident when the extent of triplet dissociation is examined. This is considered in the next section of this chapter.

In Figs. 31 and 33, the two contributions to the total emission are shown separately. Phosphorescence has a maximum between 4900 and 5000 Å, at both temperatures and at 25° there is a smaller peak near 4600 Å. The fluorescence extends to 6000 Å, with a maximum close to 4300 Å at each temperature. Fig. 32 shows how the total emission is greatly increased on cooling the gas.

The ratio of phosphorescence to fluorescence is

$$\frac{\phi_7}{\phi_5} = \frac{k_4 k_7}{k_5(k_7+k_8+k_9)},$$

independent of pressure.

At the two temperatures studied, this ratio (Table 9) is

$$\left(\frac{\phi_7}{\phi_5}\right)_{25^\circ} = 2.77, \qquad \left(\frac{\phi_7}{\phi_5}\right)_{-78^\circ} = 9.95.$$

Furthermore, from run 3, after allowing for a small change in absorption coefficient with temperature

$$\frac{(\phi_7 + \phi_5)_{-78^\circ}}{(\phi_7 + \phi_5)_{25^\circ}} = 16.7$$

These figures show that phosphorescence increases with decreasing temperature to a much greater extent than fluorescence:

$$\frac{(\phi_7)_{-78^\circ}}{(\phi_7)_{25^\circ}} = 20.7, \qquad \frac{(\phi_5)_{-78^\circ}}{(\phi_5)_{25^\circ}} = 5.75.$$

Such an effect must be at least partly due to the fact that triplet dissociation, which competes with phosphorescence at 25°, is completely absent at the lower temperature (c.f. the linear plot in Fig. 22).

The data in runs 4 and 5, Table 9 allow absolute emission yields to be estimated. Taking ϕ_{11}(4358 Å, 25°)

to be 0.15 (48), we obtain

$$\phi_7(25^\circ) = \left[\frac{\phi_{11}(\text{sensitized})}{\phi_{11}(4358\ \text{Å})}\right]\left[\frac{\phi_7+\phi_5}{\phi_{11}(\text{sens})}\right]\left[\frac{\phi_7}{\phi_7+\phi_5}\right]\phi_{11}(4358\ \text{Å})$$

$$= .025$$

Hence $\phi_7(-78^\circ) = 0.51$. Corresponding values* for the fluorescence yields are $.009(25^\circ)$ and $.051(-78^\circ)$.

It must be stressed that these last figures are subject to a considerable accumulated error - perhaps up to 30%. Nevertheless the results definitely show that at low temperature, phosphorescence in a major, perhaps predominant, primary reaction.

Radiationless conversion (reaction 9) evidently competes with phosphorescence much less effectively as the temperature is decreased. With $\phi_4 = 0.45$ and $\phi_7 + \phi_8 = 0.25$ at 25°, the ratio k_9/k_7 is about 10. At -78°, with $\phi_7 \sim 0.5$, this same ratio cannot be much greater than unity. If, as is likely, k_7 is temperature independent, then k_9 would have an apparent activation energy of at least 0.6 kcal/mole. This fact, together with any corresponding changes in k_4 and k_6 with temperature, may be another reason for the greater degree of enhancement of phosphorescence, as compared to fluorescence, as the temperature is decreased

* All these absolute yields refer to 33 mm of HFA irradiated with 3130 Å.

The data here do not allow any further deductions to be made about this aspect of the primary process.

It would be of interest to measure relative emission efficiencies as a function of pressure at -78°. The greatly increased intensity should allow observations to be made at low concentrations, where any effects of multistage deactivation might become evident (18).

The Intersystem Crossing Reaction.

The values for ϕ^{∞} (pages 66-69) are of considerable interest. At high concentrations, with the mechanism under consideration, all $^1A^m$ molecules are deactivated before they can dissociate from the singlet state, so the yield arises solely from triplet dissociation:

$$\phi^{\infty} \equiv \phi_8^{\infty} = \left(\frac{k_4}{k_4+k_5+k_6}\right)\left(\frac{k_8}{k_1+k_8+k_9}\right) \qquad (5.2)$$

We would not expect this quantity to be wavelength dependent at all, but this is contrary to the observed results: at 3340 and 3130 Å ϕ_8^{∞} is close to 0.2, whereas at 2652 Å, it must be very much less than this, if indeed it is non-zero. The exact values at 3020 and 2804 Å are subject to some uncertainty, since they were obtained by extrapolation.

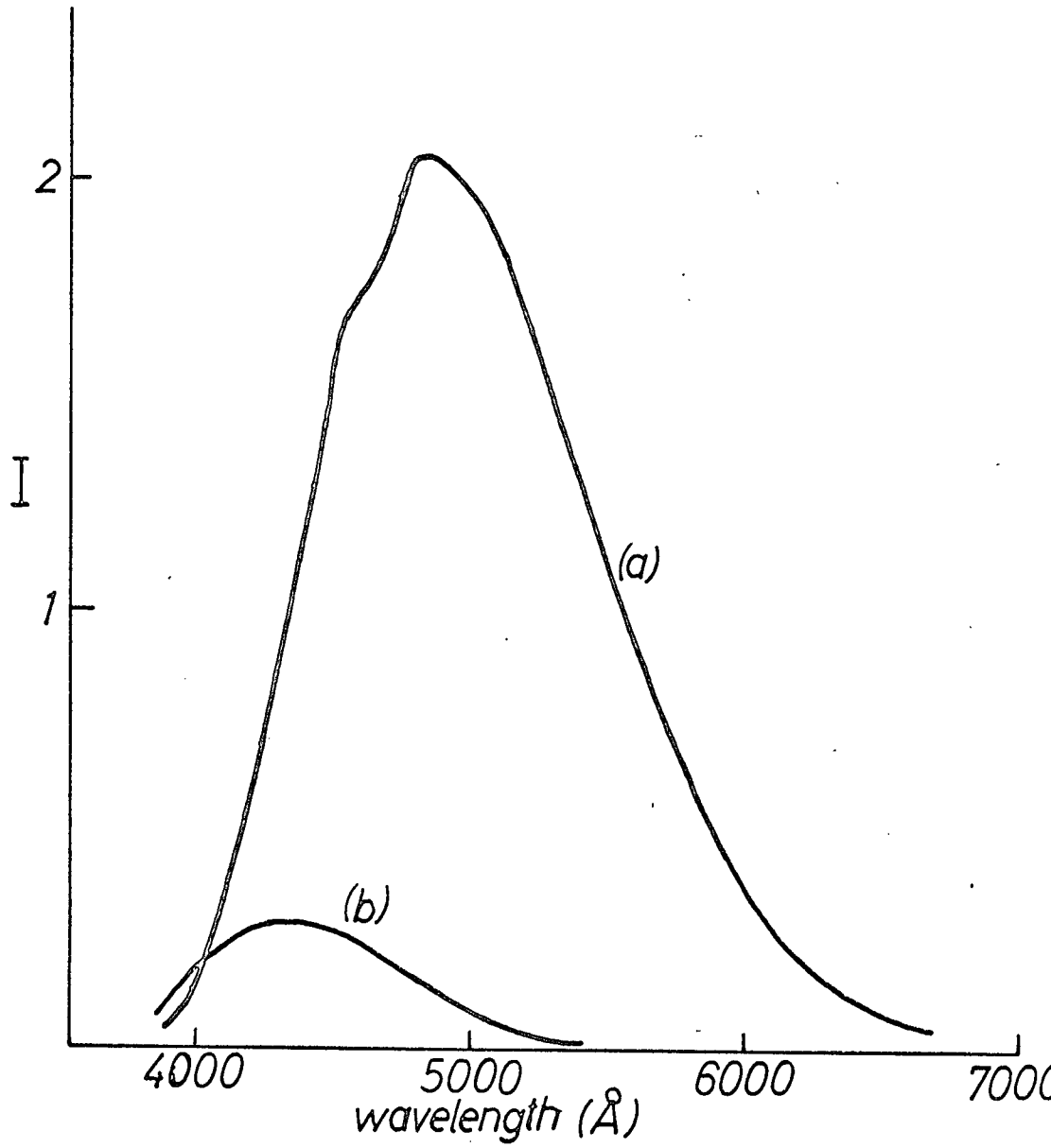

Fig. 31. Phosphorescence (a) and fluorescence (b), from 30 mm HFA at -78°, using 3130 Å. Instrumental corrections have been applied.

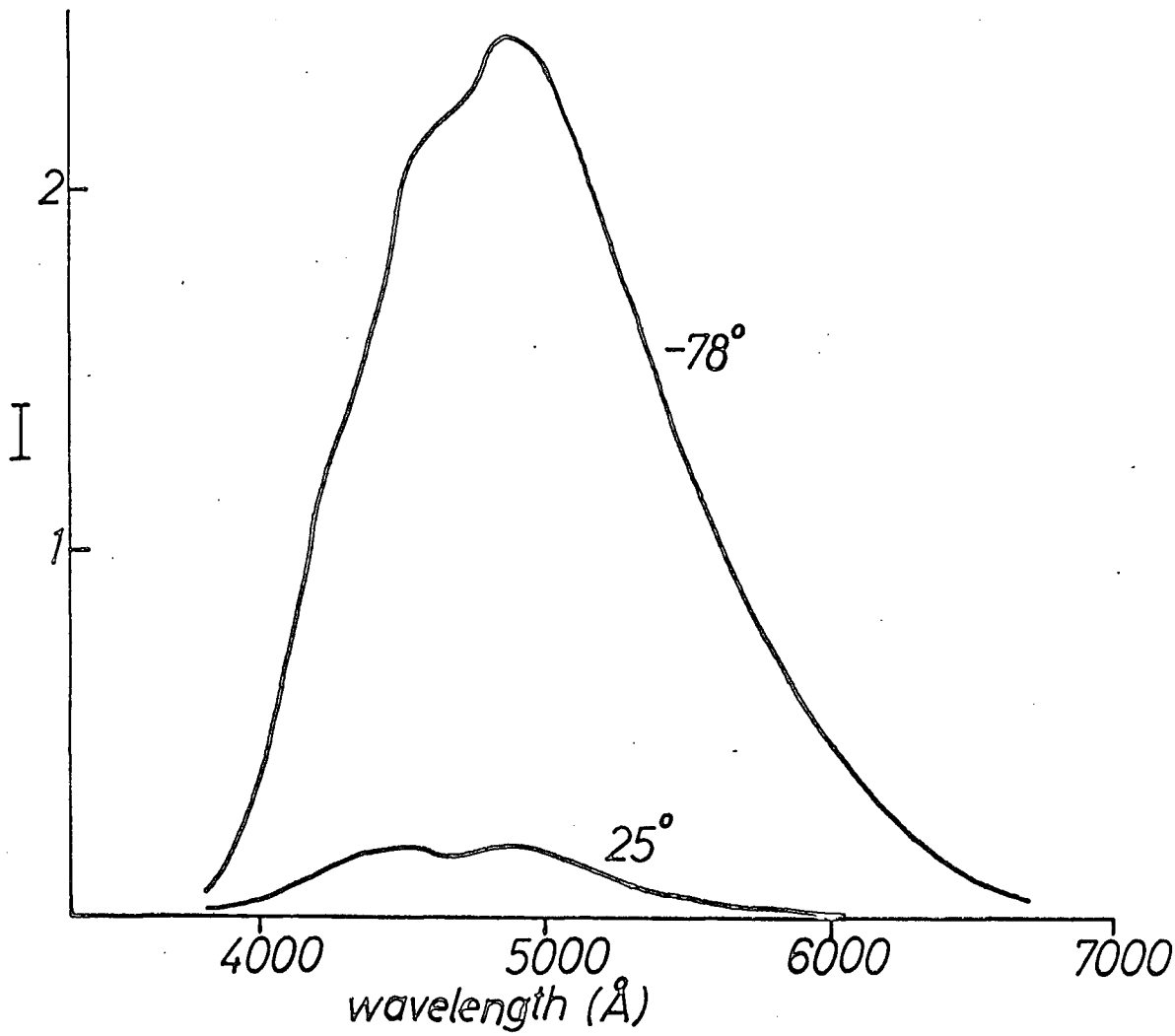

Fig. 32. The total emission of HFA (30 mm) at -78°, compared with that at 25°, using 3130 Å. Instrumental corrections have been applied.

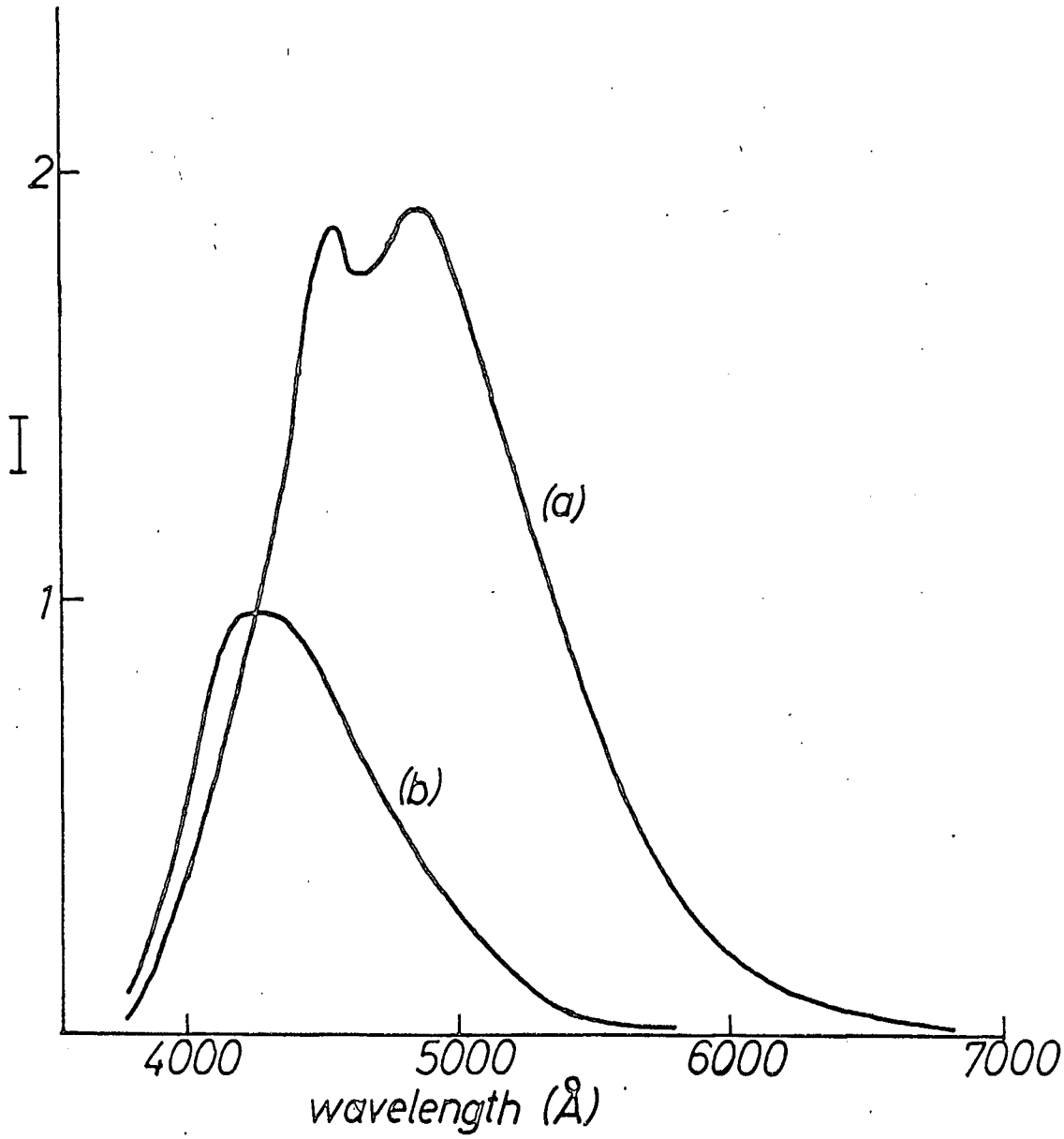

Fig. 33. Phosphorescence (a) and fluorescence (b), from HFA (110 mm) at 25°, using 3130 Å. Instrumental corrections have been applied.

Fig. 21 shows how $^1/\phi$ vs. [A] plots for 3130 and 2652 Å intersect around 100 mm. At high pressures, the quantum yield is greater when less energetic excitation is used. Experimental scatter is rather large in this region, but the trend is clear.

Another fact is that Okabe and Steacie found the spectral distribution of fluorescence to be the same, whatever wavelength was used for excitation. This suggests that $^1A^o$ species are involved in each case, and rather overrules the possibility that another excited singlet state may be involved at the shorter wavelength. The smooth, apparently continuous absorption band in Fig. 12 gives no clear evidence either way.

Any modification to the sequence of primary events must involve an additional reaction to $^1A^m$. If first-order, such a reaction would have to lead to dissociation, since $\phi^o = 1$. The only possibility is a direct inter-system crossing:

$$^1A^m \longrightarrow {}^3A^q \qquad (4a)$$

$$^3A^q \longrightarrow \text{Dissociation} \qquad (4b)$$

$$^3A^q + A \longrightarrow {}^3A^o + A \qquad (4c)$$

There is some support for including this third path to dissociation, in that observed quantum yields at 3130 Å at 25° are definitely higher for intermediate pressures than those expected if only reactions 2 to 9 occur. In the same way, the triplet yields in Fig. 30 give ϕ^{∞} too large. We are therefore inclined to include the reaction sequence 4a, b, c as part of the primary process. This complication, however, has little effect on the overall features of the kinetics: in particular ϕ^{∞} would still be given by equation 5.2, and should not vary with exciting wavelength.

Several possible second order processes may be envisaged:

(a) Dissociation: $^1A^m + A \longrightarrow \text{Diss.} + A$ (2a)

This seems unlikely. The low temperature and biacetyl-quenched data indicate that at 3130 Å, singlet dissociation can be described in terms of a simple linear relationship between $^1/\phi$ and [A], and at 2652 Å, this linearity is evident at 25°. Inclusion of reaction 2a would not give this behaviour, even if reaction 2 were also retained.

(b) Internal Conversion: $^1A^m + A \longrightarrow 2A$ (1a)

To explain the results, we might postulate that at 3130 Å, a fraction α of the collisions between $^1A^m$ and heat bath molecules, induces reaction 1a, while the remainder remove vibrational energy according to reaction 3. At 2652 Å a fraction $\beta(>\alpha)$ would be deactivated by reaction 1a, so that relatively fewer molecules undergo reactions 3 and 4 and subsequent triplet dissociation. That is, ϕ_8^∞ might be very small if $k_{1a} \gg k_3$ at short wavelengths.

With this modification, the fluorescence yield ϕ_5^∞ ought also to be much smaller at 2652 Å than at 3130 Å. The available data (Fig. 3) are somewhat inconclusive on this point: if anything, the trend suggests the values for ϕ_5^∞ to be comparable at both wavelengths.

(c) Intersystem Crossing: $^1A^m + A \longrightarrow {}^3A^o + A$ (3a)

It seems reasonable to suppose that if an encounter did lead to intersystem crossing, then the perturbing molecule would also carry off the excess vibrational energy of $^1A^m$ in the usual way. Whether or not the Franck-Condon principle is applicable for such a transition would depend on the nature and

duration of the encounter. In any case, the principle need not be violated if we imagine the two effects - crossing and deactivation - to be consecutive rather than simultaneous.

The efficiency of reaction 3a,

$$\alpha = \frac{k_{3a}}{k_{3a} + k_3}$$

might then very well depend on the magnitude of the vibration excitation, for this would determine the probability that $^1A^m$ be found in a favorable crossing region of the singlet potential energy hypersurface, at the instant of a collision.

To explain the dissociation data here, α would be very small at 2652 Å, and reaction 4 need not be included. The scheme would also predict ϕ_5^∞ (2652 Å) > ϕ_5^∞ (3130 Å), which again is not conclusively ruled out by the curves in Fig. 3.

Full responsibility for the apparent wavelength dependence of ϕ_8^∞ cannot be definitely placed on any one of the above alternatives. Reaction 3a is the only one completely consistent with the interpretation put on

the remainder of the data. Photolysis at a higher temperature ought to magnify the effect: the increased triplet dissociation would mean that ϕ(3130 Å) would exceed ϕ(2652 Å) at lower, more accessible concentrations. It would also be desirable to examine the emission spectrum at 2652 Å: to be consistent with the dissociation data, the ratio of phosphorescence to fluorescence should be much smaller than that found at 3130 Å.

The extent of dissociation in our experiments at 3130 Å at 25°, is considerably larger than that found by Ayscough and Steacie, who estimated ϕ^{∞} to be about .04. One source of the discrepancy could be in their use of an internal actinometer (acetone), while external ferrioxalate actinometry was used in our experiments. Small differences in absorption coefficients might also have a large effect. However, it is a fact that rate constants for singlet dissociation are in good agreement at both 2652 Å and 3130 Å. In view of this, the most likely explanation seems to be that in the earlier study of HFA, some impurity was present, which almost completely inhibited phosphorescence and dissociation from the triplet state.

BIBLIOGRAPHY

1. O. Stern and M. Volmer, Physik Z. 20 183(1919).

2. W. A. Noyes Jr., G. B. Porter, and J. E. Jolley, Chem. Rev. 56 49(1956)

3. Advances in Photochemistry. Vol. I ed. W. A. Noyes Jr., and J. N. Pitts. (Interscience, 1963)

4. R. M. Hochstrasser and G. B. Porter, Quart. Rev. Chem. Soc. XIV 146(1960)

5. P. B. Ayscough and E. W. R. Steacie, Proc. Roy. Soc. A 234 476(1956)

6. H. Okabe and E. W. R. Steacie, Can. J. Chem. 36 137 (1958)

7. G. Giacometti, H. Okabe and E. W. R. Steacie, Proc. Roy. Soc. A 250 287(1959)

8. A. S. Gordon, J. Chem. Phys. 36 1330(1962)

9. B. G. Tucker and E. Whittle, Proc. Chem. Soc. March 1963

10. G. B. Porter, personal communication

11. L. O. Moore and J. W. Clark, 2nd Int. Symp. on Fluorine Chem., Ester Park, Colorado (1962)

12. L. M. Whittemore and M. Szwarc, J. Phys. Chem. 67 2492(1963)

13. G. B. Porter and B. T. Connelly, J. Chem. Phys. 33 81(1960)

14. L. J. Kassel, Kinetics of Homogeneous Gas Reactions (Chemical Catalog Company Inc., New York, 1932)

15. O. K. Rice and H. C. Ramsberger, J. Am. Chem. Soc. 49 1617(1927)

16. S. Glasstone, K. J. Laidler and H. Eyring, The Theory of Rate Processes (McGraw Hill Book Company Inc., New York, 1941)

17. G. A. Taylor and G. B. Porter, J. Chem. Phys. 33 1353 (1962)

18. D. J. Wilson, B. Noble and B. Lee, J. Chem. Phys. 34 1392(1961)

19. M. Boudart and J. T. Dubois, J. Chem. Phys. 23 223 (1955)

20. B. Stevens and M. Boudart, Ann. N.Y. Acad. Sci. 67 570(1957)

21. B. Steiner, C. F. Giese and M. G. Inghram, J. Chem. Phys. 34 189(1961)

22. W. A. Chupka and J. Berkoivite, J. Chem. Phys. 32 1546 (1960)

23. H. M. Rosenstock, M. B. Wallenstein, A. L. Wahrhaftig and H. Eyring, Nat. Acad. Sci. (U.S.) 38 667(1952)

24. N. B. Slater, Theory of Unimolecular Reactions (Cornell U. P., 1959)

25. M. Wolfsberg, J. Chem. Phys. 1072(1962)

26. R. A. Marcus, J. Chem. Phys. 20 359(1952)

27. R. A. Marcus and O. K. Rice, J. Phys. Coll. Chem. 55 894(1951)

28. D. W. Setser and B. S. Rabinovitch, Can. J. Chem. 40 1425(1962)

29. B. S. Rabinovitch, R. F. Kubin and R. E. Harrington, J. Chem. Phys. 38 405(1963)

30. J. Dubois and B. Stevens, Luminescence of Organic and Inorganic Materials Ed. H. P. Kallman and G. M. Spruch (Wiley, New York 1962)

31. G. Porter and F. Wilkinson, Luminescence of Organic and Inorganic Materials Ed. H. P. Kallman and G. M. Spruch (John Wiley & Sons, New York, 1962)

32. J. Heicklen and W. A. Noyes, Jr., J. Am. Chem. Soc. 81 3858(1959)

33. J. Heicklen, J. Am. Chem. Soc. 81 3862(1959).

34. D. S. Weir, J. Am. Chem. Soc. 83 2629(1961).

35. J. K. Michael and W. A. Noyes Jr., J. Am. Chem. Soc. 85 1027(1963).

36. D. J. LeRoy, Can. J. Res. B28 492(1950).

37. W. A. Noyes Jr. and P. A. Leighton, The Photochemistry of Gases (Reinhold Publishing Corpn., New York, 1941).

38. C. G. Hatchard and C. A. Parker, Proc. Roy. Soc. A235 518(1956).

39. R. E. Hunt and T. L. Hill, J. Chem. Phys. 15 111(1947).

40. R. E. Harrington, B. S. Rabinovitch and M. R. Hoare, J. Chem. Phys. 33 744(1960).

41. E. K. Gill and K. J. Laidler, Proc. Roy. Soc. A250 121(1959).

42. H. N. Rosenstock, J. Chem. Phys. 34 2182(1961).

43. G. B. Porter, J. Chem. Phys. 32 1587(1960).

44. H. L. J. Bäckström and K. Sandros, Acta Chem. Scand. 14 48(1960).

45. G. F. Sheats and W. A. Noyes Jr., J. Am. Chem. Soc. 77 142(1955).

46. H. Okabe and W. A. Noyes, Jr., J. Am. Chem. Soc. 79 801(1957).

47. P. Ausloos and E. Murad, J. Phys. Chem. 65 1519(1961).

48. G. M. Almy and P. R. Gillette, J. Chem. Phys. 11 188(1943).

49. B. S. Rabinovitch and R. W. Diesen, J. Chem. Phys. 30 735(1959)